HAL open science

Network optimization for wireless microwave backhaul

Napoleao Nepomuceno

To cite this version:

Napoleao Nepomuceno. Network optimization for wireless microwave backhaul. Computer Science [cs]. Université Nice Sophia Antipolis, 2010. English. NNT : . tel-00593412

HAL Id: tel-00593412

https://theses.hal.science/tel-00593412v1

Submitted on 15 May 2011

HAL is a multi-disciplinary open access archive for the deposit and dissemination of scientific research documents, whether they are published or not. The documents may come from teaching and research institutions in France or abroad, or from public or private research centers.

L'archive ouverte pluridisciplinaire **HAL**, est destinée au dépôt et à la diffusion de documents scientifiques de niveau recherche, publiés ou non, émanant des établissements d'enseignement et de recherche français ou étrangers, des laboratoires publics ou privés.

UNIVERSITÉ DE
NICE - SOPHIA ANTIPOLIS
ÉCOLE DOCTORALE SCIENCES ET
TECHNOLOGIES DE L'INFORMATION
ET DE LA COMMUNICATION

UNIVERSIDADE
FEDERAL DO CEARÁ
PROGRAMA DE
PÓS-GRADUAÇÃO EM
CIÊNCIA DA COMPUTAÇÃO

PHD THESIS

to obtain the title of

Docteur en Sciences
de l'Université de
Nice - Sophia Antipolis
Mention : INFORMATIQUE

Doutor em Ciências
da Universidade
Federal do Ceará
Menção : COMPUTAÇÃO

Defended by

Napoleão NEPOMUCENO

Network optimization for wireless microwave backhaul

Thesis Advisors: **Jean-Claude BERMOND**,
David COUDERT, and **Manoel CAMPÊLO**

prepared at INRIA Sophia Antipolis, MASCOTTE Team

defended on 17th December 2010

Reviewers :	Ricardo CORRÊA	-	Professor U. Federal do Ceará
	Fabrice VALOIS	-	Professor INSA Lyon
	Di YUAN	-	Professor Linköping University
Examinators :	Jean-Claude BERMOND	-	Research Director CNRS
	Simon BRYDEN	-	Engineer SME 3Roam
	Manoel CAMPÊLO	-	Professor U. Federal do Ceará
	David COUDERT	-	Researcher INRIA
	Arie KOSTER	-	Professor RWTH University

Dedicated to my family.

Acknowledgments

I would like to record my gratitude to my Ph.D advisors. I am indebted to them more than they know.

It is a pleasure to convey my acknowledge to my coauthors, and I hope to keep up our collaboration in the future.

I have also benefited by advice, guidance, and help from people from SME 3Roam, and I am very grateful to them.

I am immensely thankful to my Ph.D. referees for their critical and constructive comments on this thesis.

I gratefully acknowledge to my colleagues for providing a stimulating and fun environment in which to work and learn.

I would like to thank my family for the support and love they provided me throughout my entire life.

And, in particular, I wish to thank Tarciana for being there and for being so nice. Obrigado, Pretinha.

Network optimization for wireless microwave backhaul

Abstract: Technological breakthroughs have transformed the telecommunications industry aiming at providing capacity and efficiency to support the increasing demand for wireless broadband services. With the advances in access technologies, the capacity bottleneck of cellular networks is gradually moving from the radio interface towards the backhaul – the portion of the network infrastructure that provides interconnectivity between the access and core networks. The ability for microwave to be rapidly and cost-effectively deployed is being a crucial point for successfully tackling the backhaul bottleneck problem.

However, backhaul solutions available with this technology have received little attention from the scientific community. Nevertheless, the growth of microwave backhaul networks and their increasing complexity give rise to many interesting optimization problems. In fact, unlike wired networks, the capacity of a microwave radio link is prone to variations, either due to external factors (e.g., weather) or by the action of the network operator. This fundamental difference raises a variety of new issues to be addressed appropriately. Therefore, more refined approaches for dealing with network optimization in wireless microwave backhaul need to be conceived.

In this thesis, we investigate network optimization problems related to the design and configuration of wireless microwave backhaul. We are concerned with a general class of problems expressed in terms of minimum cost multicommodity flows with discontinuous step increasing cost functions on the links of the network. These problems are among the most important and challenging problems in network optimization. Generally, they are computationally very difficult and, in practice, can only be solved approximately. We introduce mathematical models for some of these problems and present solution approaches essentially based on general mixed integer programming, chance-constrained programming, relaxation techniques, cutting plane methods, as well as hybrid metaheuristics.

This work was done in collaboration with the SME 3Roam, and partially developed within the scope of the joint project RAISOM (Réseaux de collecte IP sans fil optimisés), among INRIA Sophia Antipolis, SME 3Roam, and SME Avisto. This thesis was developed under joint PhD thesis supervision between the University of Nice-Sophia Antipolis and the Federal University of Ceará.

Keywords: Wireless communications, mathematical programming, network optimization, multicommodity flows, microwave backhaul networks.

Optimisation dans des réseaux backhaul sans fil

Résumé: Les avancées technologiques poussent l'industrie des télécommunications à fournir la capacité et la qualité nécessaire pour satisfaire la demande croissante de services sans fil à haut débit. De plus, avec les progrès des technologies d'accès, le goulot d'étranglement des réseaux cellulaires se déplace progressivement de l'interface radio vers le backhaul – la partie de l'infrastructure du réseau qui fournit l'interconnexion entre les réseaux d'accès et de coeur. Aussi, la possibilité de déployer rapidement des liens radio micro-ondes efficaces est essentielle pour apporter des solutions crédibles au problème de l'engorgement des réseaux backhaul.

Toutefois, les solutions de backhaul disponibles avec cette technologie ont reçu peu d'attention de la communauté scientifique. Pourtant, la croissance des réseaux backhaul et l'augmentation de leur complexité posent de nombreux problèmes d'optimisation très intéressants. En effet, contrairement aux réseaux filaires, la capacité d'un lien radio micro-ondes est sujette à variation, soit due à des facteurs extérieurs (météo), soit par l'action de l'opérateur. Cette différence fondamentale soulève une variété de nouvelles questions qui doivent être abordées de façon appropriée. Il faut donc concevoir des méthodes adéquates pour l'optimisation des réseaux backhaul.

Dans cette thèse, nous étudions les problèmes d'optimisation de réseaux liés à la conception et la configuration des liaisons terrestres sans fil à micro-ondes. Nous nous intéressons en particulier à la classe des problèmes de multiflot de coût minimum avec des fonctions de coût en escalier sur les liens du réseau. Ces problèmes sont parmi les problèmes d'optimisation combinatoire les plus importants et les plus difficiles dans l'optimisation des réseaux, et il n'est généralement possible de les résoudre que de façon approchée. Nous introduisons des modèles mathématiques pour certains de ces problèmes et présentons des approches de solution basées essentiellement sur la programmation entière mixte, la programmation sous contraintes probabilistes, des techniques de relaxation, des méthodes de coupe, ainsi que des méta-heuristiques hybrides.

Ces travaux ont été effectués en collaboration avec la PME 3Roam, et partiellement dans le cadre du projet RAISOM (Réseaux de Collecte IP sans fil optimisés) entre le projet Mascotte et les PMEs 3Roam et Avisto. Cette thèse a été développée en co-tutelle entre l'Université de Nice-Sophia Antipolis et l'Université Federale du Ceará.

Mots-clés: Communications sans fil, programmation mathématique, optimisation réseau, multiflots, réseaux micro-ondes backhaul.

Otimização em redes de backhaul sem fio

Resumo: Inovações tecnológicas têm transformado a indústria de telecomunicações visando fornecer capacidade e eficiência para suportar a crescente demanda por serviços de banda larga sem fio. Com os avanços das tecnologias de acesso, o gargalo de capacidade das redes celulares está gradualmente passando da interface de rádio para o backhaul – a parte da infraestrutura de rede que fornece interconexão entre as redes de acesso e o backbone. A implantação rápida e econômica da infraestrutura de comunicação sem fio está se mostrando um ponto crucial para se resolver o problema do gargalo de capacidade do backhaul.

No entanto, soluções de backhaul disponíveis com essa tecnologia têm recebido pouca atenção da comunidade científica. À medida que as redes de backhaul sem fio se tornam maiores e mais complexas, diversos problemas interessantes de otimização de rede surgem nesta área em desenvolvimento. De fato, ao contrário das redes cabeadas clássicas, a capacidade de um canal de rádio microondas está sujeita a alterações, quer seja por fatores externos (condições climáticas), quer seja pela ação do operador de rede. Esta diferença fundamental levanta uma série de novas questões a serem ainda abordadas de forma apropriada. Devemos, portanto, desenvolver métodos de otimização adequados ao contexto das redes de backhaul sem fio.

O tema central de investigação nesta tese são importantes e desafiadores problemas de otimização de rede relacionados com a concepção e a configuração de redes de backhaul sem fio, dentre os quais destacam-se problemas de multifluxo de custo mínimo com funções de custo em escada dos liames da rede. Estes são problemas difíceis a um ponto tal que, diante de instâncias oriundas de situações reais, somente soluções aproximadas são factíveis de serem obtidas computacionalmente. Nesse contexto, nós propomos modelos matemáticos para alguns destes problemas e apresentamos métodos de resolução baseados essencialmente em programação inteira mista, programação sob restrições probabilísticas, técnicas de relaxação, métodos de corte, bem como metaheurísticas híbridas.

Este trabalho foi realizado em colaboração com a empresa 3Roam, e foi parcialmente desenvolvido no âmbito do projeto conjunto RAISOM (Réseaux de Collecte IP sans fil optimisés), entre o INRIA Sophia Antipolis, a empresa 3Roam e a empresa Avisto. Esta tese foi desenvolvida em co-tutela entre a Universidade Federal do Ceará e a Universidade de Nice-Sophia Antipolis.

Palavras-chave: Comunicação sem fio, programação matemática, otimização em redes, multifluxo, redes de backhaul sem fio.

Contents

List of abbreviations xiii

List of Figures xv

List of Tables xvii

1 Introduction 1
- 1.1 Context and motivation . . . 1
- 1.2 Our contribution . . . 4
- 1.3 Outline of this thesis . . . 6

2 Microwave communications 9
- 2.1 Microwave radio system . . . 9
  - 2.1.1 Capital and operational costs . . . 11
  - 2.1.2 Radio spectrum . . . 11
  - 2.1.3 Performance analysis . . . 13
- 2.2 Link power budget . . . 16
  - 2.2.1 Basic terminology . . . 16
  - 2.2.2 Power budget calculations . . . 19
  - 2.2.3 Vigants–Barnett model . . . 20
  - 2.2.4 Crane rain fade model . . . 20
- 2.3 *3Link* . . . 21
  - 2.3.1 Models, input and output . . . 22
  - 2.3.2 About *3Link* . . . 23
- 2.4 Conclusion . . . 23

3 Bandwidth assignment for reliable backhaul 29
- 3.1 Context and motivation . . . 29
- 3.2 Chance-constrained programming . . . 31
- 3.3 Mathematical formulations . . . 32
  - 3.3.1 Separate chance constraints . . . 32
  - 3.3.2 Joint chance constraints . . . 35
- 3.4 Valid inequalities . . . 37
- 3.5 Computational results . . . 39
- 3.6 Conclusion . . . 43

4 Power-efficient radio configuration 47
- 4.1 Context and motivation . . . 47
- 4.2 Mathematical formulations . . . 49
  - 4.2.1 Discontinuous step increasing cost functions . . . 49
  - 4.2.2 Piecewise linear convex cost functions . . . 52

4.3 Hybrid algorithm 54
4.4 Computational results 57
4.5 Conclusion 62

5 Reoptimizing power-efficient configurations 65
5.1 Performance investigation 65
5.2 Relaxation improvements 68
5.3 Lagrangian relaxation 70
5.4 Benders' decomposition 74
5.5 Conclusion 76

6 Conclusion and perspectives 79

A Tradeoffs in routing reconfiguration problems 81
A.1 Introduction 81
A.1.1 Definitions and previous results 84
A.1.2 Our results 87
A.2 Complexity results 88
A.2.1 Definition of some useful digraphs 88
A.2.2 NP-completeness 89
A.3 Behaviour of ratios in general digraphs 90
A.4 Behaviour of ratios in symmetric digraphs 94
A.5 The routing reconfiguration problem 98
A.6 Conclusion 101

Bibliography 103

List of abbreviations

3G/4G	Third- and Forth-Generation Cellular Networks
BER	Bit Error Rate
BPSK	Binary Phase Shift Keying
BSC	Base Station Controller
BTS	Base Transceiver Station
CAPEX	Capital expenditure
FCC	Federal Communications Commission
FDD	Frequency-Division Duplexing
IDU	Indoor Unit
ILP	Integer Linear Programming
IP	Internet Protocol
ITU	International Telecommunications Union
LOS	Line-of-Sight
LTE	Long Term Evolution
MCF	Multicommodity Flow
MCMCF	Minimum Cost Multicommodity Flow
MPLS	Multiprotocol Label Switching
MSC	Mobile Switching Center
ODU	Ourdoor Unit
OPEX	Operating expenditure
PSTN	Public Switched Telephone Network
QAM	Quadrature Amplitude Modulation
QPSK	Quadrature Phase Shift Keying
RF	Radio Frequency
SNR	Signal-to-Noise Radio
WDM	Wavelength-Division Multiplexing
WiMAX	Worldwide Interoperability for Microwave Access

List of Figures

1.1 Access, backhaul, and core networks. 1
1.2 Hierarchical and mesh backhaul topologies. 2

2.1 A schematic illustration of a microwave link. 10
2.2 QPSK and 16-QAM constellations. 15
2.3 Theoretical capacity versus practical bitrate. 16
2.4 *3Link* input screen: scenario and performance parameters. 24
2.5 *3Link* output screen: configurations and performance summary. . . . 25
2.6 *3Link* flowchart diagram. 26

3.1 Adaptive modulation for a microwave link. 31
3.2 Discrete probability distribution function. 34
3.3 Cumulative probability distribution function. 35
3.4 Illustration of a cutset in a network. 38
3.5 5×5 network grid instance. 40
3.6 Bandwidth cost as a function of the infeasibility tolerance. 41
3.7 Optimality gap, best solution and lower bound values. 43
3.8 Comparison of the performance of different formulations. 44

4.1 Power-efficient configuration points. 49
4.2 Step increasing energy cost function on the links. 50
4.3 Exclusive multi-arc representation of a 168 Mbps link. 50
4.4 Piecewise linear convex energy cost function on the links. 52
4.5 Progressive multi-arc representation of a 112 Mbps link. 53
4.6 Example of solutions obtained by the different methods. 55
4.7 Conceptualization of the hybrid algorithm. 56
4.8 Power utilization as a function of the traffic volume. 58
4.9 Power utilization gap as a function of the traffic volume. 59
4.10 Very different solutions (Grid 5×5, $\lambda = 0.05$). 61
4.11 Similar solutions (Grid 5×5, $\lambda = 0.70$). 61
4.12 Very similar solutions (Grid 5×5, $\lambda = 1.30$). 61
4.13 Bad integer solution (Grid 10×10, $\lambda = 0.30$). 62

5.1 Power-efficient configuration points. 66
5.2 Convex linear combination of power-efficient points. 67
5.3 Piecewise linear convex combination of power-efficient points. 68
5.4 Execution time for linear and convexification-based relaxations. . . . 69
5.5 Execution time for the different relaxations. 71
5.6 Convergence of lagrangian relaxations. 73
5.7 Execution time for the lagrangian relaxations. 74

A.1 Different process strategies for a symmetric digraph D. 83
A.2 $mfvs_p(D)$ function of p for a digraph D. 87
A.3 Digraph $D_{n,k}$ described in Theorem 4 and Corollary 3. 91
A.4 Proof of Lemma 1 95
A.5 Symmetric digraph SD_n of Lemma 2 and instance of SD_5. 96
A.6 Instance of the reconfiguration problem. 98
A.7 Scheme of the transformation in the proof of Theorem 5 100

List of Tables

2.1 Example of capital expenditure for one microwave link. 12
2.2 Example of operational expenditure for one microwave link. 12
2.3 Bandwidth efficiency and SNR requirement for QAM schemes. . . . 16

3.1 Different formulations w.r.t the valid inequalities. 42

4.1 Power-efficient configurations data. 57

CHAPTER 1

Introduction

1.1 Context and motivation

The increasing demand for high-speed data connections, motivated by the growth in the number of mobile users and the tremendous uptake of wireless broadband services, has driven an outstanding development in telecommunications over the last years. New transmission technologies and system architectures are emerging in an attempt to meet users' needs for bandwidth-intensive services.

Advanced access technologies such as Worldwide Interoperability for Microwave Access (WiMAX) and Long Term Evolution (LTE), which typically rely on a packet-based infrastructure – using Internet Protocol (IP) as a unifying service delivery protocol and Ethernet as a universal physical transport layer –, arise as a promising alternative to provide high-bandwidth capability to users [Boc09, Lit09].

With the advances in access technologies, the capacity bottleneck of cellular networks is gradually moving from the radio interface towards the *backhaul* – the portion of the network infrastructure that provides interconnectivity between the access and core networks, as illustrated in Figure 1.1.

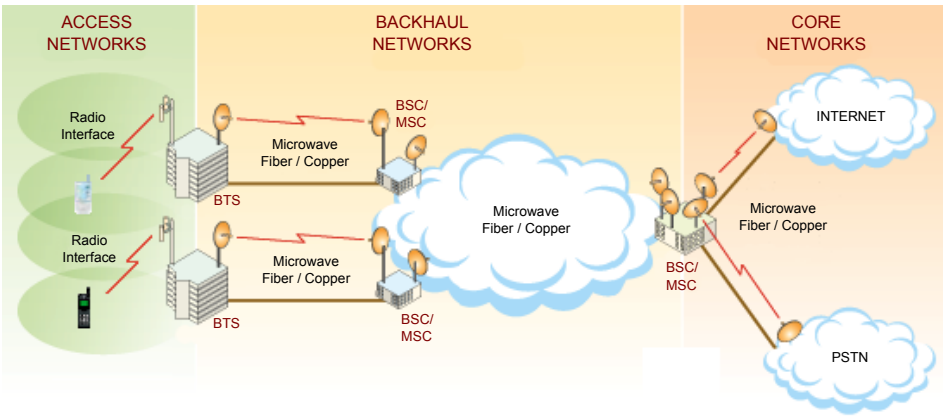

Figure 1.1: Access, backhaul, and core networks.

The backhaul basically comprises two functionalities within the cellular network. The first, often referred to as *last mile*, is the connection between the base transceiver stations (BTS) – which furnish radio coverage over a geographical area to support communications with individual mobile handsets – and the base station

controller (BSC) – which performs as an intermediate traffic aggregation point. The second, commonly referred to as *middle mile*, is the connection between the BSC and the handoff point to the core network, typically a mobile switching center (MSC) – which provides interconnection into the public switched telephone network (PSTN) or the Internet.

Regarding the choice among the transmission technologies widely used in backhaul networks – copper, fiber, and microwave –, operators must consider miscellaneous aspects such as cost, capacity, and availability. Copper offers the advantage of being widely available in some geographies, but this medium is neither cost-effective nor scalable. Fiber, thanks to its virtually unlimited capacity, would be the perfect medium in an ideal world. Unfortunately, fiber availability is extremely restricted due to deployment challenges and high installation costs. Microwave, in turn, can be deployed rapidly and cost-effectively, but it does not provide the same capacity as fiber lines.

As operators deploy third- (3G) and fourth-generation (4G) cellular networks, microwave comes forth as a key answer to ease backhaul bottlenecks. In fact, microwave has become a common preference to build backhaul networks, particularly in emerging countries and remote locations where classical copper or fiber lines are too costly or simply unavailable.

Given the expected high density of sites for 4G systems, the classical topologies used in microwave network design [Put00] – star and ring – are also evolving to provide the necessary data capacity at contained costs. Besides, the migration to an all IP-based network allows that much of the network functionality shifts to the base stations and, as a consequence, the traditional hierarchical topology is evolving to one that is flatter, as shown in Figure 1.2. As the network architecture becomes flatter, mesh connectivity would be more appropriate for ensuring capacity efficiency and routing flexibility [Boc09, CGB09].

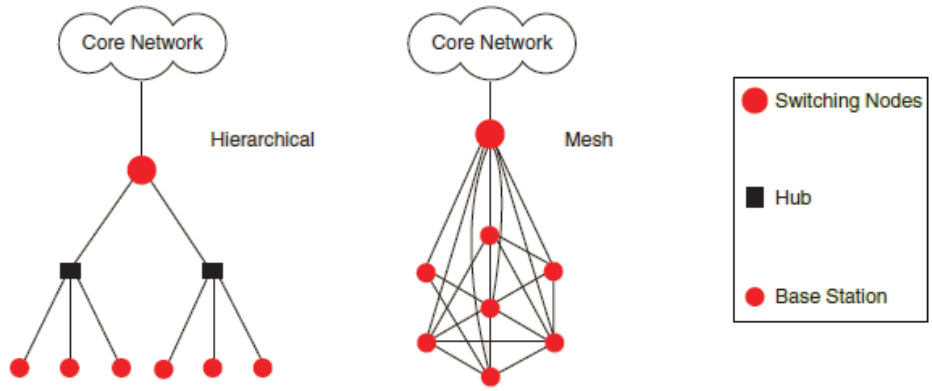

Figure 1.2: Hierarchical and mesh backhaul topologies.

As a whole, technological breakthroughs have transformed the telecommunications industry aiming at providing backhaul capacity and efficiency to support

the demand for wireless broadband services. The ability for microwave backhaul networks to be rapidly and cost-effectively deployed is being a crucial point for successfully tackling the backhaul bottleneck problem, and it is not a coincidence that over 50% of the world's base transceiver stations are connected using point-to-point microwave technologies [Lit09, San09].

Nevertheless, backhaul solutions available with this technology have received little attention from the scientific community. Apart from original problems in wireless communications (e.g., channel characterization, power control, and frequency assignment), several interesting problems from network optimization (e.g., facility location, capacity planning, and traffic routing) arise in this developing area when microwave backhaul networks become larger and more complex. Due to fundamental differences between wireless networks and classical wired networks, a variety of questions in this area remain to be adequately addressed and, doubtlessly, some additional considerations inherent to wireless communications must be taken into account for better responding some of them.

First, the design of microwave links requires special engineering considerations related to the wireless channel. In fact, while wired channels are stationary and predictable – links are always characterized by a given capacity and other parameters –, wireless links are time-varying by nature – e.g., weather conditions can introduce instantaneously variations into the communication channel – and have a dynamic behavior – e.g., modulation and coding can be adjusted according to weather conditions to keep some performance criteria.

In addition, the radio spectrum is a limited natural resource which requires sensible allocation to many different applications and systems, and coordination to promote its efficient use. Bandwidth assignment, which is closely related to network capacity planning, is a highly specialized task requiring a tremendous amount of engineering and normally subject to renewal upon payment of renewal fees. Besides, frequency planning plays a critical role to avoid interference within one's own network and between other operators' networks [AHK+07, HTRS10].

Furthermore, the design of microwave backhaul networks presents particular constraints. It is essential for microwave links to have a clear line-of-sight (LOS) – i.e., there is a direct path without any obstruction (such as buildings, trees, or mountains) between the communication endpoints –, which strongly dictates the network topology. In addition, microwave backhaul networks usually have a significant dependency on the core network, which impacts the decision of where to install network nodes and links in order to interconnect all the points of interest to the core network [Dar07].

Therefore, more refined approaches for dealing with network optimization in wireless microwave backhaul networks need to be conceived. Besides the technical task of microwave link engineering, we are especially concerned about network optimization problems that consider the random variations of wireless channels and the dynamic behavior of microwave links. This is the main issue that we address in this thesis, which was partially developed within the scope of the joint project *RAISOM* (*Réseaux de collecte IP sans fil optimisés*), among INRIA Sophia An-

tipolis, SME 3Roam, and SME Avisto, and financed by the SME 3Roam and the Région PACA through a PhD grant. This thesis was developed under joint PhD thesis supervision between the University of Nice-Sophia Antipolis and the Federal University of Ceará.

1.2 Our contribution

In this thesis, we investigate network optimization problems related to the design and configuration of wireless microwave backhaul. We are concerned with a general class of problems expressed in terms of minimum cost multicommodity flows (MCMCF), which is largely used for optimal design and dimensioning of telecommunication networks [Ken78, Min06]. These problems basically consist of transporting different commodities, from their respective sources to their destinations, which simultaneously use the network and are coupled through either the links' capacities or the cost function to be minimized. Obviously, there should be enough capacity in the network to simultaneously carry all the traffic requirements (given as an input). The interested reader is also referred to the following books on network optimization [Ber98, PM04].

Various special cases of the MCMCF problem are reported in [Min06], each of them associated with an appropriate choice of link cost function. Generally, the optimization criterion refers to the total cost of the equipment to be installed on the various links of the network. When the cost function is considered to be linear, then the MCMCF problem can be formulated as a large scale continuous linear program, and many efficient algorithms are available to tackle it (see the survey [Ken78]). By contrast, when considering realistic situations, we have commonly to deal with piecewise linear concave cost functions or step increasing cost functions, giving rise to large scale integer linear programs, much more difficult to solve in practice (see [GKM99] and references therein).

Particularly, the problems studied here rely on a MCMCF with discontinuous step increasing cost functions on the links of the network. These problems are among the most important and challenging problems in network optimization. Generally, they are computationally very difficult (they belong to the NP-hard complexity class [TLM84] and, in practice, can only be solved approximately [GM97]). We introduce mathematical models for some of these problems and present solution approaches essentially based on general mixed integer programming, chance-constrained programming, relaxation techniques, cutting plane methods, as well as hybrid metaheuristics. Our contribution can be summarized as follows.

First, we have developed an optimization tool, *3Link*, for helping engineers on the technical task of conceiving a microwave link. Driven by commercial and technical requirements, *3Link* provides an easy way to calculate the link budget and determine which configurations are available for the new microwave link to deploy. This work was done under the supervision of Simon Bryden from SME 3Roam

(http://www.3roam.com), a company which provides high-capacity microwave transmission equipments for wireless and packet networks convergence. *3Link* is distributed by SME 3Roam with its *Wireless Ethernet Starter Kit*.

Besides, the effort devoted to this practical activity provided an important background for understanding and modelling the problems studied here. In fact, we could identify the main parameters (e.g., channel bandwidth, modulation scheme, and transmission power) that determine the capacity of a microwave link. These parameters represent information of different natures – some of them are network engineer's decisions while others are closely related to the conditions on the communication channel. Furthermore, we could identify how these parameters impact the network costs (e.g., renewal fees of licenses and power utilization) while considering different scenarios of optimization.

In addition, we have proposed a chance-constrained programming approach to determine the optimal bandwidth assignment for the links of a microwave backhaul network under outage probability constraints. This problem differs from classical capacity planning problems in the sense that microwave links vary in time. In fact, the capacity of microwave links is basically determined by the channel bandwidth and the modulation scheme used to transmit data. On the one hand, the assigned bandwidth for each link is a network engineer's decision. On the other hand, in response to channel fluctuations, we assume that the modulation scheme is a random factor. Therefore, the optimal solution must somehow consider such random variations for guaranteeing a reliability level of the solution (without leading to the inefficient use of the radio spectrum). This work was done in collaboration with David Coudert from Mascotte team, Grit Claßen and Prof. Arie M. C. A. Koster from RWTH Aachen University, and it was recently submitted to an international conference [CCKN].

Moreover, we have presented mathematical models to generate power-efficient radio configurations as a function of the network traffic. Since microwave links present a dynamic behavior (transmission power and modulation scheme can be properly adjusted on the fly), the traffic fluctuation over the time offers an opportunity to power mitigation when microwave links are underused. The main goal is to reduce interference among systems that share the same spectrum, especially when the number of base transceiver stations and microwave links increases. This work was done in collaboration with David Coudert from Mascotte team and Hervé Rivano from CITI Lab INSA Lyon, and it has originated many publications [CNR09a, CNR09b, CNR10]. Subsequent discussions with Prof. Manoel Campêlo and Prof. Ricardo Corrêa from Universidade Federal do Ceará, and Prof. Arie M. C. A. Koster from RWTH Aachen University led to several improvements on the problem modelling and solving.

Finally, we have also addressed the routing reconfiguration problem that occurs in connection-oriented networks such as telephone, multiprotocol label switching (MPLS), or wavelength-division multiplexing (WDM) networks. This problem involves moving from an initial routing (set of paths connecting pairs of nodes) to another, treating sequentially each connection. It requires a proper

scheduling to avoid conflicts in accessing resources but, incidentally, connection interruptions may happen during the reconfiguration process. Two different objectives arise: (1) minimize the total number of interruptions or (2) minimize the maximum number of simultaneous interruptions. We study tradeoffs between these conflicting objectives and give several complexity results about this problem. This work was done in collaboration with many people from Mascotte team, and it has originated national and international publications [CCM+10a, CCM+10b]. Since this work does not belong to the main subject of this thesis, it will be presented as an appendix.

1.3 Outline of this thesis

The remainder of this thesis is organized as follows:

Chapter 2 is devoted to the technical task of conceiving a microwave link. Along with the fundamentals of wireless communications – e.g., channel capacity, modulation schemes, and fading models –, we present *3Link*, an optimization tool that we have developed for helping engineers who are faced with designing and planning microwave links.

Chapter 3 covers the minimum cost bandwidth assignment problem under outage probability constraints. We introduce (joint) chance-constrained mathematical programs to tackle this problem and derive their integer linear programming (ILP) counterparts. To enhance the performance of ILP solvers, we propose cutset-based valid inequalities. We present a comparative study on the performance of the different formulations and illustrate the price of reliability.

Chapter 4 investigates on determining feasible radio configurations for microwave wireless backhaul, focusing on power efficiency. We introduce an exact mathematical formulation for this problem and propose a piecewise linear convex function that provides a good approximation of the power utilization on the links. We present a relaxation of the exact formulation and heuristic algorithms to produce feasible radio configuration solutions. Our models are validated through extensive experiments that are reported and discussed.

Chapter 5 presents a preliminary study of different mathematical formulations related to the power-efficient configuration problem. We provide several refinements to the previous formulations aiming at reducing the execution time of the problem solving. In addition, we implement a lagrangian relaxation to this problem and present a Benders' decomposition based on constraint generation.

Chapter 6 is devoted to the general conclusion and perspectives of this thesis. Along with the final remarks of our work, we discuss some remaining challenges in wireless microwave backhaul networks that we envisage as future research.

Appendix A focuses on a different research work with which we have been involved during the PhD program. It covers the routing reconfiguration problem through a game played on digraphs. In this game, we study the tradeoff between two conflicting parameters: the total number of interruptions and the maximum number of simultaneous interruptions. We show that minimizing one of these parameters while the other is constrained is NP-complete. We also prove that there exist digraphs for which minimizing one of these parameters arbitrarily impairs the quality of the solution for the other one. Conversely, we exhibit classes of digraphs for which good tradeoffs can be achieved. We finally detail the relationship between this game and the routing reconfiguration problem.

CHAPTER 2

Microwave communications

In this chapter, we first introduce the fundamentals of microwave communications, such as channel capacity, modulation schemes, radio spectrum, link power budget, and fading models. In Section 2.1, we present the basic blocks of a microwave radio system, along with generally accepted assumptions and simplifications concerning microwave communications. In addition, we present some considerations about microwave costs and frequency spectrum, and introduce a performance analysis of microwave radio systems. In Section 2.2, mathematical models for microwave link engineering are contemplated. We present different calculations and models used to predict the availability of a microwave link. The interested reader is also referred to these books on wireless communications [Rap02, Gol05] and microwave transmission [And03, Man09, Leh10]. Finally, in this chapter, we present *3Link*, an optimization tool that we have developed (under the supervision of the SME 3Roam, which distributes the software with its *Wireless Ethernet Starter Kit*) for helping engineers who are faced with designing and planning microwave links.

2.1 Microwave radio system

Microwave, in general, denotes the technology of transmitting information by the use of the radio waves whose wavelengths are conveniently measured in small numbers of centimeters. In the context of this thesis, microwave refers to terrestrial point-to-point digital radio communications[1], usually employing highly directional antennas in clear line-of-sight (LOS) and operating in licensed frequency bands from 6 GHz to 38 GHz[2].

A microwave radio system is a system of radio equipment used for microwave data transmission. A modern microwave radio, based on a split-mount model,

[1]It is important to remember that not all microwave systems are point-to-point. Cellular telephone networks, commercial and government mobile radio systems, and oneway television and radio broadcast systems are all examples of point-to-multipoint microwave networks. Usually, it consists of one or more broad-beam antennas that are designed to radiate toward multiple end-user terminals. [And03, Leh10]

[2]Wireless technology continues to expand the frequency range at which commercially viable communication systems can be built and deployed. Millimeter-wave is a new generation of point-to-point radio communication operating at very high frequencies, typically including 71–76 GHz, 81–86 GHz, and 92–95 GHz. Frequencies up to 300 GHz are also the subject of wireless communications research. [Man09, Leh10]

consists of three basic components: the *indoor unit* (IDU) which performs all digital processing operations, containing the baseband and digital modem circuitry and, optionally, a network processing unit that provides advanced networking capabilities such as routing and load balancing; the *outdoor unit* (ODU) which houses all the radio frequency (RF) modules for converting a carrier signal from the modem to a microwave signal; and the *antenna* used to transmit and receive the signal into/from free space, which is typically located at the top of a communication tower, as illustrated in Figure 2.1. Antennas used in microwave links are highly directional, which means they tightly focus the transmitted and received energy mainly into/from one specific direction. To avoid waveguide losses, the antenna is directly attached to the ODU which, in turn, is connected to the IDU by means of a single coaxial cable. The distance between the indoor and outdoor equipment can sometimes be up to 300 meters. Two microwave radios are required to establish a microwave link (usually operating in duplex mode[3]) between two locations that can be several kilometers apart. It should be noted that a single IDU can support multiple ODUs in a same site and, thus, multiple microwave links between different locations.

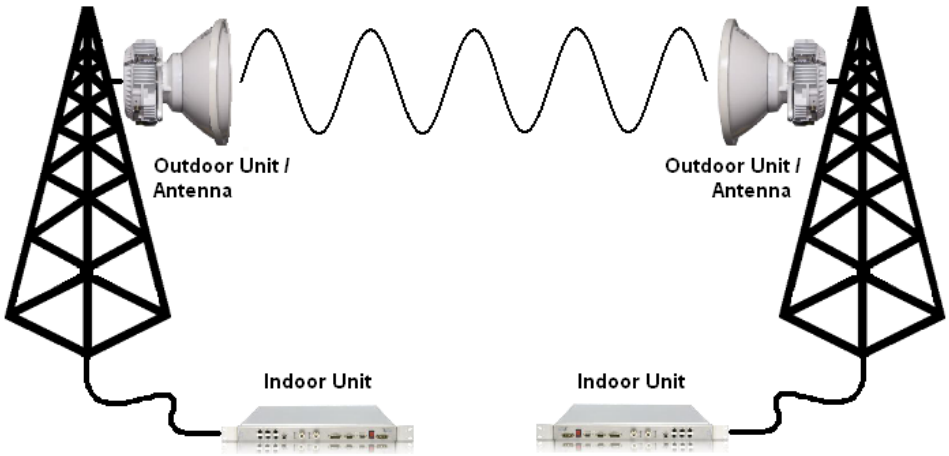

Figure 2.1: A schematic illustration of a microwave link.

In a microwave radio system, communication starts with an information source that can be audio, video, or data in many forms. The IDU accesses a service signal, prompting baseband processing, multiplexing and intermediate frequency (IF) modulation. The signal is then sent to the ODU via coaxial cable for RF processing, before being finally transmitted. The energy radiated by the RF transmitter is amplified by the transmitting antenna before propagating in the form of radio

[3]Duplex operation means that each RF channel consists of a pair of frequencies for the transmit and receive directions, respectively. Both the transmit and receive frequencies are combined onto one antenna using frequency-division duplexing (FDD), where the duplexer provides the coupling of the two signals onto one antenna, and the isolation required to ensure that the transmit signal does not leak through to the receiver [Man09].

waves in the directions determined by the design and orientation of the antenna. As a radio wave travels through the atmosphere, it experiences different propagation phenomena – e.g., free-space loss, reflection, diffraction, and scattering – which negatively impact the perceived energy at the receiving antenna. Besides the transmitted signal, the electromagnetic fields from the interference and noise sources are also converted to power at the RF receiver, likely leading to imprecise interpretation of the transmitted signal. Finally, the RF receiver processes this power in an effort to recover exactly the source information that was originally transmitted.

2.1.1 Capital and operational costs

Microwave generally has lower costs associated with it when compared to copper and fiber lines [Boc09, San09]. As a common solution, self-build microwave involves capital expenditure (CAPEX) and operating expenditure (OPEX). Basically, CAPEX includes the investment in equipment and infrastructure, as well as installation costs. Note that a pair of IDUs, ODUs, and antennas are required to establish one microwave link. The installation costs are closely tied to the site location and equipment dimensions (size of antennas).

Conversely, OPEX comprises the recurrent costs, such as spectrum licenses, tower rentals, maintenance, and energy consumption. As further discussed in this chapter, the spectrum price is usually a function of the amount of the assigned bandwidth. The tower rentals normally represent an important contribution to the total OPEX. However, the operator may also decide for the construction of the communication towers and, in this case, all the cost is associated with the total CAPEX. The maintenance costs are usually assumed to be a percentage of the equipment cost on an annual basis. In addition, we must consider the energy consumption to keep equipment in operation.

Since the conditions differ greatly on a project-by-project basis, it is very difficult to provide even typical information to determine CAPEX and OPEX expenses [Leh10]. An illustrative example is given in Tables 2.1 and 2.2. It should be note that, unlike copper and fiber lines, microwave costs remain relatively distance-insensitive within the range for each deployed link. We want to note also that the energy costs are mainly associated with the operation of IDU (100 W per device) and ODU (60 W per device) equipment. Although energy cost commonly represents less than 5% of the total OPEX of microwave radio systems, the rising demand for energy has yielded a strong social and economical incentive for energy savings in communications networks [GS03].

2.1.2 Radio spectrum

The radio frequency spectrum is a limited natural resource worldwide regulated by the International Telecommunications Union (ITU) [ITU10], an intergovernmental organization whose function is to ensure the rational, equitable, efficient

Table 2.1: Example of capital expenditure for one microwave link.

Item	Quantity	Cost (€)	Total (€)
IDU	2	4,000	8,000
ODU	2	2,500	5,000
Antenna	2	2,500	5,000
Installation	1	5,000	5,000
Total			23,000

Table 2.2: Example of operational expenditure for one microwave link.

Item	Quant.	Cost (€/year)	Total (€/year)
License	2	5,000	10,000
Tower	2	5,000	10,000
Energy	1	500	500
Maintenance	1	1,500	1,500
Total			22,000

and economic use of frequency bands. In conjunction with ITU regulations, national legislation instruments establish the availability of frequency bands for specific applications and the procedures for issuing licenses, as well as the rights and obligations resulting from using the spectrum.

It is important to distinguish two terms related to the radio spectrum utilization: allocation and assignment. Allocation refers to the administration of the radio frequency spectrum performed by the ITU, which sets out its use by one or more communication services. An allocation then is a distribution of frequencies to radio services. Assignment is the authorization given by an administration for a radio station to use a radio frequency under specified conditions. An assignment then is a distribution of a frequency to a given radio station [ICT10].

There are a number of frequency bands that have been allocated throughout the world for use by licensed fixed broadband services. Within the general ITU band designations, individual countries may elect to implement polices, such as those by the Federal Communications Commission (FCC) [FCC10] in the United States, that allow those frequencies to be licensed and used within their country boundaries. In a given band, there may be requirements for maximum radiated power levels, particular efficient modulation types, and even standards for the radiation patterns of directional antennas. These criteria are established to reduce or minimize interference among systems that share the same spectrum, and to ensure that the spectrum efficiency is sufficiently high to justify occupying the spectrum [And03].

Therefore, obtaining a license (assignment) is a highly specialized task requiring a tremendous amount of engineering and a careful review and functional understanding of the administrative rules that govern the use of the intended licensed spectrum space. In addition, frequency spectrum licenses are normally subject to renewal upon payment of renewal fees. Administrative methods of setting spectrum prices are increasingly being supplemented by the use of market-based methods for determining spectrum prices [ICT10].

The major policy objective for spectrum pricing is that it should be done in a way which promotes spectrum efficiency. Spectrum efficiency does come with a cost and the spectrum manager should attempt to find an optimal cost/benefit tradeoff. Secondly, use of the spectrum provides considerable benefit to the national and regional economies, and this benefit should be maximized. Next, managing radio frequency spectrum costs money and, as a principle, those who benefit from the use of the spectrum should be the ones to pay these costs [ICT10].

In practice, the price of a frequency spectrum for microwave communications is usually a function of the amount of spectrum (bandwidth) with which a license is associated, but it may also vary according to the frequency band to reflect the level of congestion, the market demand and the relative cost of deploying network infrastructures. In some countries, the spectrum is sold to an operator, either by auction or by competitive tender. Because of specific differences from country to country, a comprehensive tabulation of spectrum prices is beyond the scope of this thesis. As an illustrative instance, in France, the annual renewal fee R in euro can be determined by [ARC07]:

$$R = l \cdot bf \cdot lb \cdot es \cdot K \tag{2.1}$$

where

$$\begin{aligned} R &= \text{the annual renewal fee (€)} \\ l &= \text{channel bandwidth (MHz)} \\ bf &= \text{factor related to the frequency} \\ lb &= \text{factor related to the frequency and other technical criteria} \\ es &= \text{factor related to the frequency and other technical criteria} \\ K &= \text{reference value (€/ MHz)} \end{aligned}$$

For example, the annual renewal fee for a bandwidth of 7 MHz at the 8 GHz frequency band is about €1,800, while for a bandwidth of 28 MHz at the same frequency band is about €7,000.

2.1.3 Performance analysis

The performance analysis of microwave radio systems involves detailed knowledge of the physical channels through which the data is transmitted. Traditionally, it is focused on computing signal levels at the receiver [Rap02, Leh10], and the

first step is the link power budget (See Section 2.2). The result is an estimation of the signal-to-noise ratio (SNR) value, from which we can obtain some implications in terms of channel capacity and bit error rate (BER). Given the assigned channel bandwidth B and the signal-to-noise ratio value S/N, expressed as a linear power fraction, we can determine an upper bound for the channel capacity C, in bits per second (bps), assuming that the BER approaches zero when the data transmission rate is below the channel capacity, according to Shannon's capacity theorem [Sha48]:

$$C[bps] = B[Hz] \cdot \log_2 \left(1 + \frac{S[W]}{N[W]}\right) \tag{2.2}$$

The degree to which a microwave radio system can approximate this limit depends on receiver noise and modulation techniques [ZP00]. The receiver noise is generated by components used to implement the communication system, and it is closely tied to the bandwidth. The receiver noise can be calculated by:

$$N = kTB \tag{2.3}$$

where

$$\begin{aligned} N &= \text{receiver noise (W)} \\ k &= \text{Boltzman's constant } (1.38 \times 10^{-23}\ \text{J/K}) \\ T &= \text{system temperature (usually assumed to be 290 K)} \\ B &= \text{bandwidth (Hz)} \end{aligned}$$

Other sources of noise may arise externally to the system, such as electrical noise from industry machinery and interference from other users of the radio channel[4].

With regard to the modulation technique, there are several features that influence the preference for some modulation scheme, such as bandwidth efficiency and power efficiency. These requirements are conflicting, and existing modulation schemes do not simultaneously perform both of them. Power efficiency describes the ability of the system to reliably send information at the lowest practical power level. Bandwidth efficiency describes the ability of a modulation scheme to accommodate data within a limited (as small as possible) bandwidth. The most power-efficient modulation methods, like binary phase shift keying (BPSK) and quadrature phase shift keying (QPSK), present a rather modest bandwidth efficiency. Since spectrum is a very expensive and highly regulated commodity (as previously discussed in Subsection 2.1.2), good bandwidth efficiency with low BER is a priority for designers of microwave radio systems [And03, Man09, Leh10].

The most commonly used modulation method for microwave radio systems is quadrature amplitude modulation (QAM), which employs a combination of am-

[4]Noise is usually differentiated from interference in that it may not be identifiable to a given source and does not carry any useful information. Interference generally refers to identifiable man-made transmissions [And03].

plitude and phase techniques[5]. Instead of transmitting one bit at a time, two or more bits are transmitted simultaneously according to the QAM scheme in use. An m-QAM scheme presents m different combinations of amplitude and phase, each one representing a n-bit pattern called a symbol (with $n = \log_2 m$ and integer). In practice, given the assigned channel bandwidth B and the m-QAM scheme in use, we can determine the channel capacity C by:

$$C[bps] = n \cdot B[Hz] \tag{2.4}$$

where $n = \log_2 m$. To increase bandwidth efficiency, symbols that convey more information bits are required. For example, 16-QAM is more bandwidth-efficient than 4-QAM (most known as QPSK). However, since the constellation states are closer together (see Figure 2.2), high-level QAM schemes (e.g., 16-QAM) are more susceptible to errors due to noise, interference, and channel impairments than low-level QAM schemes (e.g., QPSK). In fact, for a given transmitting power, it becomes increasingly difficult to correctly detect which signal state has been transmitted as the number of symbol states increases. Hence, as a higher modulation technique is used, a better SNR value is needed to maintain an acceptable BER level (typically 10^{-6}). Figure 2.3 shows the theoretical capacity (given by Shannon's theorem) and the practical bitrate (using QAM schemes), as a function of the SNR value given in dB, achieved for a typical microwave link using 28 MHz of bandwidth. In Table 2.3, we present the bandwidth efficiency, the SNR requirement (BER 10^{-6}), along with the channel capacity for different QAM schemes.

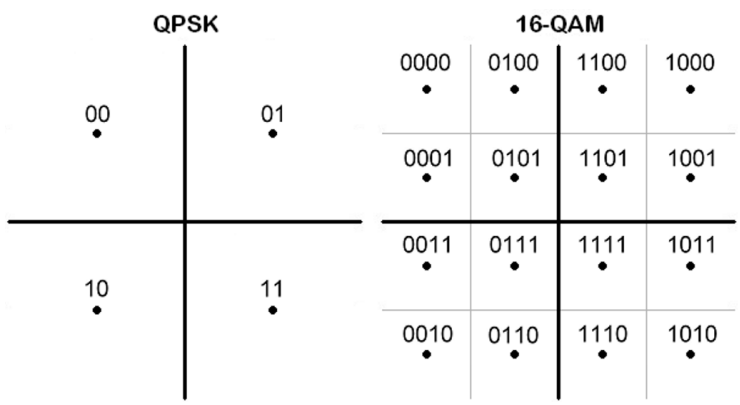

Figure 2.2: The rectangular representation for QPSK and 16-QAM constellations.

[5]A radio wave has three fundamental characteristics – frequency, amplitude, and phase – which can be modulated individually or in combination to convey information [Rap02, And03, Leh10].

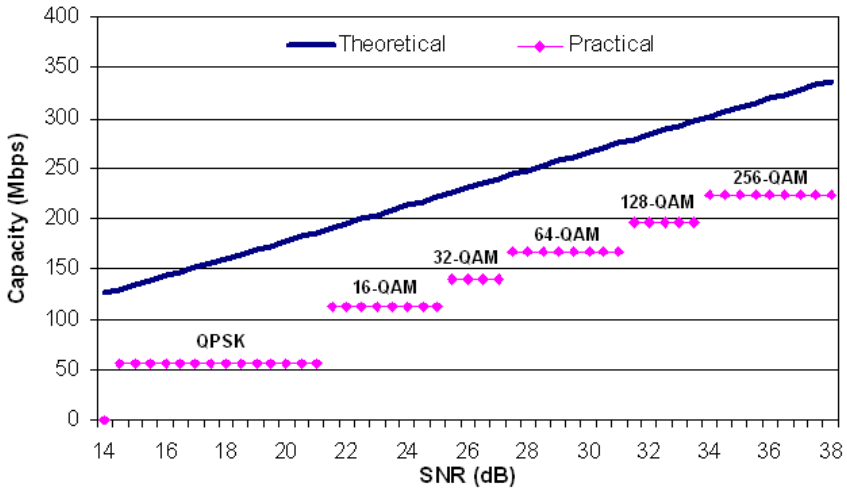

Figure 2.3: Theoretical capacity versus practical bitrate.

Table 2.3: Bandwidth efficiency and SNR requirement for different QAM schemes.

Modulation scheme	Bandwidth efficiency	SNR requirement	Capacity for 7 MHz	Capacity for 28 MHz
QPSK	2 bps/Hz	14.21 dB	14 Mbps	56 Mbps
16-QAM	4 bps/Hz	21.02 dB	28 Mbps	112 Mbps
32-QAM	5 bps/Hz	25.24 dB	35 Mbps	140 Mbps
64-QAM	6 bps/Hz	27.45 dB	42 Mbps	168 Mbps
128-QAM	7 bps/Hz	31.10 dB	49 Mbps	196 Mbps
256-QAM	8 bps/Hz	33.78 dB	56 Mbps	224 Mbps

2.2 Link power budget

The design process of a microwave radio system makes use of many mathematical models to predict the system operation before it is actually built. These models are based on highly accurate measurements, as well as on imprecise prediction of the signal levels at the receiver [And03, Leh10]. In the sequence, along with the basic terminology, we present the models used to assess performance and availability of microwave radio systems.

2.2.1 Basic terminology

Transmitter output power. This is the RF power of the link transmitter on the transmission channel, usually expressed in dBm (dB relative to one milliwatt). Normally, the link is operated with the maximum possible transmitter power, according to the link operating frequency and modulation scheme. However, it is a

good practice to keep some power reserve available to flexibly respond to fade or interference from other links.

Circulator loss. Normally, the output of a transmitter is combined with the receiver input when the transmitter and receiver share the same antenna. This duplexing device has some loss associated with it. This loss value in dB is obtained from the equipment manufacturer.

Line loss. This is the loss in dB from the transmission line connecting the transmitter with the antenna (or the antenna with the receiver). This loss depends on the waveguide type and length.

Connector loss. This is the loss in dB introduced by the use of connectors between transceivers devices, transmission lines, and antennas. This loss depends on the quantity and the quality of the connectors that are used.

Antenna gain. The antenna gain value, usually given in dBi (dB relative to an isotropic radiator), is obtained from the antenna manufacturer. It depends on the antenna type and link operating frequency. The antenna is one of the link system elements that the design engineer can change to improve link performance.

Antenna radome loss. Special covers for antennas called radomes are available to protect the horn feed and reduce the wind loading on the tower. The radome cover on the antenna introduces some loss. This loss value in dB is obtained from the antenna manufacturer.

Antenna polarization. Polarization is a physical phenomenon of radio signal propagation and refers to the orientation of the electric field vector in the radiated wave. It is related to the construction and orientation of the antenna and impacts the link availability in rain fading conditions.

Effective radiated power. This is the sum of the transmitter output power and transmitter antenna gain minus the losses from the circulator, waveguide, and radome. It is normally expressed in dBm.

Frequency. This is the operating frequency of the link, usually expressed in MHz. Normally, the nominal center frequency of the channel is used to find the path loss.

Bandwidth. This is the frequency range occupied by a modulated carrier wave to transmit the data.

Path length. This is the distance, usually expressed in km, from the transmitting antenna to the receiving antenna.

Free space path loss. This is the loss in signal strength, normally expressed in dB, that occurs when an electromagnetic wave travels over a line of sight path in free space.

Atmospheric absorption loss. This is the total atmospheric absorption loss along the link path. This loss, usually expressed in dB, depends on the path length and link operating frequency.

Total path loss. This is the sum of the free space and other loss factors along the path, expressed in dB.

Received signal level. This is the signal strength, usually measured in dBm, at the input of the radio receiver.

Receiver sensitivity. This is the minimum signal strength, expressed in dBm, at the input of the radio receiver required to perform a specific BER (normally 10^{-6}). It depends on the equipment manufacturer and the modulation scheme.

Fade margin. This is the difference, measured in dB, between the received signal level and the receiver sensitivity. This is an important result for the link availability calculations and one of the ultimate results of the link budget calculation.

Receiver noise. This is the noise generated by thermal agitation of electrons in a conductor, expressed in dBm. It depends on channel bandwidth and system temperature (usually assumed to be 290 K).

Signal-to-noise ratio. This is the ratio, usually measured in dB, between the received signal level and the receiver noise.

Required SNR. This is the SNR value needed at the input of the radio receiver to achieve a specific BER (normally 10^{-6}). This value is found on the equipment specifications for each modulation scheme.

Link availability. This represents the probability that the BER is at or below a given quality threshold level (normally 10^{-6}). Conversely, an outage is the time when the link is not available. It can occur for a variety of reasons, including multipath fades, rain fades, and equipment failures.

2.2.2 Power budget calculations

The microwave link design starts with a link power budget, i.e., a calculation involving the gains and losses associated with the antennas, transmitters, receivers, transmission lines, as well as the signal attenuation due to propagation in order to obtain the mean signal level (and other related parameters) at the receiver. These values can then be used to assess the availability of the link under a variety of fading mechanisms. For a microwave link in clear line-of-sight, a power budget equation might look like this:

$$P_{RX} = P_{TX} - L_{TX} + G_{TX} - L_{PL} + G_{RX} - L_{RX} \tag{2.5}$$

where

$$\begin{aligned}
P_{RX} &= \text{received signal level (dBm)} \\
P_{TX} &= \text{transmitter output power (dBm)} \\
L_{TX} &= \text{transmitter losses (circulator, line, connectors, radome) (dB)} \\
G_{TX} &= \text{transmitter antenna gain (dBi)} \\
L_{PL} &= \text{total path loss (free space, absortion) (dB)} \\
G_{RX} &= \text{receiver antenna gain (dBi)} \\
L_{RX} &= \text{receiver losses (circulator, line, connectors, radome) (dB)}
\end{aligned}$$

For a line-of-sight microwave radio system, the primary source of loss is the decrease of the signal power due to uniform propagation, proportional to the inverse square of the distance. The free space path loss equation can be written as follows:

$$L_{PL} = 32.44 + 20 \cdot \log_{10}(f) + 20 \cdot \log_{10}(d) \tag{2.6}$$

where

$$\begin{aligned}
L_{PL} &= \text{free space path loss (dB)} \\
f &= \text{frequency (MHz)} \\
d &= \text{path length (km)}
\end{aligned}$$

The received signal level P_{RX} can be used to assess other important parameters, such as the signal-to-noise ratio and fade margin. As previously discussed, the SNR value is a determinant of the channel capacity. The fade margin, in turn, is used to calculate the link availability under fading conditions. Fading is a broad term that is applied to a wide range of variations observed in the signal amplitude, phase, and frequency characteristics [And03]. Fading phenomena are described in statistical terms, and the probability of fades of a particular magnitude can be evaluated through analytical techniques [Bar72, Vig75, Cra80, Cra96], from which we can estimate the probability of outage and hence the link availability.

2.2.3 Vigants–Barnett model

The Vigants–Barnett method is a multipath fading model based on the published work of two microwave system researchers at AT&T Bell Labs [Bar72, Vig75]. This work used both analytical and experimental data to create semiempirical equations for fade depth probability for the received signal. This model was specifically created for fade depths greater than 15 dB, i.e., deep fades. The average probability of a fade of depth A using this method is given by:

$$P_F = 6.0 \times 10^{-10} C f d^3 10^{\frac{-A}{10}} \tag{2.7}$$

where

$$\begin{aligned} P_F &= \text{probability of a fade as a fraction of time} \\ d &= \text{path length (km)} \\ f &= \text{frequency (MHz)} \\ C &= \text{propagation conditions factor} \\ A &= \text{fade depth (dB)} \end{aligned}$$

The propagation conditions factor C is selected on the basis of the type of environment in which the link is to operate. There exist maps that provide an indication of the appropriate C factor for the area where the link will be deployed [And03].

2.2.4 Crane rain fade model

The Crane rain method [Cra80, Cra96] is used to predict the attenuation by rain on terrestrial propagation path. The degree of attenuation due to rain is a function of the rain intensity or rain rate. Rain rates are given in terms of the probability that the average millimeters of rain that fall over an hour will be exceeded. Calculating the outage is an iterative process that is based on the calculation of the attenuation. The rain attenuation is calculated by the Crane method as follows:

$$A_R = kR_p^\alpha \left(\frac{e^{\mu\alpha d} - 1}{\mu\alpha} - \frac{b^\alpha e^{c\alpha d}}{c\alpha} + \frac{b^\alpha e^{c\alpha D}}{c\alpha} \right) [dB], d \leq D \leq 22.5\text{km} \tag{2.8}$$

$$A_R = kR_p^\alpha \left(\frac{e^{\mu\alpha D} - 1}{\mu\alpha} \right) dB, D < d \tag{2.9}$$

where

$$
\begin{aligned}
b &= 2.3R_p^{-0.17} \\
c &= 0.026 - 0.03\ln(R_p) \\
d &= 3.8 - 0.6\ln(R_p) \\
\mu &= \ln(be^{cd})/d \\
R_p &= \text{rain rate (mm/h)} \\
D &= \text{path length (km)} \\
k, \alpha &= \text{regression coefficients w.r.t frequency and polarization}
\end{aligned}
$$

The rain rate values in mm/h are directly related to the geographical area where the link will operate. There exist maps and tables that provide an indication of the appropriate rain rate values for the area where the link will be deployed [And03]. To find the rain outage percentage with the Crane rain model, A_R is iteratively calculated with increasing rain rates for the appropriate zone until the value of rain attenuation A_R equals the fade margin. The percentage of time corresponding to that rain rate is the rain outage percentage P_R.

For path lengths greater than 22.5 km, the calculation is done for $D = 22.5$ km and the final adjusted outage probability is calculated as:

$$P_R = P_{22.5}\left(\frac{D}{22.5}\right) \tag{2.10}$$

where P_R is the final rain outage percentage and $P_{22.5}$ is the rain outage percentage for a path length of 22.5 km. The annual outage probability may be multiplied by the number of seconds in a year to yield the total number of seconds per year that the link is unavailable because of rain outages.

2.3 *3Link*

The design of microwave radio systems commonly makes use of software tools that implement appropriate and widely accepted propagation prediction models. Most microwave design tools are developed by radio manufacturers and therefore are typically biased toward the manufacturers' own equipment. Many commercial tools, such as Pathloss 5.0, are also available upon purchase. These tools basically calculate the performance of a given configuration and, finally, determine whether it meets the client's objectives. If the modelling process shows that the system performance is inadequate, then the configuration can be adjusted until the predicted performance meets the service objectives (if possible), what can take several iterations.

SME 3Roam decided to develop its own software tool, *3Link*, that is provided with its Wireless Ethernet Starter Kit. The main advantage of *3Link* lies in the fact that, besides implementing the classical link power budget to assess the microwave link performance and availability, it determines the different configura-

tions available for the microwave link to be deployed according to customers requirements. Essentially, *3Link* helps microwave link engineers to answer these following questions:

1. Will the microwave link transmit data fast enough for the user?
2. Will the microwave link be reliable enough for the user?
3. Which configurations will be available for the microwave link?

2.3.1 Models, input and output

The performance predictions obtained by *3Link* are intrinsically related to the models, calculations, and data used to perform such predictions. *3Link* implements the widely accepted propagation models and calculations, discussed in this chapter, that are used to predict LOS paths for anywhere in the world. With respect to the data, much information was obtained from technical specifications of radio equipment and precise parameters available in the literature [And03, Man09, Leh10]. Radio equipment parameters, frequency and channel tables, antenna models, and so on are defined in XML and stored in the parameters database for easy retrieval.

Input. The basic input data are parameters related to the scenario and required performance targets for the new microwave link to be deployed (See Figure 2.4). Some of them are informed by the user, while others are retrieved from the *3Link* database. The parameters entered by the user are:

- The path length between the communication sites;
- The requirements in terms of capacity;
- The requirements in terms of availability;
- The band frequency for the microwave link;
- The set of antennas available and polarization;
- The geographic region for the microwave link;
- The lines and connectors used to interconnect radio equipment.

Then, *3Link* can determine other parameters, such as the set of bandwidth choices according to the frequency, the set of modulation schemes depending on the frequency and bandwidth, and the applicable range of output power for each frequency, bandwidth and modulation combination.

Output. The basic output computed by *3Link* are all valid configurations for the new microwave link (See Figure 2.5). Each configuration consists of the choice of antennas, bandwidth, modulation scheme, and output power. In addition, for each valid configuration, *3Link* presents a performance summary that shows how well the microwave link is predicted, as follows:

- The receiver noise value;
- The total path loss;
- The received signal level;
- The signal-to-noise ratio;
- The fade margin value;
- The link's capacity;
- The link's availability.

Models. The *3Link* flowchart diagram is illustrated in Figure 2.6. For each configuration (antenna, bandwidth, output power, modulation, etc) *3Link* first performs the noise (Equation (2.3)), path loss (Equation (2.6)), and power budget (Equation (2.5)) calculations, from which we can estimate the received signal level and receiver noise. The signal level is used to compute the SNR (which depends on receiver noise) and fade margin. According to the SNR requirements (Table 2.3) and the estimated SNR value, we can determine which modulations are available and, thus, the link's capacity (Equation (2.4) multiplied by an encoding factor less than 1). The fade margin is used to compute the link's availability (Vigants–Barnett and Crane models). Finally, *3Link* determines which configurations successfully meet the performance requirements.

2.3.2 About *3Link*

All mathematical models and calculations were implemented by Napoleão Nepomuceno from Mascotte team. The interfaces and layouts were conceived by Sebastien Martagex from SME 3Roam. This work has been supervised by Simon Bryden from SME 3Roam.

2.4 Conclusion

In this chapter, we presented the main considerations related to the technical task of conceiving a microwave link. Along with the fundamentals of wireless communications and the basic blocks of microwave radio systems, we introduced *3Link*, an optimization tool that we have developed for the designing and planning of microwave links. This work, developed under SME 3Roam supervision, represents

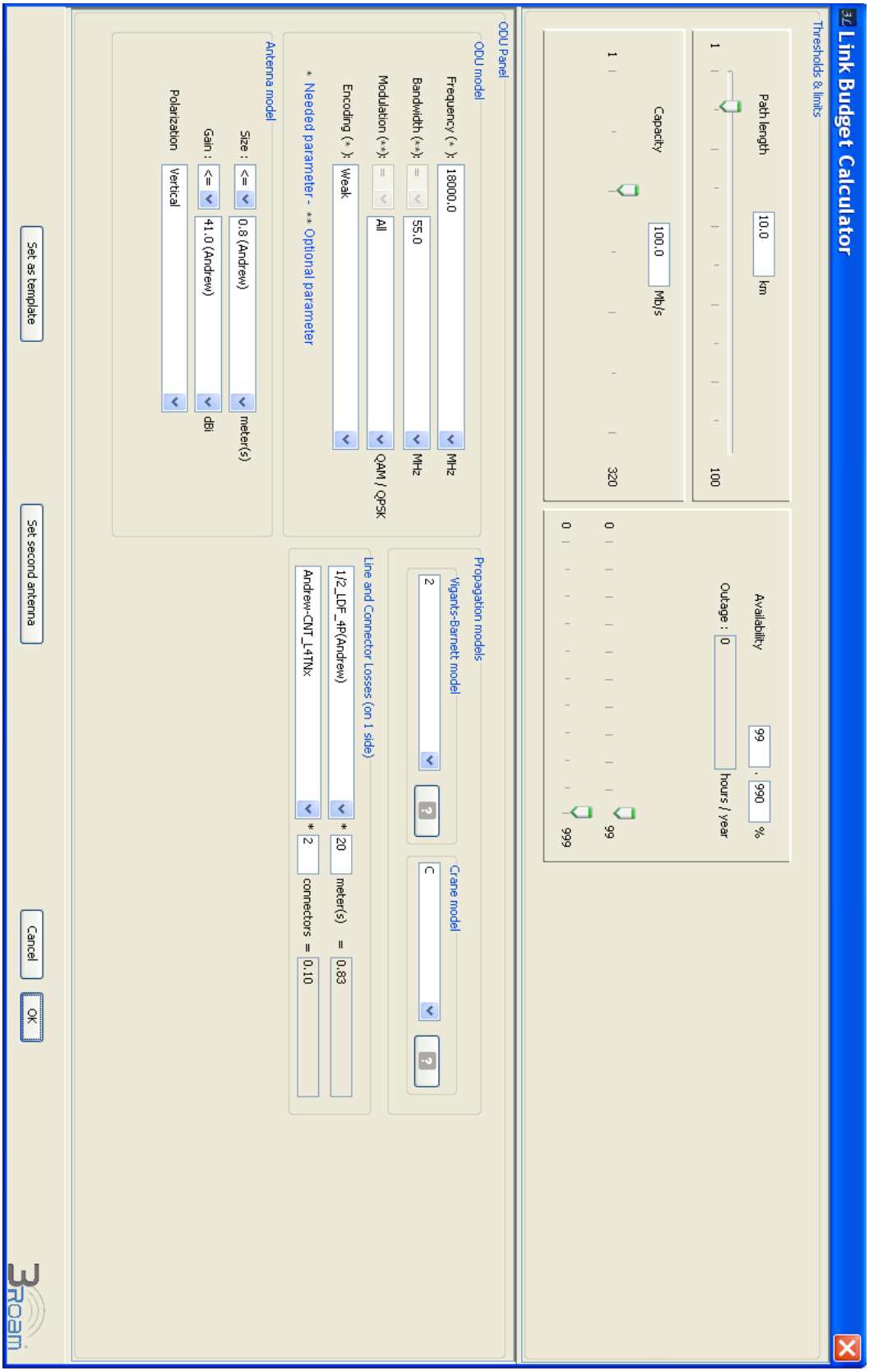

Figure 2.4: *3Link* input screen: scenario and performance parameters.

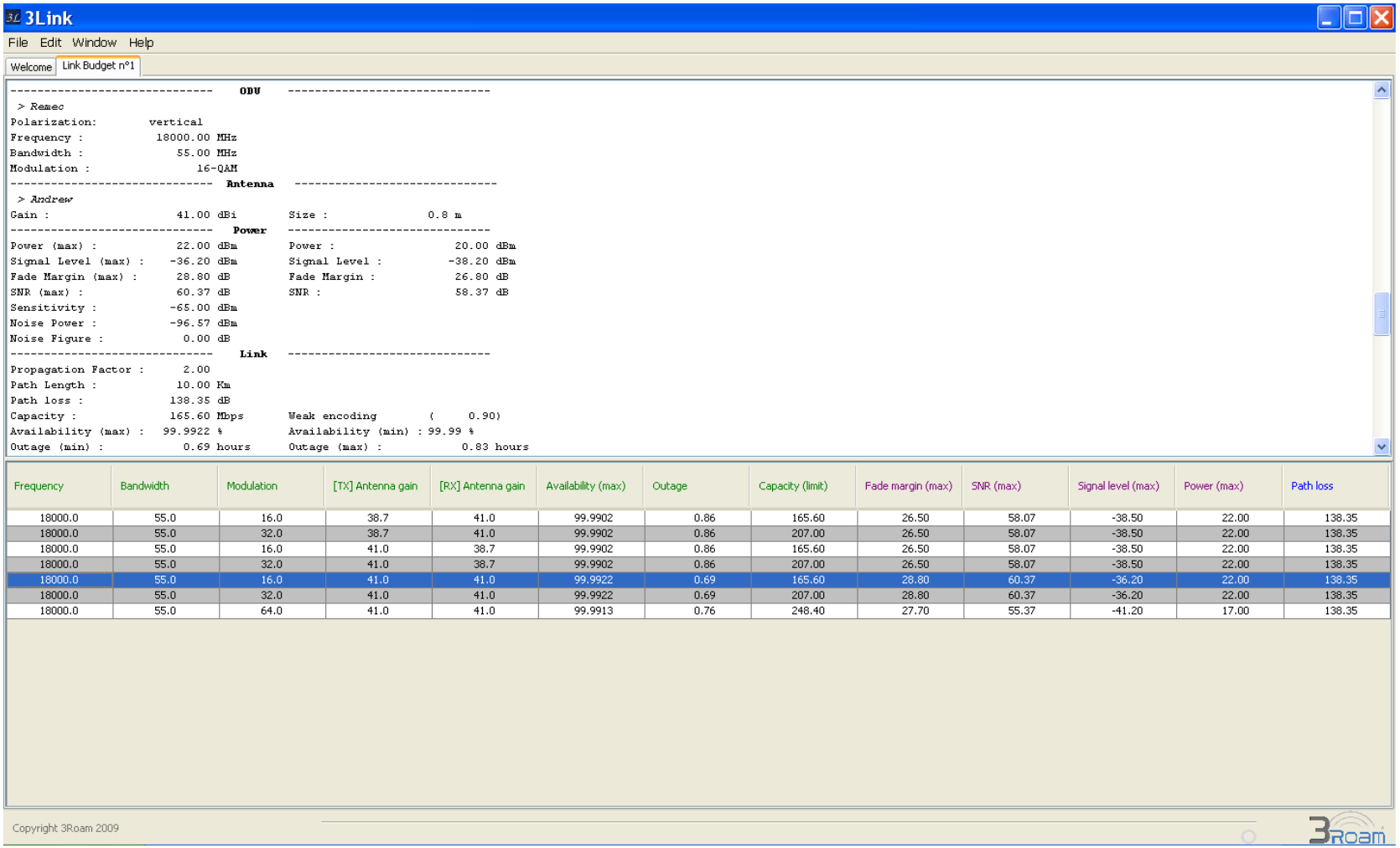

Frequency	Bandwidth	Modulation	[TX] Antenna gain	[RX] Antenna gain	Availability (max)	Outage	Capacity (limit)	Fade margin (max)	SNR (max)	Signal level (max)	Power (max)	Path loss
18000.0	55.0	16.0	38.7	41.0	99.9902	0.86	165.60	26.50	58.07	-38.50	22.00	138.35
18000.0	55.0	32.0	38.7	41.0	99.9902	0.86	207.00	26.50	58.07	-38.50	22.00	138.35
18000.0	55.0	16.0	41.0	38.7	99.9902	0.86	165.60	26.50	58.07	-38.50	22.00	138.35
18000.0	55.0	32.0	41.0	38.7	99.9902	0.86	207.00	26.50	58.07	-38.50	22.00	138.35
18000.0	55.0	16.0	41.0	41.0	99.9922	0.69	165.60	28.80	60.37	-36.20	22.00	138.35
18000.0	55.0	32.0	41.0	41.0	99.9922	0.69	207.00	28.80	60.37	-36.20	22.00	138.35
18000.0	55.0	64.0	41.0	41.0	99.9913	0.76	248.40	27.70	55.37	-41.20	17.00	138.35

Figure 2.5: *3Link* output screen: configurations and performance summary.

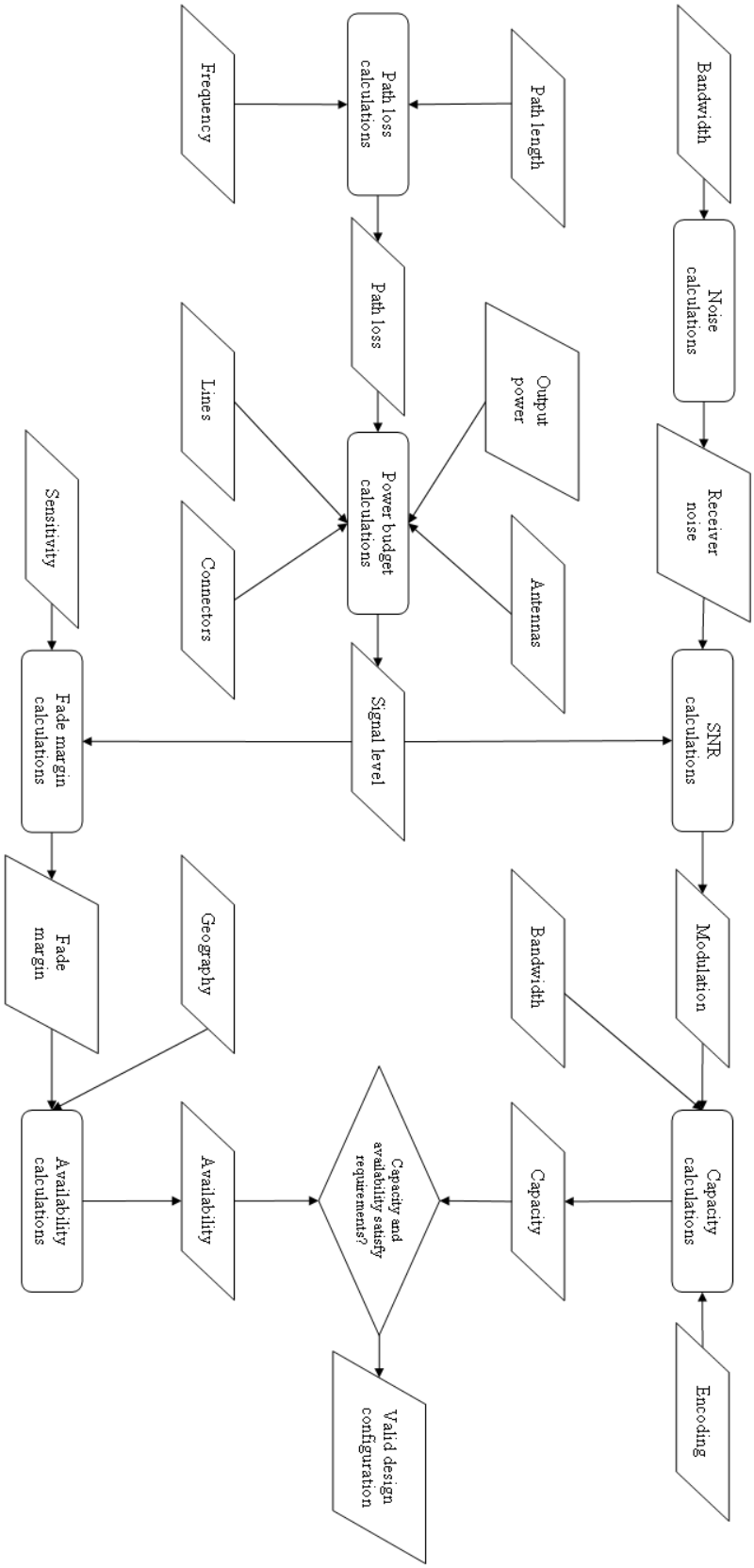

Figure 2.6: *3Link* flowchart diagram.

an important contribution of this thesis, and the effort devoted to it has provided an indispensable technical background used throughout this thesis.

The methods and analyses presented in this chapter are also used for designing microwave backhaul networks, and it would be very interesting to conceive a complete network design tool driven by technical constraints – e.g., LOS considerations, sites locations, frequency availability, etc – and performance criteria – e.g., network CAPEX and OPEX costs, traffic requirements, network reliability, etc – for determining network topology and configuration solutions. In general, the optimization problems involved in this task are NP-hard [Dar07]. From a technical viewpoint, these problems also present high complexity [HART10].

In the following chapters, we focus on two different optimization problems related to the planning and configuration of microwave backhaul networks. We consider the main parameters (e.g., channel bandwidth, modulation scheme, and transmission power) that determine the capacity of a microwave link and impact the network costs (e.g., renewal fees of licenses and power utilization), while regarding different scenarios of optimization.

CHAPTER 3

Bandwidth assignment for reliable backhaul

In this chapter, we investigate on conceiving reliable microwave backhaul networks under outage probability constraints. We introduce a joint optimization of data routing and bandwidth assignment that minimizes the total renewal fees of licenses, while handling all the traffic requirements simultaneously with a prescribed reliability level. It can be seen as a special case of the minimum cost multicommodity flow (MCMCF) with discontinuous step increasing cost functions on the links [Ken78, Min06]. In addition, we must consider probabilistic constraints to deal with random parameters (viz., modulation schemes) that impact the capacity of microwave links.

We then propose a (joint) chance-constrained mathematical programming approach to tackle this problem. Chance-constrained programming aims at finding the best solution remaining feasible for a given infeasibility probability tolerance. This approach is still considered as very difficult and widely intractable since the feasible region defined by a probabilistic constraint generally is not convex. In addition, among the vast literature on chance-constrained programming, few research work has been carried out to tackle combinatorial problems [Klo10, LAN10]. Given these difficulties, we derive an equivalent ILP formulation for the case where the outage probabilities of the microwave links are independent and propose cutset-based valid inequalities to obtain strengthened formulations for this problem.

The remainder of this chapter is organized as follows. In Section 3.1, we present the context and motivation of this study. In Section 3.2, we give a brief introduction to chance-constrained programming. In Section 3.3, we introduce exact formulations for the application considered here. Section 3.4 is devoted to cutset-based valid inequalities to improve these formulations. In Section 3.5, we discuss preliminary computational results illustrating the price of reliability and present a comparative study on the performance of the different formulations. In Section 3.6, some final remarks and comments on future work conclude the chapter.

3.1 Context and motivation

As previously discussed in Chapter 2, the design of wireless networks differs fundamentally from wired network design. First, the radio frequency spectrum is a

limited natural resource which has been regulated worldwide to promote its efficient use. Second, the radio channel is a random and difficult communication medium. Actually, environment conditions can introduce instantaneously variations into the communication channel, likely leading to outage events. Therefore, capacity planning for wireless microwave backhaul requires additional reliability investigation.

In a single microwave link design, a basic calculation of the link's performance can be used to determine whether it meets the required service and reliability. Essentially, the link availability under fading conditions can be determined from the fade margin derived from the link budget. However, determining the reliability of a network with several microwave links is a much more difficult task. In fact, the overall system's reliability is not just a function of the availability of single links, but it also depends on the network capacity and data connections to be established.

The capacity of microwave links is basically determined by the channel bandwidth and the modulation scheme used to transmit data. On the one hand, the assigned bandwidth for each link is a network engineer's decision subject to obtaining licenses upon payment of renewal fees whose values are usually in accordance with the amount of spectrum (e.g., in MHz) with which a license is associated. The amount of spectrum is generally available in modules, resulting in discontinuous step increasing cost functions on the links.

On the other hand, in response to channel fluctuations, we assume that the modulation scheme is a random factor. In fact, to overcome outage events, modern wireless communication systems employ adaptive modulation which has been shown to considerably enhance radio link performance [GC97, GC98]. Adaptive modulation refers to the automatic modulation (and other radio parameters) adjustment that a wireless system can make to prevent weather-related fading from causing communication on the link to be disrupted.

Since communication signals are modulated, varying the modulation also varies the amount of traffic that is transferred per signal. Therefore, in order to keep the quality of the communication in terms of BER, this technique entails the variability of the links' capacity, as shown in Figure 3.1. For instance, 256-QAM modulation can deliver approximately four times the throughput of QPSK.

Microwave backhaul solutions, although having limited bandwidth and suffering channel impairments, must degrade gracefully as environment conditions degrade. As a common practice, backhaul operators highly overprovision bandwidth during capacity planning to avoid traffic bottlenecks under adverse scenarios (when the performance of some links deteriorates). This approach, however, incurs additional investments that do not result in resource- and cost-efficient networks, besides leading to the inefficient use of the radio spectrum.

Therefore, establishing better wireless backhaul solutions is not just a matter of adding bandwidth, but it also entails a complex decision aiming at enhancing network reliability to cope with channel fluctuations.

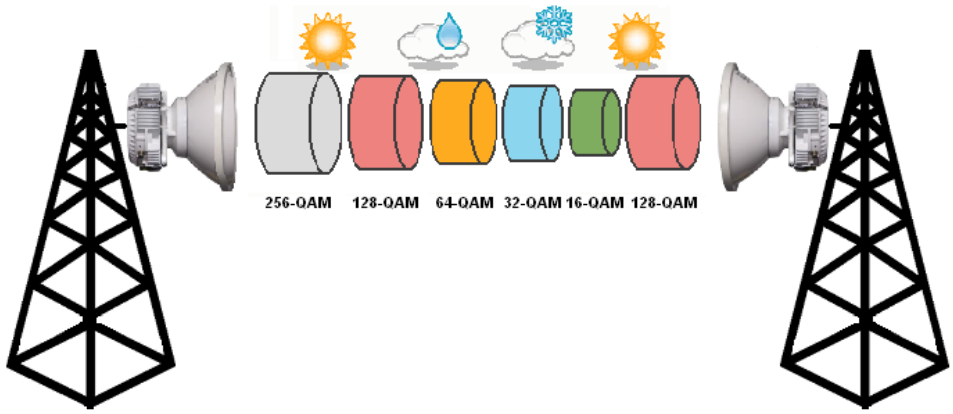

Figure 3.1: Adaptive modulation for a microwave link.

3.2 Chance-constrained programming

Chance-constrained programming appears as a specific model of stochastic optimization for dealing with random parameters in optimization problems. These random parameters take part of the inequalities, and sometimes of the objective function as well, describing the proper working of the system under consideration. Chance-constrained programming remains one of the main challenges of modern stochastic programming. The main difficulty of such models is due to optimal decisions that have to be taken prior to the observation of random parameters.

Chance-constrained programming is suitable when one can hardly find any decision which would definitely exclude later constraint violation caused by unexpected random effects. Actually, there exist situations where constraint violation can almost never be avoided because of unexpected extreme events. When knowing or approximating the distribution of the random parameters, it makes sense to call decisions feasible (in a stochastic meaning) whenever they are feasible with high probability (i.e., only a low percentage of realizations of the random parameters leads to constraint violation under this fixed decision). This can be expressed in terms of chance constraints (or probabilistic constraints). The constraints

$$\mathcal{P}(h_j(x,\zeta) \geq 0) \geq 1 - \varepsilon, j \in \mathcal{J} \tag{3.1}$$

are called separate chance constraints, while the constraint

$$\mathcal{P}(h_j(x,\zeta) \geq 0, j \in \mathcal{J}) \geq 1 - \varepsilon \tag{3.2}$$

is called a joint chance constraint, where

$$
\begin{aligned}
\mathcal{P} &= \text{probability measure} \\
x &= \text{vector of decision variables} \\
\zeta &= \text{vector of random parameters} \\
h(x,\zeta) \geq 0 &= \text{finite system of inequalities} \\
\mathcal{J} &= \text{index set of the inequalities} \\
\varepsilon &= \text{infeasibility tolerance} \in [0,1]
\end{aligned}
$$

We require that $h_j(x,\zeta) \geq 0$ (or $h(x,\zeta) \geq 0$) shall hold at least with some prescribed probability $1-\varepsilon \in [0,1]$, rather than for all possible realizations of ζ. The value ε is chosen by the decision maker in order to model the reliability requirements. Note that the former formulation (separate chance constraints) does not ensure reliability of the solution as a whole. Usually, the infeasibility tolerance is strictly fixed with a low value (e.g., ε=0.01,0.05). Of course, lower values of ε lead to fewer feasible decisions x in (3.1) or (3.2), hence to optimal solutions at higher costs. Fortunately, it turns out that usually ε can be decreased over quite a wide range without affecting too much the optimal value of some problem, until it closely approaches zero and then a strong increase of costs becomes evident, or even feasible solutions do not exist. In this way, models with chance constraints can also give a hint to a good compromise between costs and reliability of the solutions.

Bibliography on chance-constrained programming can be found in books about stochastic programming [Pré95, ASR09]. An introduction to chance-constrained programming is also available at the Stochastic Programming Community home page [COS10]. In what follows, we introduce a (joint) chance-constrained mathematical programming approach to conceive reliable microwave backhaul networks.

3.3 Mathematical formulations

In this section, we first study the optimization problem of bandwidth assignment with a separate chance constraint for every microwave link and afterwards the joint chance-constrained model. We assume in both models that, for each link and bandwidth, the modulation choice is associated with a random variable whose discrete probability distribution is known (on the basis of analytical or statistical studies).

3.3.1 Separate chance constraints

This problem can be formally stated as follows. The network's topology is modelled as a digraph $G = (V, E)$, where each node $v \in V$ denotes a base transceiver station and each arc $uv \in E$ represents a microwave link from u to v, with $u, v \in V$

and $u \neq v$. Let $\delta^+(v)$ denote the set of outneighbors of v and $\delta^-(v)$ the set of inneighbors of v. Let W_{uv} be the number of bandwidth choices available for arc $uv \in E$. Each bandwidth b^w_{uv}, for $w = 1, \ldots, W_{uv}$, is associated with its cost c^w_{uv} and a random variable η^w_{uv} that represents the number of bits per symbol of the current modulation scheme (remember that the modulation scheme varies in response to channel fluctuations). Let $\varepsilon_{uv} > 0$ be the infeasibility tolerance (typically near zero) on link uv chosen by the network engineer. The traffic requirements are defined by K oriented pairs of nodes (s^k, t^k), with $s^k, t^k \in V$ and $s^k \neq t^k$, and expected demand d^k of pair $k = 1, \ldots, K$.

We want to determine the bandwidth assignment and the traffic flows that minimize the total bandwidth cost. Let y^w_{uv} be the binary decision variable indicating whether the bandwidth b^w_{uv}, $w = 1, \ldots, W_{uv}$, is assigned or not for the arc $uv \in E$. The flow variables f^k_{uv} denote the fraction of d^k, $k = 1, \ldots, K$, routed on the arc $uv \in E$. The optimization problem can be formulated as follows:

$$\min \sum_{uv \in E} \sum_{w=1}^{W_{uv}} c^w_{uv} y^w_{uv} \tag{3.3}$$

$$s.t. \sum_{u \in \delta^-(v)} f^k_{uv} - \sum_{u \in \delta^+(v)} f^k_{vu} = \begin{cases} -1, & \text{if } v = s^k, \\ 1, & \text{if } v = t^k, \\ 0, & \text{otherwise} \end{cases} \qquad \begin{matrix} \forall v \in V, \\ k = 1 \ldots K \end{matrix} \tag{3.4}$$

$$\mathcal{P}\left(\sum_{k=1}^{K} d^k f^k_{uv} \leq \sum_{w=1}^{W_{uv}} \eta^w_{uv} b^w_{uv} y^w_{uv} \right) \geq 1 - \varepsilon_{uv} \qquad \forall uv \in E \tag{3.5}$$

$$\sum_{w=1}^{W_{uv}} y^w_{uv} = 1 \qquad \forall uv \in E \tag{3.6}$$

$$f^k_{uv} \in [0,1], y^w_{uv} \in \{0,1\} \tag{3.7}$$

In this formulation, the objective function (3.3) represents the total bandwidth cost that is to minimize. The flow conservation property is expressed by (3.4). It provides the routes for each demand pair, guaranteeing that the traffic requirements are entirely fulfilled. Constraints (3.5) ensure that the available capacity on each link (taking into account the bandwidth choice and the random modulation) supports all the traffic to be routed through it with (high) probability $1 - \varepsilon_{uv}$. Finally, the bandwidth assignment is determined by (3.6). For each link, it forces a single selection among the possible bandwidths.

Since we have to deal with a finite number of scenarios, this probabilistic program can be equivalently written as a standard integer linear program. However, this equivalent model is highly intractable due to the very large number of scenarios to be considered.

Let us examine different alternatives through an example. Consider a single microwave link and a unique demand of 70 Mbps. Assume that we have two bandwidth choices, 10 MHz and 20 MHz, and consider the same discrete proba-

bility distribution function for both bandwidth choices, given in Figure 3.2. Let $\varepsilon = 0.05$ be the infeasibility tolerance (which corresponds to a reliability level of 0.95).

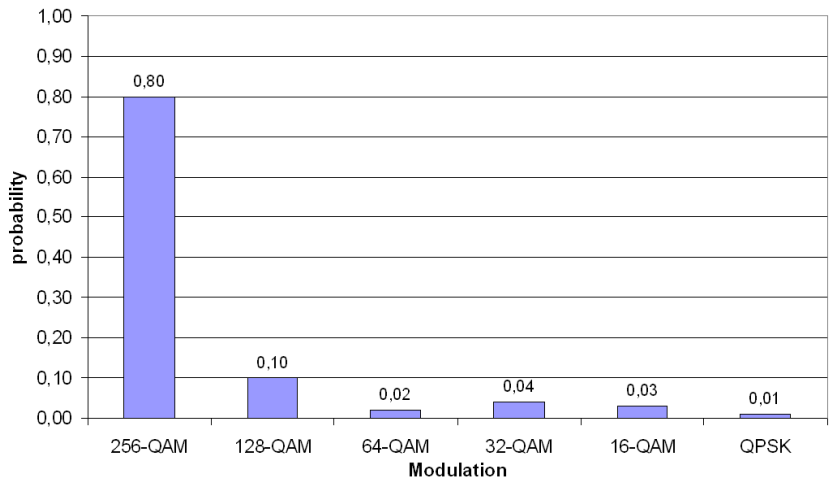

Figure 3.2: Discrete probability distribution function.

We can easily calculate the expectation value of the random variable η, $E(\eta) = 0.80 \times 8 + 0.10 \times 7 + 0.02 \times 6 + 0.04 \times 5 + 0.03 \times 4 + 0.01 \times 2 = 7.56$. Note that, if we use the expectation value for estimating the link's capacity, the bandwidth choice of 10 MHz is sufficient to carry all the demand (since the estimated capacity will be $7.56 \times 10 = 75.6$ Mbps). However, $\mathcal{P}(10 \cdot \eta \geq 70) = \mathcal{P}(\eta \geq 7) = 0.90 \leq 0.95$. Thus, this solution does not respect the infeasibility tolerance $\varepsilon = 0.05$.

Now let us assume the worst case (lowest modulation scheme) for estimating the link's capacity. This way, a feasible solution for this case will be more expensive but necessarily feasible for all other cases. However, assuming the QPSK modulation scheme (with bandwidth efficiency of 2 bps/Hz), we do not dispose enough capacity to satisfy the demand of 70 Mbps even if we consider the largest available bandwidth of 20 MHz (the estimated capacity will be $2 \times 20 = 40.0$ Mbps).

Here, we use the idea of *basic scenarios* from Klopfenstein [Klo10] and take advantage of the problem structure to obtain, in a more efficient manner, the deterministic counterparts of constraints (3.5):

$$\sum_{k=1}^{K} d^k f_{uv}^k \leq \sum_{w=1}^{W_{uv}} n_{uv}^w b_{uv}^w y_{uv}^w \qquad \forall uv \in E \tag{3.8}$$

where for each microwave link and bandwidth, the constant n_{uv}^w can be easily computed from the cumulative probability distribution of the random variable η_{uv}^w. It represents the maximum number of bits we can assume taking into account the infeasibility tolerance ε_{uv}, i.e., the highest modulation scheme whose cumulative probability value is greater than $1 - \varepsilon_{uv}$ (see Figure 3.3 for an illustration). Note

that, as the solution reliability increases (ε_{uv} approaches zero), we have to consider lower modulation schemes and, consequently, less capacity for a given bandwidth. Therefore, there is a tradeoff between the cost and the reliability of the solutions.

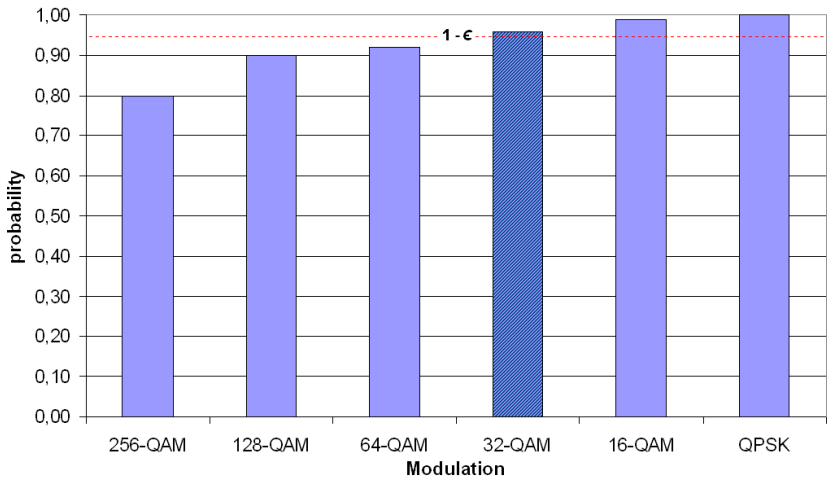

Figure 3.3: Cumulative probability distribution function.

In the example aforementioned, the modulation 32-QAM is considered to estimate the link's capacity ($n = 5$). Note that, in this case, the bandwidth choice of 10 MHz is not enough to carry all the demand (since the estimated capacity will be $5 \times 10 = 50.0$ Mbps). Conversely, using 20 MHz, we can satisfy all the demand of 70 Mbps (the estimated capacity will be $5 \times 20 = 100.0$ Mbps). In addition, $\mathcal{P}(20 \cdot \eta \geq 100) = \mathcal{P}(\eta \geq 5) = 0.96 \geq 0.95$. Since $\mathcal{P}(20 \cdot \eta \geq 70) \geq \mathcal{P}(20 \cdot \eta \geq 100)$, this solution does respect the required reliability level $1 - \varepsilon$.

Remember that, in this model, we impose separate probabilistic constraints (3.5) on each link. As a consequence, even if we consider a very small infeasibility tolerance on each link, the network reliability as a whole can be very bad when the number of links increases (i.e., the optimal solution can be infeasible with a significant probability). Therefore, this approach is worthwhile for particular cases where the network is not too large and the microwave links are engineered to have a very high availability. In the sequel, we present a joint chance-constrained program to overcome this limitation.

3.3.2 Joint chance constraints

In the subsequent formulation, we enforce an infeasibility tolerance on the entire block of capacity constraints, guaranteeing that the assigned bandwidth supports the total traffic to be routed through the network with (high) probability $1 - \varepsilon$. Thus, the constraints (3.5) are now replaced by a single chance constraint:

$$\mathcal{P}\left(\sum_{k=1}^{K} d^k f_{uv}^k \leq \sum_{w=1}^{W_{uv}} \eta_{uv}^w b_{uv}^w y_{uv}^w \qquad \forall uv \in E\right) \geq 1-\varepsilon \tag{3.9}$$

In case of independent probabilities, we can reformulate the left hand side of (3.9) as the product of probabilities. For this, we introduce the following modifications to the previous formulation: Let M_{uv}^w be the number of modulations held by the arc uv with respect to the bandwidth choice w. Let ρ_{uv}^{wm} be the cumulative probability value of the random variable η_{uv}^w regarding the modulation m. Now b_{uv}^{wm} represents the capacity on the arc uv for a given bandwidth choice w and a specific modulation m. In addition, the binary decision variables y obtain a new index m that incorporates the assumption on the modulation scheme. The problem can be rewritten as:

$$\min \sum_{uv\in E} \sum_{w=1}^{W_{uv}} \sum_{m=1}^{M_{uv}^w} c_{uv}^w y_{uv}^{wm} \tag{3.10}$$

$$s.t. \sum_{u\in\delta^-(v)} f_{uv}^k - \sum_{u\in\delta^+(v)} f_{vu}^k = \begin{cases} -1, & \text{if } v = s^k, \\ 1, & \text{if } v = t^k, \\ 0, & \text{otherwise} \end{cases} \qquad \begin{matrix} \forall v \in V, \\ k = 1..K \end{matrix} \tag{3.11}$$

$$\sum_{k=1}^{K} d^k f_{uv}^k \leq \sum_{w=1}^{W_{uv}} \sum_{m=1}^{M_{uv}^w} b_{uv}^{wm} y_{uv}^{wm} \qquad \forall uv \in E \tag{3.12}$$

$$\prod_{uv\in E} \left(\sum_{w=1}^{W_{uv}} \sum_{m=1}^{M_{uv}^w} \rho_{uv}^{wm} y_{uv}^{wm}\right) \geq 1-\varepsilon \tag{3.13}$$

$$\sum_{w=1}^{W_{uv}} \sum_{m=1}^{M_{uv}^w} y_{uv}^{wm} = 1 \qquad \forall uv \in E \tag{3.14}$$

$$f_{uv}^k \in [0,1], y_{uv}^{wm} \in \{0,1\} \tag{3.15}$$

Note that now, in the capacity constraints (3.12), we assume explicitly a hypothesis on the modulation scheme. Obviously, for a given link and bandwidth, the lower the modulation scheme is, the lower will be the capacity assumed to this link and the higher will also be the probability that the effective capacity on this link supports all the traffic to be routed through it. In other words, more conservative hypotheses on the modulation scheme will lead to more reliable solutions.

Constraint (3.13) denotes formally this relation. According to the bandwidth assignment and the hypotheses on the modulation scheme for each microwave link, this constraint guarantees that the reliability of the solutions is greater than $1-\varepsilon$. Note that constraint (3.13) is not linear. Nevertheless, we can derive an equivalent linear constraint exploiting the properties of logarithmic functions as well as constraints (3.14) stating that exactly one bandwidth and modulation scheme are chosen. First, by the monotonicity of any logarithmic function, (3.13) is equivalent to

$$\log\left(\prod_{uv\in E}\sum_{w=1}^{W_{uv}}\sum_{m=1}^{M_{uv}^{w}}\rho_{uv}^{wm}y_{uv}^{wm}\right)\geq\log(1-\varepsilon) \tag{3.16}$$

Next, we employ that the logarithm of a product is equal to the sum of the logarithms:

$$\sum_{uv\in E}\log\left(\sum_{w=1}^{W_{uv}}\sum_{m=1}^{M_{uv}^{w}}\rho_{uv}^{wm}y_{uv}^{wm}\right)\geq\log(1-\varepsilon) \tag{3.17}$$

Finally, we take advantage of the problem structure, notably of the constraint (3.14), that exactly one of the sum elements within the logarithmic function will be nonzero, to obtain the equivalent linear constraint:

$$\sum_{uv\in E}\sum_{w=1}^{W_{uv}}\sum_{m=1}^{M_{uv}^{w}}\log(\rho_{uv}^{wm})y_{uv}^{wm}\geq\log(1-\varepsilon) \tag{3.18}$$

The resulting formulation still results in large scale integer linear programs, which are very hard to solve. In what follows, we introduce some cutset-based valid inequalities to improve the solving performance for this formulation.

3.4 Valid inequalities

Constraints (3.11), (3.12), and (3.14) define the basic properties of multicommodity flow (MCF) problems studied intensively in the literature of classical network design [MMV93, MMV95, BG96, BCGT98, RKOW10]. To enhance the performance of ILP solvers, several valid inequalities have been introduced, in particular so-called cutset-based inequalities, exploiting knowledge about the required capacity on a cut in the network.

Let $S\subset V$ be a proper and nonempty subset of the nodes V and $\overline{S}=V\setminus S$ its complement. $(S,\overline{S})$ is a cutset, i.e., the set of arcs that connect a node in S to a node in $\overline{S}$, as illustrated in Figure 3.4. Also, let $K(S,\overline{S})\subseteq K$ be the set of demands having their origin in S and their destination in $\overline{S}$ and $d_{(S,\overline{S})}=\sum_{k\in K(S,\overline{S})}d^{k}$.

An appropriate aggregation of constraints (3.11), (3.12), and nonnegativity of the variables results in the following *base cutset inequality*:

$$\sum_{uv\in(S,\overline{S})}\sum_{w=1}^{W_{uv}}\sum_{m=1}^{M_{uv}^{w}}b_{uv}^{wm}y_{uv}^{wm}\geq d_{(S,\overline{S})} \tag{3.19}$$

This inequality denotes that there should be enough capacity on the arcs of the cutset in order to satisfy the demands that must be routed through it. Cutset inequalities are necessary for a capacity vector to be feasible, but it is well-known that they are not sufficient in general [CCG09]. In the sequel, we present two types of strong inequalities to our problem obtained from cutset inequalities by applying Chvátal-Gomory cutting plane methods (cf. [Wol98]).

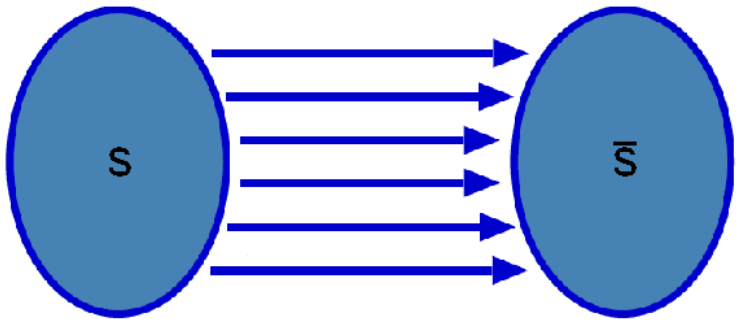

Figure 3.4: A cutset in a network consists of the arcs between the shores.

Type 1. Given a cutset $(S, \overline{S})$, let a_{uv} be the smallest capacity coefficient b_{uv}^{wm}, with respect to the arc $uv \in (S, \overline{S})$,

$$a_{uv} = \min_{w=1,\dots,W_{uv}} \min_{m=1,\dots,M_{uv}^{w}} b_{uv}^{wm}.$$

By (3.14) and $a_{(S,\overline{S})} = \sum_{uv \in (S,\overline{S})} a_{uv}$, (3.19) can be equivalently formulated as

$$\sum_{uv \in (S,\overline{S})} \sum_{w=1}^{W_{uv}} \sum_{m=1}^{M_{uv}^{w}} (b_{uv}^{wm} - a_{uv}) y_{uv}^{wm} \geq d_{(S,\overline{S})} - a_{(S,\overline{S})}. \tag{3.20}$$

Now, let a be the maximal coefficient $(b_{uv}^{wm} - a_{uv})$ at the left hand side of inequality (3.20). By Chvátal-Gomory rounding, we obtain the valid inequality *Type 1* as follows:

$$\sum_{uv \in (S,\overline{S})} \sum_{w=1}^{W_{uv}} \sum_{m=1}^{M_{uv}^{w}} 1_{uv}^{wm} y_{uv}^{wm} \geq \left\lceil \frac{d_{(S,\overline{S})} - a_{(S,\overline{S})}}{a} \right\rceil, \tag{3.21}$$

where

$$1_{uv}^{wm} = \begin{cases} 1 & \text{if } b_{uv}^{wm} > a_{uv} \\ 0 & \text{otherwise} \end{cases}.$$

In general the linear programming (LP) relaxation of (3.10)–(3.12), (3.14), (3.15), (3.18) does not satisfy (3.21) although all integer solutions have to satisfy it. Hence, the inequality is valid and can enhance the solving of the ILP. Under certain conditions, (3.21) defines a facet of the convex hull of feasible solutions indicating the importance of this inequality (cf. [RKOW10] for conditions for similar results).

Type 2. Instead of subtracting a_{uv} for all coefficients in (3.19), we can also apply Chvátal-Gomory rounding directly to (3.19) for a certain value a'. If we take

$$a' = \max_{uv \in (S,\overline{S})} a_{uv}$$

the resulting valid inequality reads

$$\sum_{uv \in (S,\overline{S})} \sum_{w=1}^{W_{uv}} \sum_{m=1}^{M_{uv}^{w}} \left\lceil \frac{b_{uv}^{wm}}{a'} \right\rceil y_{uv}^{wm} \geq \left\lceil \frac{d_{(S,\overline{S})}}{a'} \right\rceil \tag{3.22}$$

and has at least $|(S,\overline{S})|$ coefficients equal to one. Moreover, the following equality can be easily obtained as a sum of constraints (3.14) associated with the cutset $(S,\overline{S})$:

$$\sum_{uv \in (S,\overline{S})} \sum_{w=1}^{W_{uv}} \sum_{m=1}^{M_{uv}^{w}} y_{uv}^{wm} = |(S,\overline{S})|, \tag{3.23}$$

and subtracting (3.23) from (3.22), we obtain

$$\sum_{uv \in (S,\overline{S})} \sum_{w=1}^{W_{uv}} \sum_{m=1}^{M_{uv}^{w}} \left(\left\lceil \frac{b_{uv}^{wm}}{a'} \right\rceil - 1 \right) y_{uv}^{wm} \geq \left\lceil \frac{d_{(S,\overline{S})}}{a'} \right\rceil - |(S,\overline{S})| \tag{3.24}$$

which is weaker than (3.21) with a' instead of a. The same procedure can be applied for other values a'. Given a cutset $(S,\overline{S})$, let a'_{uv} be the second smallest capacity coefficient b_{uv}^{wm}, with respect to the arc $uv \in (S,\overline{S})$, of the inequality (3.19) associated with this cutset, and let a' be the largest coefficient among all a'_{uv}. The result of Chvátal-Gomory rounding is again (3.24), but this time at least two coefficients $\left(\left\lceil \frac{b_{uv}^{wm}}{a'} \right\rceil - 1 \right)$ for every arc $uv \in (S,\overline{S})$ are equal to 0, and the cutset inequality is indeed different from (3.21). We refer to the inequalities derived this way as *Type 2*. Again, it can be shown that (3.24) defines a facet of the convex hull of feasible solutions under certain conditions (beyond the scope of our study).

3.5 Computational results

Given the absence of topology instances for microwave backhaul networks available in the literature, we have performed computational experiments on a grid network (available at http://www.di.unipi.it/optimize/Data/MMCF.html) which originates from [LY04]. A particular characteristic of grid networks is the huge number of paths between any pair of nodes. In addition, the regular structure of grid networks make it easier to perform comparisons between various solutions methods. We take into account the 5×5 grid instance (25 base transceiver stations and 80 directional microwave links, as illustrated in Figure 3.5) with 50 demands taken from the original paper.

With respect to the radio scenario, we consider two bandwidth choices for each link, 7 MHz and 28 MHz, associated with costs of \$ 1,000 and \$ 6,000 respectively. We assume that links operating at 7 MHz are designed to use the 128-QAM scheme, with an availability of 99.9%. Only in fading conditions, these links will use the 16-QAM scheme. Conversely, we suppose that links operating at 28 MHz are designed to use the 256-QAM scheme, with an availability of 99.9%. The 32-QAM scheme will be used for these links in fading conditions.

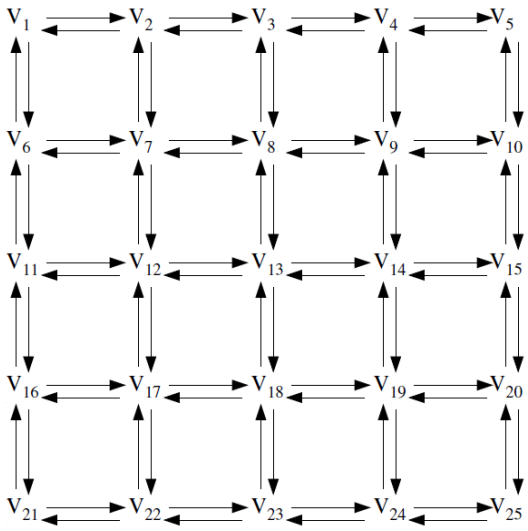

Figure 3.5: 5×5 network grid instance.

In what follows, we focused on the integer linear program associated with the joint chance-constrained formulation, since it is in general more appropriate to cope with practical instances of this problem. All the computations were carried out on a Linux machine with 3.20 GHz Intel Xeon W5580 CPU (8 Threads) and 64 GB RAM, using IBM ILOG CPLEX 12.1 [CPL10] as underlying solver.

Price of reliability. As we assume the same availability for microwave links using the highest-level modulations and under the hypothesis that the lowest-level modulations are sufficiently robust to guarantee an availability of 100%, instead of explicitly setting the infeasibility tolerance ε, we can specify the maximum number of links N that we assume using highest-level modulations. To prove that, let us rewrite (3.18) considering these assumptions ($\rho_{uv}^{w1} = 1$, cumulative probability value for lowest-level modulation, and $\rho_{uv}^{w2} = \rho$, cumulative probability value for highest-level modulation):

$$\sum_{uv \in E} \sum_{w=1}^{W_{uv}} (\log(1) y_{uv}^{w1} + \log(\rho) y_{uv}^{w2}) \geq \log(1-\varepsilon) \tag{3.25}$$

Note that, as $\log(1) = 0$, (3.25) is equivalent to

$$\log(\rho) \sum_{uv \in E} \sum_{w=1}^{W_{uv}} y_{uv}^{w2} \geq \log(1-\varepsilon) \tag{3.26}$$

Finally, in this scenario, (3.18) can be replaced by:

$$\sum_{uv \in E} \sum_{w=1}^{W_{uv}} y_{uv}^{w2} \leq \left\lfloor \frac{\log(1-\varepsilon)}{\log(\rho)} \right\rfloor = N \tag{3.27}$$

Note that, in this scenario, the parameter N directly implies the infeasibility tolerance ε and, as the former increases the latter also increases, i.e., the reliability of the solutions can become worst. Therefore, in order to observe the evolution of the bandwidth cost as a function of the infeasibility tolerance, we ran tests for $N = 0, 10, \ldots, 80$.

The solutions were obtained by solving the (enhanced) formulation D (as further described in Table 3.1 and below) to optimality, which took several hours (even days) of computation for each instance. As illustrated in Figure 3.6, the total bandwidth cost decreases as we admit larger values for the infeasibility tolerance (N augments). For $N = 0$, when we have to assume the lowest-level modulations for all radio links, the network cannot provide enough capacity to satisfy all the traffic demands, hence this problem is infeasible. For $N = 10$ ($\varepsilon = 0.01$), the bandwidth cost is 38.6% higher than the bandwidth cost for $N = 80$ ($\varepsilon = 0.077$) and 68.4% higher compared to the case where we do not use any optimization (i.e., we assign 28 MHz for every microwave link). For $N = 60, 70, 80$, the probabilistic constraint does not really affect the cost of the solutions because the number of links we need to consider using the highest-level modulations to satisfy all the traffic requirements is smaller than 60 for these instances.

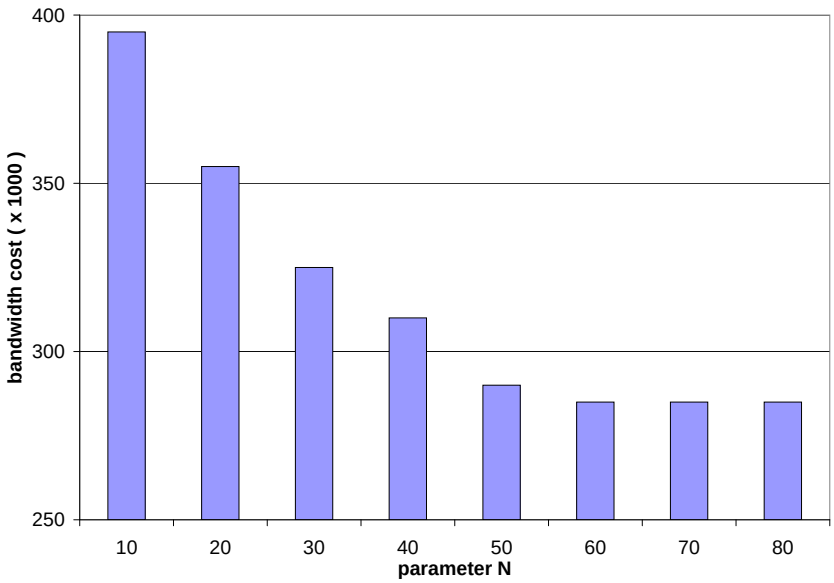

Figure 3.6: Bandwidth cost as a function of the infeasibility tolerance.

Comparison of the formulations. In addition, to study the gain of applying the valid inequalities introduced in Section 3.4, we performed tests for different formulations A, B, C, D, that consider or not such valid inequalities according to the Table 3.1. Note that, in formulations B and D, base cutset inequalities (3.19) are also

added although these do not contribute to an improvement of the objective – the ILP solver, however, can benefit from those to generate its own valid inequalities.

Table 3.1: Different formulations w.r.t the valid inequalities.

Formulation	Cutset	Type1	Type2
A	no	no	no
B	yes	no	no
C	no	yes	yes
D	yes	yes	yes

We manually identified a restricted, but sufficiently large (432 cutsets in total), set of cutsets of the type $(S, \overline{S})$ to generate the valid inequalities. As typical examples, according to the node labelling of Figure 3.5, we considered the sets S:

$$\{v_1, v_2, v_3, v_4, v_5, v_6, v_7, v_8, v_9, v_{10}\},$$
$$\{v_4, v_5, v_9, v_{10}, v_{14}, v_{15}, v_{19}, v_{20}, v_{24}, v_{25}\},$$
$$\{v_1, v_2, v_3, v_6, v_7, v_{11}\},$$
$$\{v_1, v_2, v_6, v_7, v_{11}, v_{12}\},$$
$$\{v_{18}, v_{19}, v_{20}, v_{21}, v_{22}, v_{23}, v_{24}, v_{25}\}.$$

Due to computational limitations, first a limit of 30,000 nodes (LP relaxations) of the branch-and-bound process was set for solving each instance. All other solver settings were preserved at their defaults. In addition, as the size and the complexity of the LP relaxations vary according to each formulation, instead of imposing a limit on the number of nodes, we also performed tests where we set a time limit of 1 hour of computation for each instance, preserving all other solver settings at their defaults.

Figure 3.7 illustrates, for each instance, the optimality gap (given by the ILP solver) achieved for the different formulations considering first a limit on the number of nodes (Figure 3.7(a)) and then on the execution time (Figure 3.7(b)), along with the best feasible solution (Figure 3.7(c)) and lower bound (Figure 3.7(d)) values obtained for the first scenario (limit on the number of nodes).

With respect to the optimality gap, the adding of valid inequalities improves the performance of the ILP solver in both scenarios. Formulation B, which considers only base cutset inequalities, performs significantly better than the basic problem formulation A. Formulation C, which introduces only the valid inequalities Type 1 and Type 2, also improves the basic problem formulation A for most cases, but it does not perform as well as formulation B. Actually, the valid inequalities Type 1 and Type 2 are more useful in conjunction with base cutset inequalities. In fact, formulation D presents the best results in terms of the achieved optimality gap for most cases.

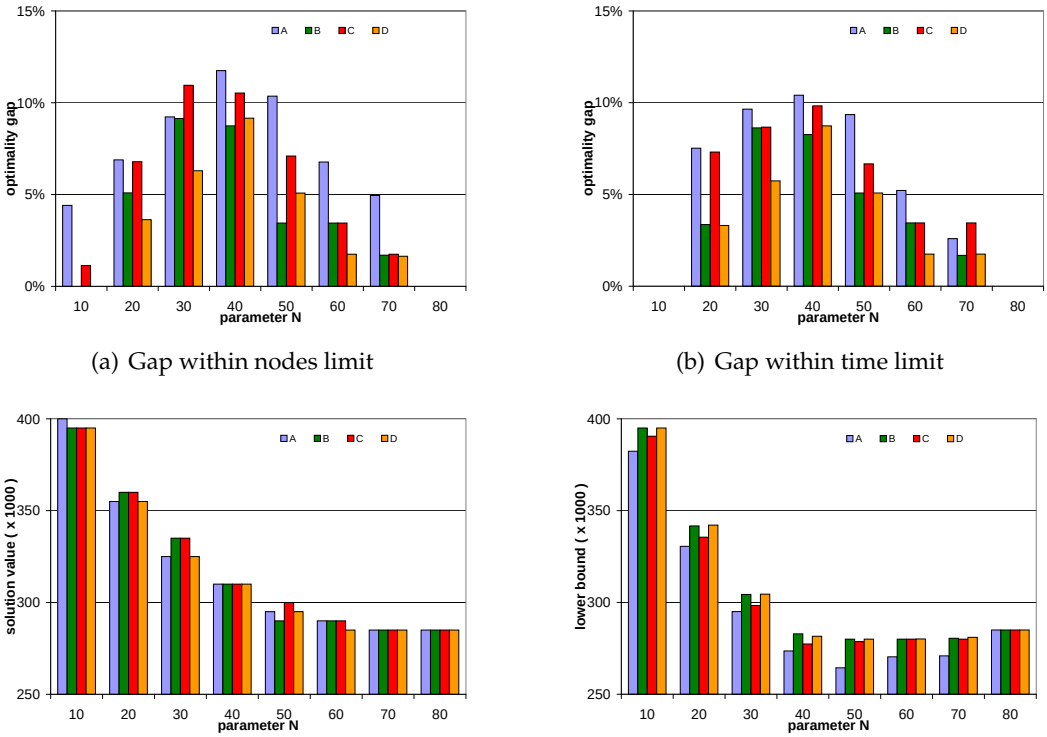

(a) Gap within nodes limit

(b) Gap within time limit

(c) Best solution

(d) Lower bound

Figure 3.7: Optimality gap, best solution and lower bound values achieved for the different formulations.

Nevertheless, there are not significant differences among feasible solutions (see Figure 3.7(c) – lower values mean better solutions) found by each formulation to explain the better performance of formulations B and D. In Figure 3.8, we show the performance of the different formulations according to the number of LP relaxations for these instances. Note that, in general, the optimality gap decreases rather quickly until finding a barrier in a given level, when the lower bounds defined by the LP relaxations improve rather slowly, suggesting that much computational effort is made to prove the optimality of the current feasible solutions. Formulations B and D coped better to the task of finding tighter lower bounds (see Figure 3.7(d) – higher values mean better lower bounds), and this explains in part why these formulations provide lower optimality gaps.

3.6 Conclusion

In this chapter, we have presented a chance-constrained programming approach to tackle the problem of assigning bandwidth for reliable microwave backhaul networks. We introduced different mathematical formulations and proposed cutset-

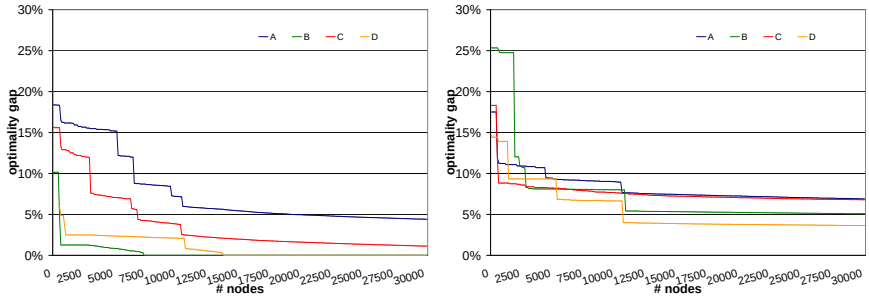

(a) N = 10

(b) N = 20

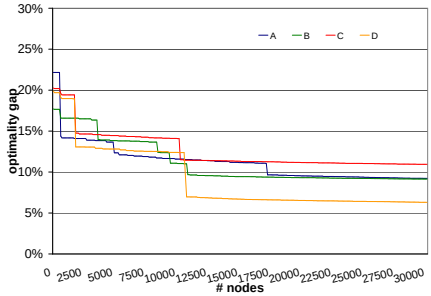

(c) N = 30

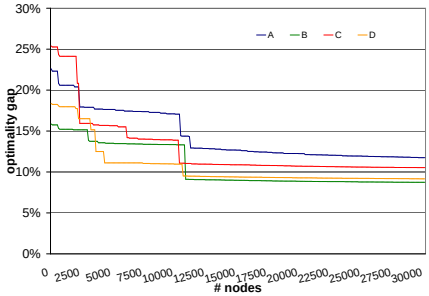

(d) N = 40

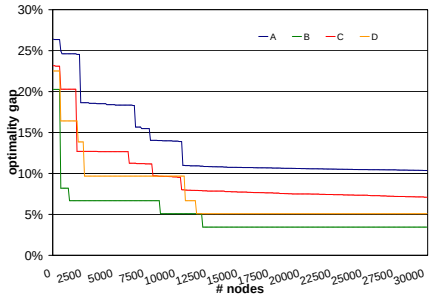

(e) N = 50

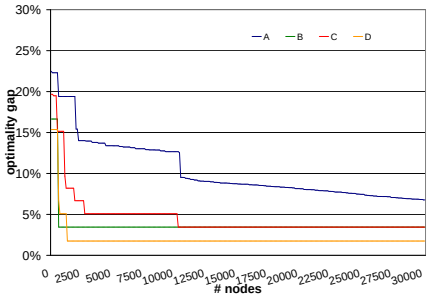

(f) N = 60

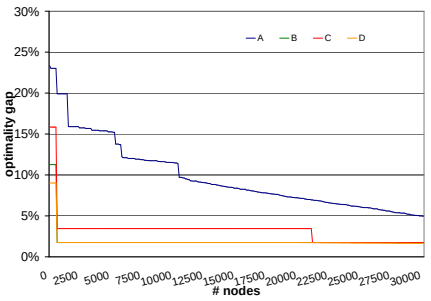

(g) N = 70

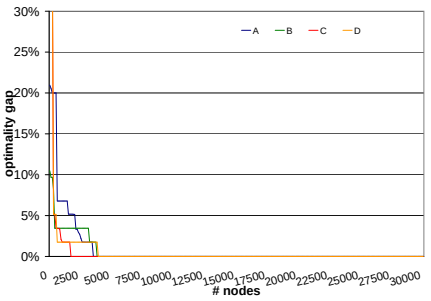

(h) N = 80

Figure 3.8: Formulations performance according to the number of LP relaxations.

based valid inequalities for this problem. In our computational studies, we discussed the price of reliability and compared the performance of the different mathematical formulations. The results show that there is a tradeoff between bandwidth assignment costs and network reliability. In addition, the cutset-based valid inequalities improved the solving performance of the basic problem formulation.

Many challenges related to this problem remain unaddressed. For example, besides the modulation scheme, we could consider other radio parameters (e.g., coding and transmission power) that vary in response to the conditions of the channel and that have a great impact on the capacity of a microwave link. Obviously, more realistic models while being more accurate also bring more difficulty on the problem solving.

In addition, it would be interesting to compare our solution to other approaches used to reduce the vulnerability of wireless networks (e.g., equipment and frequency diversity). Actually, conceiving reliable solutions for microwave backhaul networks involves many different design decisions. For example, in order to reduce the impact of signal fluctuations, it could be more cost-efficient to use an expensive antenna with very high gain than obtain licenses for using a great amount of spectrum.

As a final remark we want to note that, in contrast to wired networks where libraries of standardized benchmark instances are accessible [OPTW10], a data library with realistic data sets for microwave backhaul networks is not available so far. A characterization of the topologies and traffic behavior of microwave backhaul networks would be a great contribution for helping engineers who deal with network optimization in this challenging area.

CHAPTER 4

Power-efficient radio configuration

In this chapter, we investigate on determining feasible radio configurations in microwave backhaul networks, focusing on power efficiency. We introduce a joint optimization of data routing and radio configuration that minimizes the total power utilization, while handling all the traffic requirements simultaneously. As in the previous chapter, this problem also relies on a MCMCF with discontinuous step increasing cost functions on the links, which is very hard to optimize [Ken78, Min06].

We then propose a piecewise linear convex function, obtained by linear interpolation of power-efficient points, that provides a good approximation of the power utilization on the links, and present a relaxation that exploits the convexity of the cost functions. This yields lower bounds on the total power expenditure, and finally heuristic algorithms based on the fractional optimum are employed to produce feasible configuration solutions. Particularly, we present a hybrid algorithm that combines a metaheuristic and an exact method to improve these solutions.

The remainder of this chapter is organized as follows. In Section 4.1, we present the context and motivation to study this problem. In Section 4.2, we introduce mathematical formulations for the application considered here, and a simple heuristic algorithm based on the model relaxation is presented. In Section 4.3, a hybrid algorithm to improve heuristic configuration solutions is introduced. In Section 4.4, we discuss some computational results that we have achieved by experimenting with benchmark problem instances. In Section 4.5, some final remarks and perspectives on future work conclude the chapter.

4.1 Context and motivation

Recent studies show that the traffic demand, even being aggregated at access points, is highly dynamic and presents a nonstationary behavior over large time scales due to the diurnal and weekly working cycles [DXC+08]. Therefore, microwave backhaul operators are commonly compelled to built networks in a robust fashion to support this extremely bursty traffic behavior (and also to guarantee fault protection and future traffic expansion). As a drawback, it leads to important resources utilization to provide extra capacity which could be used only in critical situations.

As discussed earlier in Chapter 2, there is a tradeoff between bandwidth efficiency and power efficiency. Since microwave links present a dynamic behavior – radio parameters (e.g., transmission power and modulation scheme) can be suit-

ably set on the fly –, the traffic fluctuation over the time offers an opportunity to power mitigation when microwave links are underused.

Even though terrestrial microwave links are not typically concerned with power efficiency from an economical viewpoint, since they have plenty of power available and the transmitter output power is very low – usually a few dozen milliwatts of RF energy produced by the radio transmitter (which is equivalent to a few hundred watts of RF energy effectively radiated from a highly directional antenna) –, from a technical point of view it is a good practice to use low transmission power levels. In fact, reducing transmission power increases the potential for frequency reuse within a system and reduces possible interference to neighboring systems.

This is especially important in congested urban areas (containing many randomly oriented microwave links), where operators opt for equipment collocation[1]. The collocation trend in the industry can actually create compliance challenges that operators otherwise would not have encountered. The reason is they must submit compliance records for their own equipment and for the equipment owned by collocation tenants at the site. In addition, there exists a public perception of the safety of microwave radiation[2]. In certain situations, and depending on the site accessibility to the public, if emissions exceed the maximum allowed exposure levels, any company that contributes to the RF emissions in that area is responsible for mitigating the problem [Leh10].

Wireless networks have been intensively studied in recent years with a specific focus on capacity or other QoS parameters and installation costs [ZWZL05, GPR08, MPR08, ORV10]. Many researches have especially focused on minimizing energy consumption in wireless networks, such as minimum energy broadcasting, backbone construction or monitoring in sensor and ad-hoc networks [SRSW05, FKNP07]. Since a huge majority of these works consider energy-constrained devices (sensors, ad-hoc nodes, etc), most existing solutions are per-device power optimization. In our settings, in which a global optimum is sought out, system-wide approaches might be more relevant.

In what follows, we introduce a mathematical programming approach to conceive power-efficient microwave backhaul networks. Under this scenario, we can define a power-efficient configuration as the minimum transmission output power needed to achieve the SNR requirement associated with a given modulation. Every microwave link holds a finite set of power-efficient configuration points, characterized by a modulation scheme and a transmission power level (as illustrated in Figure 4.1). Note that power-efficient configurations depend on several system's

[1]Collocation is a general concept that refers to multistation sites consisting of numerous transmitters and receivers installed within a limited geographical area. The site often consists of a number of antennas, typically belonging to different operators, that are all mounted on a common tower or distributed among a small number of closely positioned towers [Leh10].

[2]It should be noted that microwaves fall within the nonionized portion of the electromagnetic spectrum, below the ionizing portion where X, gamma, and cosmic rays reside. Microwave energy thus has insufficient energy to ionize atoms and so is unable to change the DNA composition of human tissue or cause cancer [Man09].

parameters (such as the antenna gain, line losses, and distance between sites) that define the scenario of application.

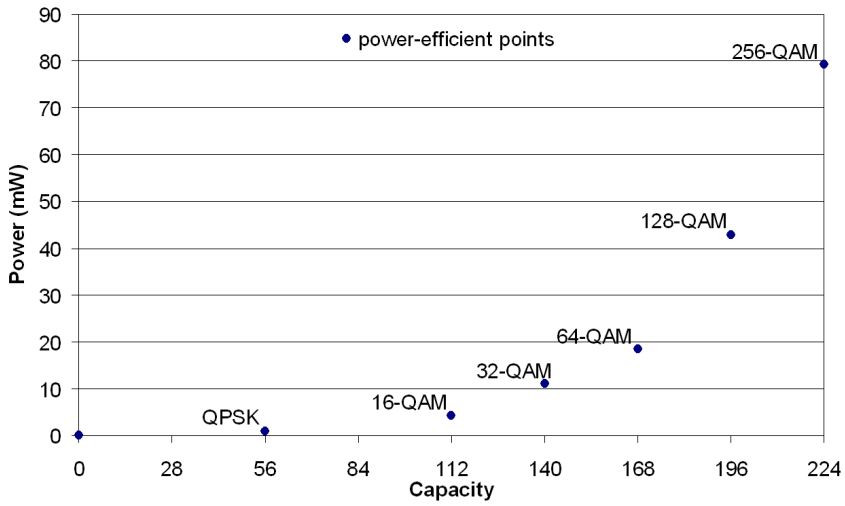

Figure 4.1: Power-efficient configuration points.

4.2 Mathematical formulations

In this section, we study the optimization problem of deciding both the network's configuration and flows that minimize the total power utilization, while handling all the traffic requirements simultaneously. Particularly, by configuration, we mean the choice of the transmission power level and the modulation scheme for each microwave link. We first introduce an exact formulation with discontinuous step increasing cost functions on the links and then we propose a relaxation using piecewise linear convex cost functions.

4.2.1 Discontinuous step increasing cost functions

In this formulation, we consider power-efficient configuration points to derive an energy cost function that is discontinuous step increasing (see Figure 4.2). Note that, for each modulation scheme, only the most right point of the curve represents a power-efficient configuration. For each modulation level, the decimal number denotes the minimum power utilization required to attain a specific SNR. These values were obtained for the link scenario used in our simulations (see Section 4.4). It is important to clarify that different values could be obtained according to the scenario in focus. Nevertheless, the shape of the function remains the same.

The power utilization on each microwave link depends on the traffic volume that is supposed to pass through it. In this formulation, we use a multi-arc representation of a microwave link, as illustrated in Figure 4.3, and enforce a single

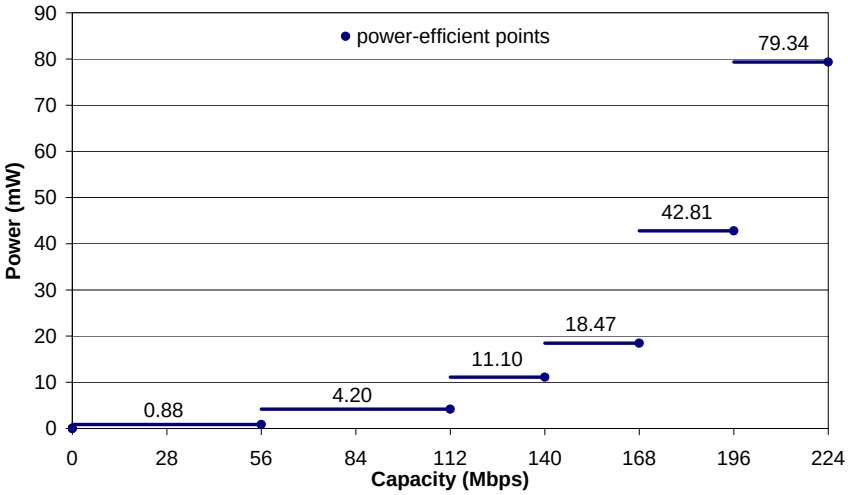

Figure 4.2: Step increasing energy cost function on the links.

arc selection (represented by a continuous line in contrast with the dashed lines). The basic idea is to set, for each link, the lowest configuration level that supports all the traffic to be routed through it. The arc selection, conditioned by the traffic volume on the link, explicitly determines its capacity and power utilization.

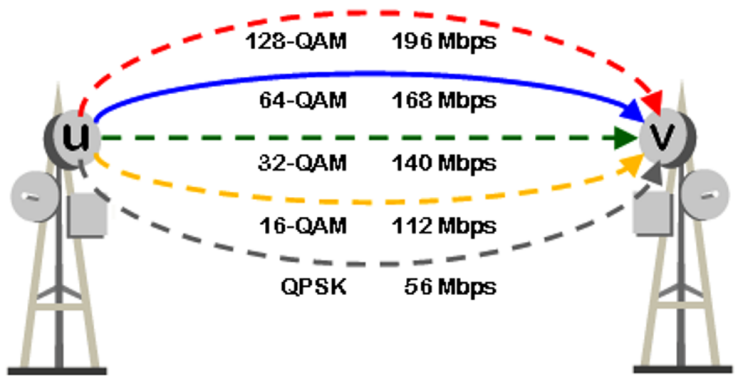

Figure 4.3: Exclusive multi-arc representation of a 168 Mbps link.

This problem can be formally stated as follows. The network's topology is modelled as a digraph $G = (V, E)$, where each node $v \in V$ denotes a base transceiver station and each arc $uv \in E$ represents a microwave link from u to v, with $u, v \in V$ and $u \neq v$. Let $\delta^+(v)$ denote the set of outneighbors of v and $\delta^-(v)$ the set of inneighbors of v. Let M_{uv} be the number of power-efficient configurations held by the arc uv, each of them associating a link capacity b^m_{uv} with its energy cost c^m_{uv}, for $m = 1, \ldots, M_{uv}$. The traffic requirements are defined by K oriented

pairs of nodes (s^k, t^k), with $s^k, t^k \in V$ and $s^k \neq t^k$, and the expected demand d^k of pair $k = 1, \ldots, K$.

We want to determine the network's configuration and flows that minimize the total energy cost. Let y^m_{uv} be the binary decision variable indicating whether the link configuration m is active or not for the arc uv, and let x^{mk}_{uv} be the flow on the arc uv under the configuration m with respect to the traffic requirement k. The optimization problem can be formulated as follows:

$$\min \sum_{uv \in E} \sum_{m=1}^{M_{uv}} c^m_{uv} y^m_{uv} \tag{4.1}$$

$$s.t. \sum_{u \in \delta^-(v)} \sum_{m=1}^{M_{uv}} x^{mk}_{uv} - \sum_{u \in \delta^+(v)} \sum_{m=1}^{M_{vu}} x^{mk}_{vu} = \begin{cases} -d^k, & \text{if } v = s^k, \\ d^k, & \text{if } v = t^k, \\ 0, & \text{otherwise} \end{cases} \quad \begin{matrix} \forall v \in V, \\ k = 1 \ldots K \end{matrix} \tag{4.2}$$

$$\sum_{k=1}^{K} x^{mk}_{uv} \leq b^m_{uv} y^m_{uv} \quad \begin{matrix} \forall uv \in E, \\ m = 1 \ldots M_{uv} \end{matrix} \tag{4.3}$$

$$\sum_{m=1}^{M_{uv}} y^m_{uv} \leq 1 \quad \forall uv \in E \tag{4.4}$$

$$x^{mk}_{uv} \in \mathbb{R}^+, y^m_{uv} \in \{0, 1\} \tag{4.5}$$

In this formulation, the objective function (4.1) represents the total power utilization that is to minimize. For each link, it counts the energy consumption due to the radio operation at a given transmission power level, defined by its configuration. The flow conservation property is expressed by (4.2). It provides the routes for each demand pair, guaranteeing that the traffic requirements are entirely attended. By (4.3), it is assured that, on each link, the available capacity according to its configuration supports all the traffic to be routed through it. Finally, the link's configuration choice is determined by (4.4). For each microwave link, it forces a single selection among the possible power-efficient configurations.

This formulation results in large scale integer linear programs, which are very hard to solve in practical cases. In addition, solution methods for this problem have received little attention in the literature. In [GM97], a relaxation that combines both column and constraint generation is used to derive lower bounds to this problem. In [AT02], a difference of convex function algorithm is applied to provide feasible solutions. These studies consider general step increasing functions, where *convexification* may derive poor approximations.

In our application, however, we perceive that the energy cost per bit rises as we assume higher modulation levels. Taking advantage of this fact, we introduce a convexification-based relaxation that takes advantage of the inherent convex shape of the energy cost functions on the links to obtain lower bounds on the power utilization and determine the network's configuration.

4.2.2 Piecewise linear convex cost functions

In the subsequent formulation, we consider a piecewise linear convex cost function (see Figure 4.4), obtained by linear interpolation of power-efficient configuration points, that provides a good approximation of the power utilization on the links. Note that, for each interval, the endpoints represent power-efficient configurations and the decimal number denotes the marginal energy cost (i.e., the additional power utilization per unit of capacity into this interval). These values were obtained for a real world scenario (see Section 4.4). Obviously, distinct scenarios lead to different cost values, but the shape of the curve remains the same. Note that the link's energy cost per unit of capacity increases as the modulation scheme changes to accommodate higher data rates.

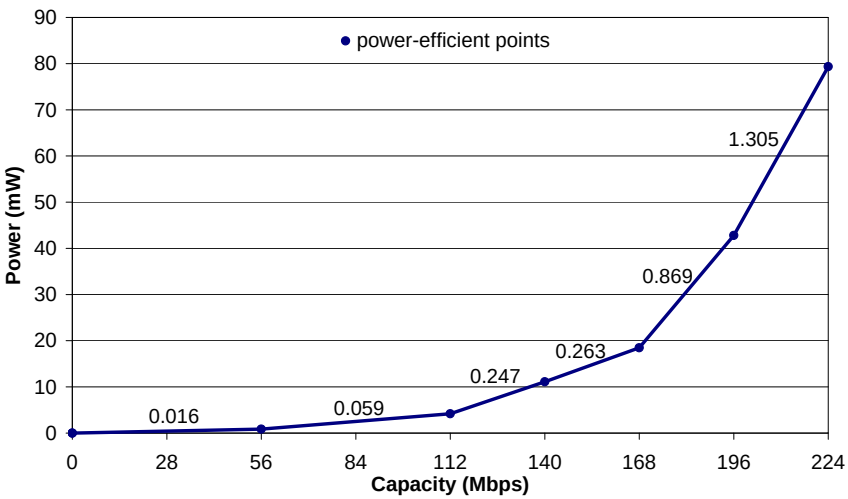

Figure 4.4: Piecewise linear convex energy cost function on the links.

Here, we still have a multi-arc representation of a radio link, as shown in Figure 4.5. However, note that now the capacity of each arc represents the maximum increment of the link's capacity when we move from a given configuration level to the immediate higher one. In addition, the arc selection (represented by the continuous lines in contrast with the dashed lines) is not exclusive anymore. Actually, as the marginal energy cost for higher configurations is always increasing, we will have a progressive utilization of the arcs from the lowest configuration level to the highest one. When the current arc becomes saturated and the link's capacity is still not enough to support all the traffic to be routed through it, we start to use the next virtual arc. The configuration can then be determined by the flow at the highest modulation scheme.

As an example, if we need a capacity of 140 Mbps, then the power utilization on the link will be given by $(56 - 0) \times 0.016 + (112 - 56) \times 0.059 + (140 - 112) \times 0.247 = 11.116$ mW, which is the expected value in Figure 4.2 since it corresponds to a possible power-efficient radio configuration (some difference is

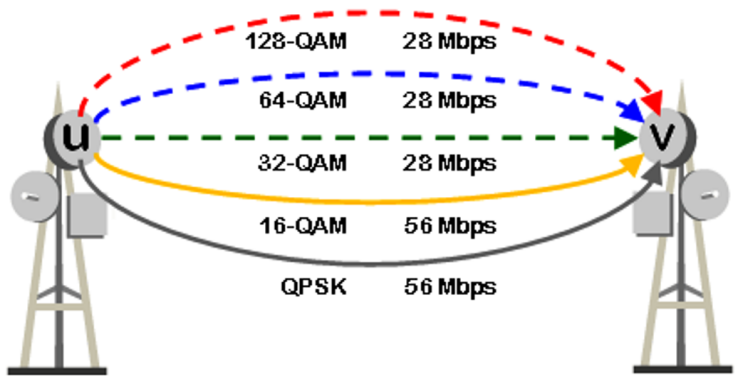

Figure 4.5: Progressive multi-arc representation of a 112 Mbps link.

due to the decimal format representation of the marginal energy costs). Conversely, if we want a capacity of 150 Mbps, the power utilization will be given by $(56-0)\times 0.016+(112-56)\times 0.059+(140-112)\times 0.247+(150-140)\times 0.263 = 13.746$ mW. Note that this later in reality does not represent a possible power-efficient radio configuration.

The problem can be rewritten as a MCMCF with piecewise linear convex cost functions. Consider the problem statement, as in the previous subsection, and the following modifications: now b^m_{uv} represents the maximum increment of capacity on the arc uv when we move from the configuration $m-1$ to the immediate higher level m, and c^m_{uv} denotes the marginal energy cost into this configuration. As the marginal cost for routing an amount of traffic over higher QAM schemes is always increasing, the modulation and the transmission power for each radio link can be implicitly determined by the variable x of highest configuration level and nonzero value, i.e. by the flow at the highest QAM scheme. The problem can be then formulated as follows:

$$\min \sum_{uv\in E}\sum_{m=1}^{M_{uv}}\sum_{k=1}^{K} c^m_{uv}x^{mk}_{uv} \tag{4.6}$$

$$s.t. \sum_{u\in\delta^-(v)}\sum_{m=1}^{M_{uv}} x^{mk}_{uv} - \sum_{u\in\delta^+(v)}\sum_{m=1}^{M_{vu}} x^{mk}_{vu} = \begin{cases} -d^k, & \text{if } v=s^k,\\ d^k, & \text{if } v=t^k,\\ 0, & \text{otherwise}\end{cases} \qquad \forall v\in V,\ k=1...K \tag{4.7}$$

$$\sum_{k=1}^{K} x^{mk}_{uv} \le b^m_{uv} \qquad \forall uv\in E,\ m=1\dots M_{uv} \tag{4.8}$$

$$x^{mk}_{uv}\in\mathbb{R}^+ \tag{4.9}$$

The total energy cost is now given by a continuous linear function (4.6). The flow conservation constraints (4.7) remain as in the previous model and implicitly provide, besides the routes for each demand pair, the network's configuration.

Finally, by (4.8), we guarantee that, through every link, the flow over each configuration level does not exceed its capacity.

This formulation gives rise to continuous linear programs and can be easily solved even if we have to deal with very large problem instances. Despite the fact that the resulting optimal solution of the associated linear program is not a practical one, it yields lower bounds on the energy consumption. Furthermore, quite satisfactory solutions can be obtained by means of simple heuristics based on the fractional optimum.

Particularly, we consider a direct heuristic algorithm that contemplates the optimal solution of the relaxation and reassigns, for each microwave link, the lowest configuration level that supports the network's flows (obtained by the continuous linear program) through it. In other words, this heuristic establishes feasible solutions by rounding up the links' capacity to meet a possible power-efficient configuration. In some cases, it can lead to the underuse of many links that operate at higher modulation levels to carry a small extra amount of traffic that could be routed through other links. In what follows, we present an algorithm to overcome this problem and improve the configuration solutions.

4.3 Hybrid algorithm

In this section, we introduce a hybrid algorithm[3] that combines a metaheuristic[4] and an exact method to improve radio configuration solutions. The basic idea is summarized as follows. Given the solution obtained by the relaxation model, instead of indistinctively rounding up the capacity of all links to the immediate higher power-efficient configuration (which clearly provides a feasible solution), we use a metaheuristic to decide which links will have their capacity rounded up and which links will have their capacity pruned down. As some possible network's radio configurations produced during this process could not represent a feasible solution to the problem, we must check at each iteration the existence of a flow assignment that satisfies all the problem's constraints, i.e. we have to verify if the current network's radio configuration supports all the traffic requirements.

As an example, consider 4 base transceiver stations A, B, C, D, 4 oriented microwave links AB, AC, CD, DB, and a traffic matrix with 4 demands of 10 Mbps

[3] It is only rather recently that methods which combine ideas from metaheuristics and other operations research techniques into more powerful algorithms (commonly referred to as *hybrid metaheuristics* [Rai06]) have been proposed. These algorithms have been shown a very promising strategy, as they typically represent complementary perspectives over the problem solving process as a whole. Some of them mainly aim at providing optimal solutions in shorter time, while others primarily focus on getting better heuristic solutions [PR05].

[4] Metaheuristics (e.g., simulated annealing, genetic algorithms, and ant colony optimization) have succeeded in providing a suitable balance between the efficiency and effectiveness criteria while tackling many nontrivial optimization problems, even though they cannot furnish any sort of guarantee of finding optimal solutions. This success can be evidenced by the diversity of works about this topic found in the literature (see [BR03, GK03] and references therein).

each, AB, AC, CD, DB, as illustrated in Figure 4.6. Let us also assume the power-efficient configuration data for the link scenario used in our simulations (see Table 4.1). The relaxation routes the demands on different links, for an overall cost of $4 \times 10 \times 0.016 = 0.64$ mW. Note that the relaxation computes the energy cost assuming a capacity of 10 Mbps for each link. Actually, this solution does not represent a possible radio configuration. Thus, in order to obtain a feasible solution, the heuristic rounds up the capacity of all links from 10 Mbps to 56 Mbps, for a total energy cost of $4 \times 0.88 = 3.52$ mW. The exact model, however, avoids the use of the link AB, routing the demand AB through the links AC, CD, DB, for an overall energy cost of $3 \times 0.88 = 2.64$ mW. Starting from the relaxation solution, the hybrid algorithm can also find this optimal solution by rounding up the capacity of the links AC, CD, DB, while pruning down the capacity of the link AB.

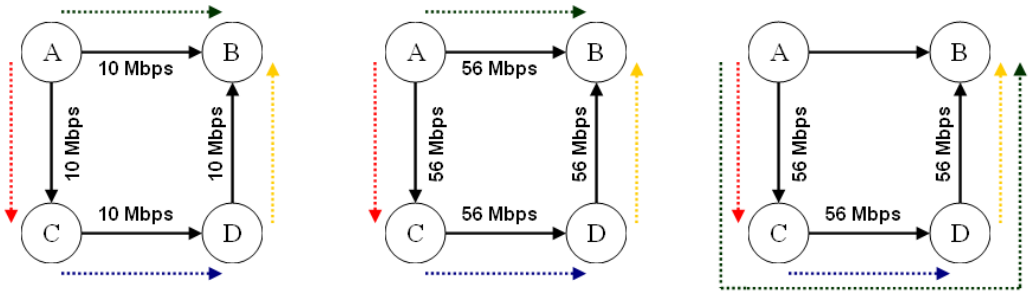

(a) Relaxation (b) Heuristic (c) Hybrid

Figure 4.6: Example of solutions obtained by the different methods.

Conceptually, the hybrid algorithm prescribes the integration of two components, as illustrated in Figure 4.7. A metaheuristic engine implemented in the form of a simulated annealing (SA) algorithm [KGV83] works as a generator of possible network's radio configurations, according to the basic idea described before and having as a starting point the heuristic solution based on the fractional optimum. From every network's configuration, we can derive a multicommodity flow (MCF) problem instance. These instances, in turn, are solved by an exact method (viz., linear programming (LP) solver) that acts as a filter to the metaheuristic search process, attesting the feasibility of each MCF instance and, as a straightforward consequence, of the network's configuration. Finally, the best solution obtained throughout the whole metaheuristic process is deemed to be the final solution to the problem.

In our implementation of the SA algorithm, we consider that each microwave link possesses only one or two possible configurations, according to what follows. On the condition that the traffic volume through a link (given by the optimal solution of the relaxation model) already meets the capacity of a power-efficient configuration, we keep this configuration throughout the entire process. Otherwise, we

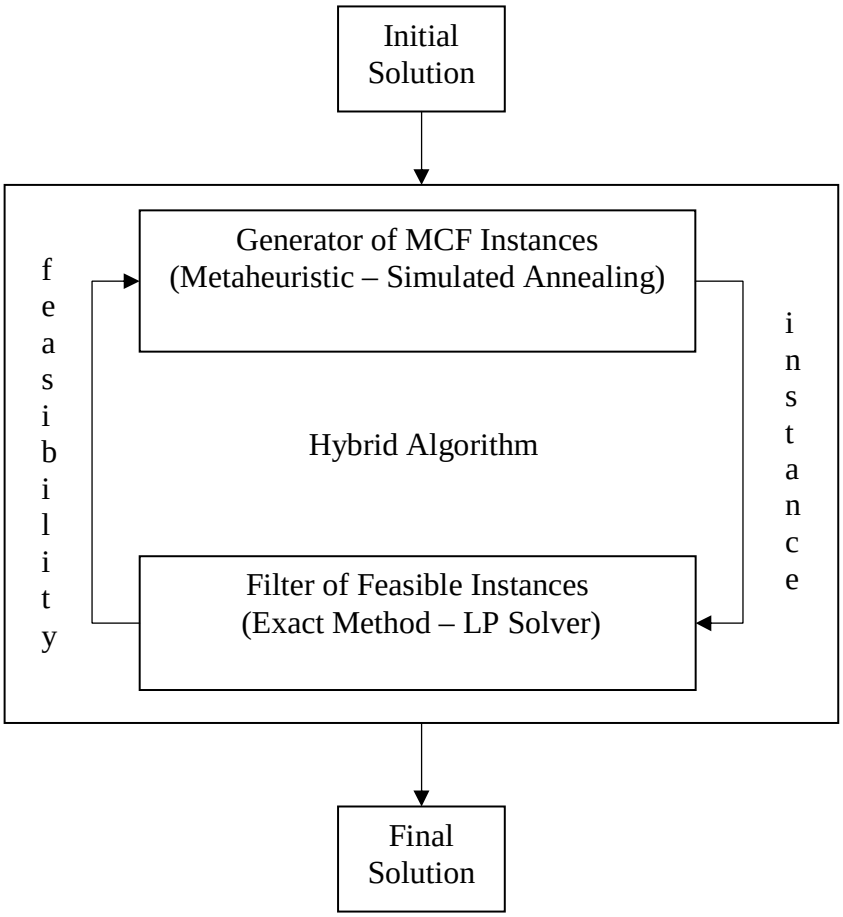

Figure 4.7: Conceptualization of the hybrid algorithm.

consider the two power-efficient configurations that are derived from the rounding up and pruning down operations. Thus, the search space of the metaheuristic becomes limited to a subset of possible network's radio configurations. More precisely, the cardinality of the search space is given by 2^n, where n is the number of links whose flows do not meet the capacity of a power-efficient configuration.

At each iteration of the simulated annealing process, a new network configuration is generated from the current solution by switching the configuration of a single link randomly chosen (among those that present two possible configurations). Then, we apply the filter to check if this new configuration leads to a feasible solution. In the affirmative case, we attribute the total power utilization as energy score value of this solution. Otherwise, we generate another network configuration. We then follow the original description of the simulated annealing process [KGV83], where the algorithm replaces the current solution by the new solution with a probability that depends on the difference between the corresponding energy score values and a global parameter T (called the temperature).

4.4 Computational results

To testify the potentialities behind the novel approach, we have performed computational experiments on standard benchmark grid instances [LY04] (available at http://www.di.unipi.it/optimize/Data/MMCF.html). We take into account the 5×5 grid instance (25 base transceiver stations and 80 directional microwave links) with 50 demands and the 10×10 grid instance (100 base transceiver stations and 360 directional microwave links) with 100 demands.

With respect to the radio scenario, we consider that the base transceiver stations use directional antennas, the transceiver devices present identical characteristics, and all microwave links are operated at the same frequency and bandwidth. We assume here the free-space path loss attenuation model and do not consider interference, but receiver noise. The following parameters are assumed:

- Channel Bandwidth: 28 MHz;
- Operated Frequency: 13 GHz;
- Antenna Gain: 30 dBi;
- Receiver Sensitivity: -90 dBm;
- Distance: 1,000 m.

By means of a link budget, we can then compute the information related to the power-efficient configurations. Table 4.1 shows the modulation schemes supported, along with the channel capacities, the transmission power levels, the marginal energy costs, and the SNR requirements for a BER of 10^{-6}.

Table 4.1: Power-efficient configurations data.

Modulation	Capacity	Power	Marginal Cost	SNR
QPSK	56 Mbps	0.88 mW	0.016 mW	14.21 dB
16-QAM	112 Mbps	4.20 mW	0.059 mW	21.02 dB
32-QAM	140 Mbps	11.10 mW	0.247 mW	25.24 dB
64-QAM	168 Mbps	18.47 mW	0.263 mW	27.45 dB
128-QAM	196 Mbps	42.81 mW	0.869 mW	31.10 dB
256-QAM	224 Mbps	79.34 mW	1.305 mW	33.78 dB

We used IBM ILOG CPLEX 12.1 [CPL10] as ILP solver to execute both the exact formulation and the model relaxation, as well as to implement the filter of the hybrid algorithm. As we adopted a time limit of two hours of computation for the exact formulation, the best feasible solutions found within this limit (from now on referred to as integer solutions) are not supposed to be optimal. The same time limit was assumed to the hybrid algorithm. On the other hand, few seconds of

computation are required to solve the model relaxation and generate basic heuristic solutions. The relaxation solutions yield lower bounds on the power utilization, however they do not represent possible network radio configurations. Conversely the integer, heuristic and hybrid solutions correspond to practical network radio configurations.

In order to observe the evolution of the power utilization as a function of the traffic amount, we have multiplied the demand matrix by a traffic volume factor λ, initiated at 0.05 and increased by 0.05 until the network's infrastructure does not support all the traffic volume anymore. As illustrated in Figure 4.8, the total power utilization evolves exponentially as the traffic volume increases.

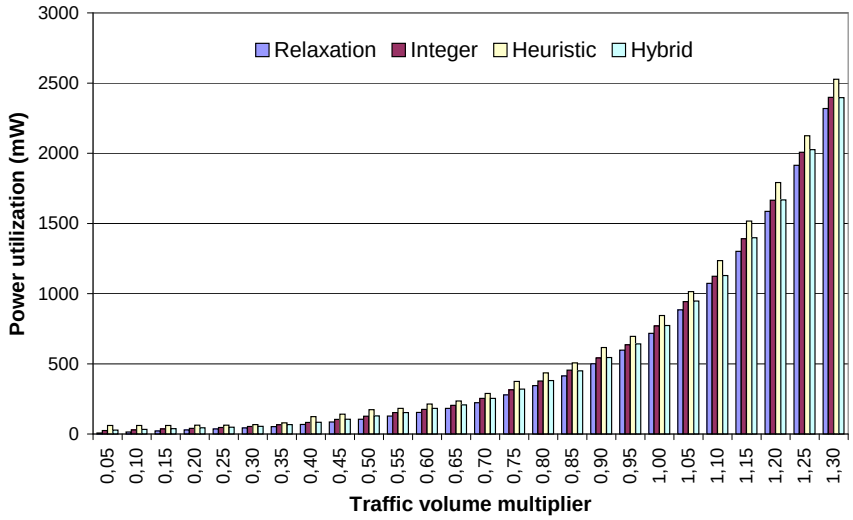

(a) Grid 5×5

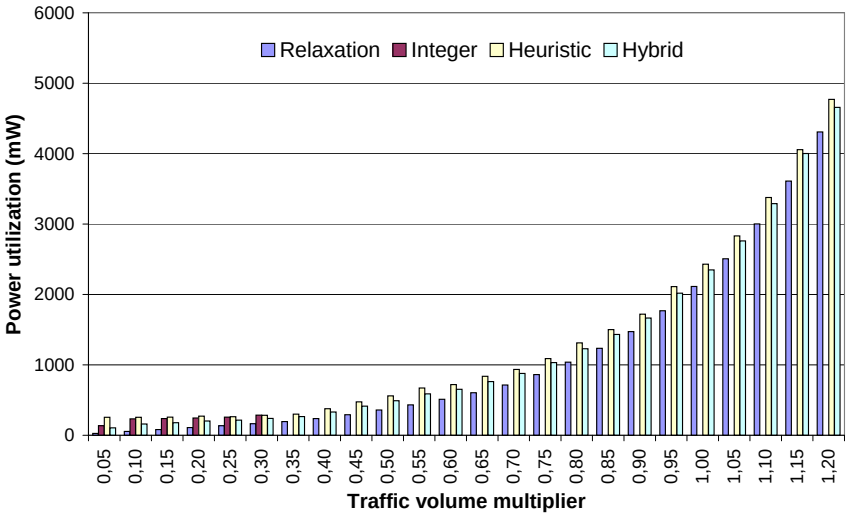

(b) Grid 10×10

Figure 4.8: Power utilization as a function of the traffic volume.

Figure 4.9 illustrates the gap of the hybrid solutions compared to both the relaxation and integer solutions. Remember that the relaxation solutions just give lower bounds on the power utilization, and the integer ones are the best feasible solutions found for the exact formulation within the time limit assumed.

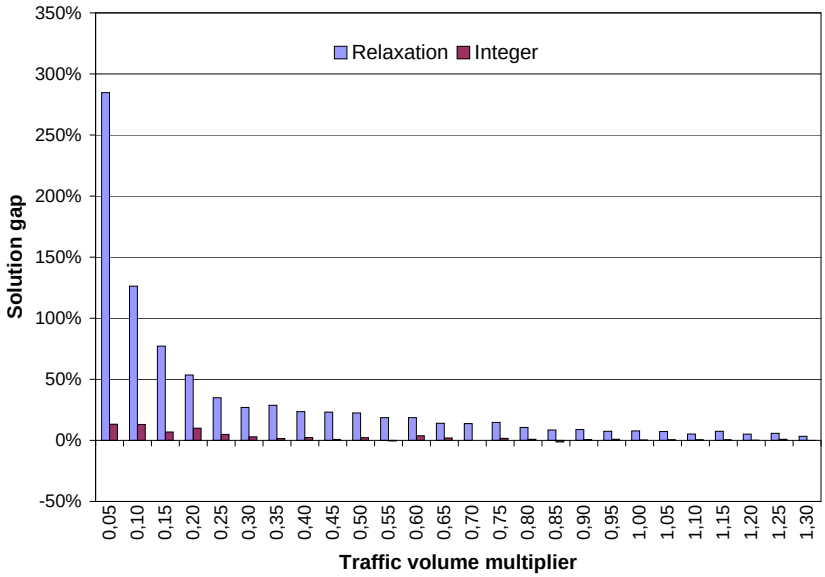

(a) Grid 5×5

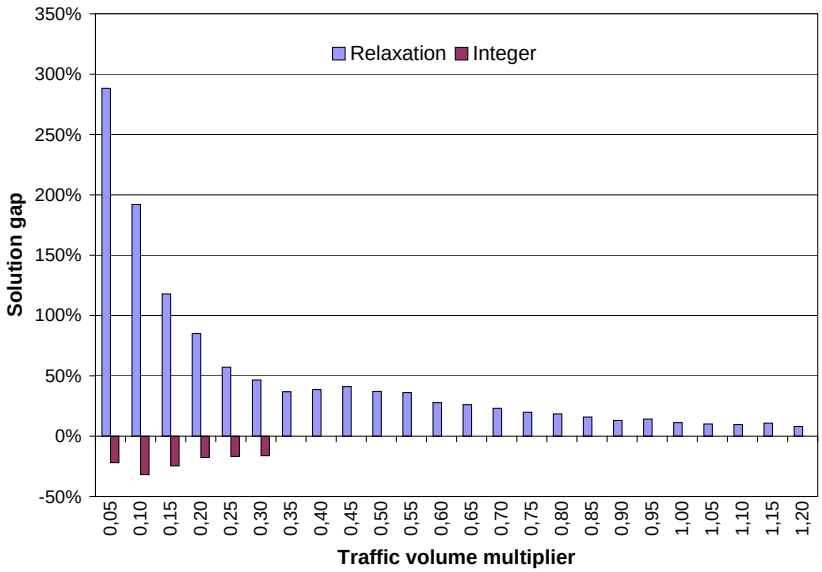

(b) Grid 10×10

Figure 4.9: Power utilization gap as a function of the traffic volume.

Note that the gap between the power utilization of the hybrid and relaxation solutions abruptly decreases as the network becomes more charged. The hybrid algorithm also induces a very satisfactory integrality gap (difference between the power utilization of the hybrid and integer solutions in terms of percent of the power utilization of the integer solution), particularly for instances on which the amount of traffic is not small.

The exact approach performed well for all 5×5 grid instances, providing good integer solutions within 2 hours of computation. However, for the 10×10 grid instances, integer solutions were found just for the first six cases. Moreover, the quality of these solutions was not satisfactory. These problem instances are associated with huge search spaces, and the ILP solver could not keep up with the task of exploring well some promising regions within the time limit. None of the integer solutions was proven to be optimal.

Heuristic feasible solutions based on the fractional optimum of the model relaxation were generated for all problem instances, and the execution time has never exceeded a few seconds. As a drawback, instances on which the network's traffic was small have not presented good heuristic solutions. The hybrid algorithm, in turn, clearly improved the heuristic solutions. In addition, for large instances, the hybrid algorithm achieves solutions that are even better than the integer ones.

These results are evidenced by the graphical representation of the solutions, as illustrated in Figures 4.10– 4.13. The figures show the different solutions, side by side, achieved by each method. In this representation, each arc is labelled by its capacity. The dash-dotted arcs (in red) of the heuristic solutions represent the links that have their capacity pruned down by the hybrid algorithm. On the other hand, the dashed arcs (in blue) of the hybrid and integer solutions represent the links of each of these solutions that operate at higher configuration levels with respect to each other.

For a small traffic volume (Figure 4.10), the basic heuristic is inefficient mainly because the relaxation blindly spreads the traffic among several radio links. Therefore, by rounding up the links' capacity, many links may use a higher modulation level to carry a small extra amount of traffic that could be routed through other links. The hybrid algorithm, in turn, has overcome this difficulty by aggregating the traffic flow. Moreover, despite the fact that the hybrid and integer solutions present very different link distributions, they are both basically composed of connected oriented circuits.

As the traffic volume increases (Figures 4.11 and 4.12), the network configurations become more and more similar. Nevertheless, the hybrid algorithm can still fine-tune the heuristic solutions to achieve results as good as the integer method. Finally, for large instances (Figure 4.13), the hybrid algorithm copes better with the problem complexity than the integer approach.

In general, the computational results show that the hybrid method overachieves the heuristic algorithm (reducing the total power utilization of the basic heuristic solutions) and the exact approach (solving instances that are not

reachable by executing the exact mathematical model and finding better solutions within the same execution time for large instances).

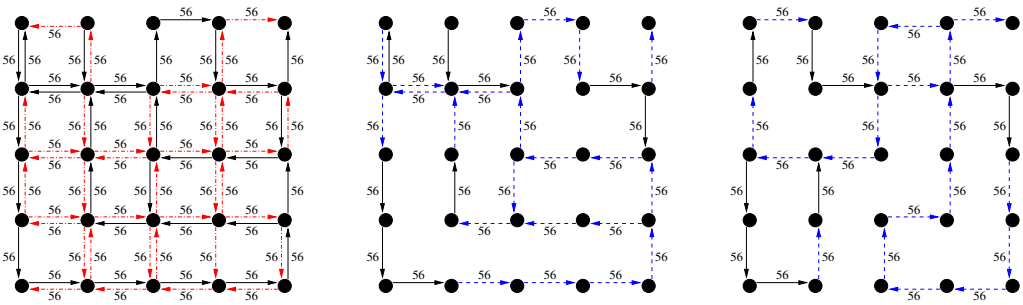

(a) Heuristic (b) Hybrid (c) Integer

Figure 4.10: Very different solutions (Grid 5×5, $\lambda = 0.05$).

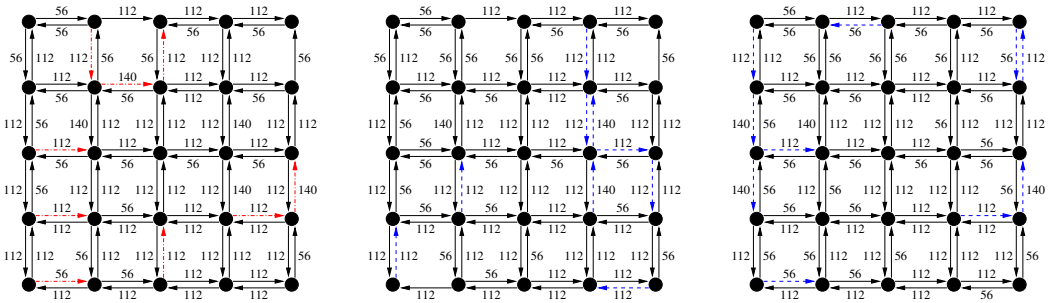

(a) Heuristic (b) Hybrid (c) Integer

Figure 4.11: Similar solutions (Grid 5×5, $\lambda = 0.70$).

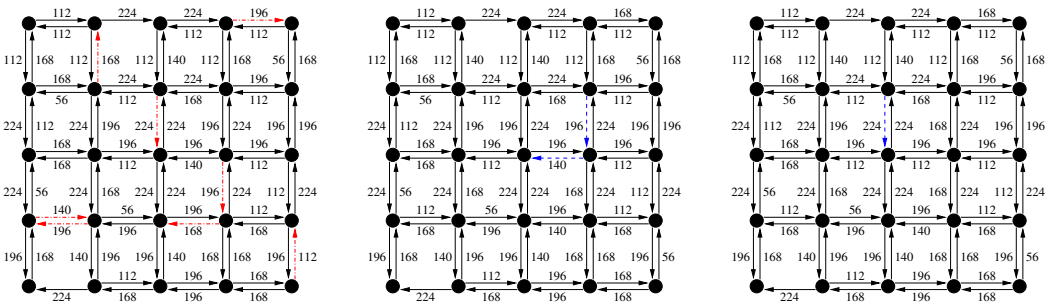

(a) Heuristic (b) Hybrid (c) Integer

Figure 4.12: Very similar solutions (Grid 5×5, $\lambda = 1.30$).

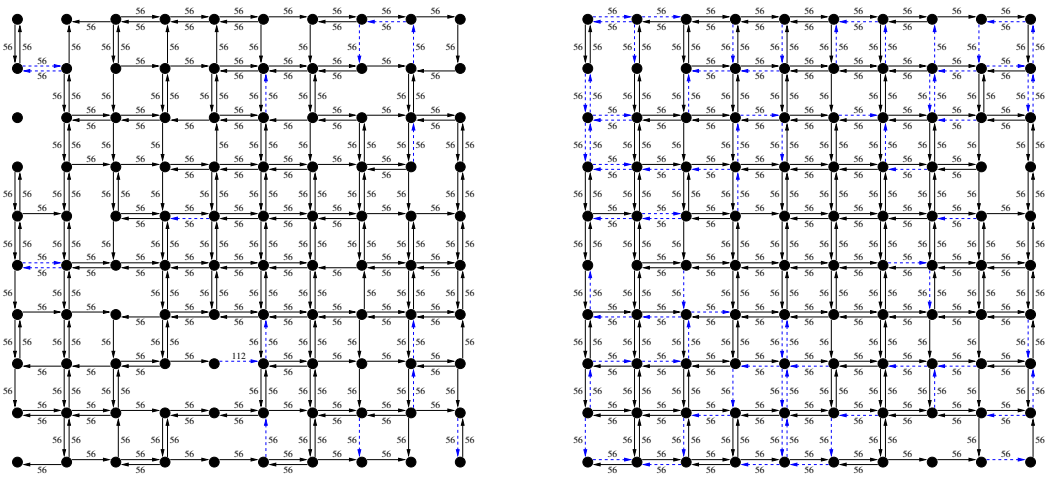

(a) Hybrid (b) Integer

Figure 4.13: Bad integer solution (Grid 10×10, $\lambda = 0.30$).

4.5 Conclusion

In this chapter, we have presented mathematical formulations for determining feasible radio configurations in microwave backhaul networks, focusing on power efficiency. We introduced a joint optimization of data routing and radio configuration that minimizes the total power utilization while handling all the traffic requirements simultaneously. In particular, we proposed an approximation of the power utilization on the links by a piecewise linear convex cost function. A heuristic based on the fractional optimum was applied to generate feasible solutions. Finally, we introduced a hybrid algorithm to improve radio configuration solutions.

The basic idea behind our approach is to provide a power-aware solution that takes advantage of the traffic fluctuation to keep power-efficient radio configurations. Besides increasing the potential for frequency reuse and reducing possible interference to neighboring systems, this approach can also improve the performance of the operator's own system since it favors the use of more robust modulation schemes whenever possible. In view of the scenarios to come, given the expected high density of sites for 4G systems, this approach is of critical importance to ensure the proper functioning of the telecommunications infrastructure necessary to support the growing demand for wireless broadband services.

Nevertheless, note that this method presents rather modest energy savings compared to those achieved by switching off communication devices [CMN09, IOR+10]. In fact, the operation of outdoor and indoor units represents the bulk of the energy consumption of microwave radio systems. The impact of saving energy is significant, particularly in the developing world where energy is a scarce resource. In this sense, we have some preliminary work, in collaboration with David Coudert and Issam Tahiri from Mascotte team. Basically, we investigate on

saving energy by selectively turning off idle ODU and IDU communication devices in low-demand scenarios.

Finally, given the computational complexity of the problem studied in this chapter and knowing the necessity of obtaining efficient solutions in a more reasonable time, we conducted a performance study to investigate alternative models and solution methods to cope with the task of finding power-efficient configurations in microwave backhaul networks. This study is presented in the following chapter.

CHAPTER 5

Reoptimizing power-efficient configurations

In this chapter, we revisit the mathematical formulations related to the power-efficient configuration problem. The main goal here is to obtain alternative mathematical formulations aiming at reducing the execution time of the problem solving. Actually, given the dynamic nature of this problem (since an optimal network configuration for a given scenario may quickly become inefficient with changes in the traffic requirements), we need to generate power-efficient network configurations in a more reasonable time, even though we cannot provide any sort of guarantee of the optimality of solutions.

Therefore, our study is mainly directed towards the improvement of the convexification-based relaxation that we have proposed for this problem in the previous chapter. First, we show the advantages of our relaxation compared to a classical linear relaxation of the exact formulation, and present computational results that corroborate the gain in terms of time efficiency obtained by using the convexification-based relaxation. Then, we introduce some modifications in this formulation that reduces the number of decision variables and thus the problem dimension. Moreover, we apply classical optimization techniques (viz., lagrangian relaxation and Benders' decomposition) that are commonly used to tackle multi-commodity network design problems [Hol95, SP00, LY04, CCG09, BCC10].

The remainder of this chapter is organized as follows. In Section 5.1, we present a performance study of the different mathematical formulations proposed in Chapter 4 for the power-efficient configuration problem. In Section 5.2, we provide several refinements to the previous formulations aiming at reducing the execution time of the problem solving. In Section 5.3, we implement a lagrangian relaxation of the convexification-based formulation. Finally, in Section 5.4, we present a Benders' decomposition formulation to the exact mathematical model.

5.1 Performance investigation

In this section, we present a performance investigation of the mathematical formulations introduced in Chapter 4. Let us first retrieve the exact mathematical formulation with discontinuous step increasing cost functions on the links.

$$\min \sum_{uv \in E} \sum_{m=1}^{M_{uv}} c_{uv}^{m} y_{uv}^{m} \tag{5.1}$$

$$s.t. \sum_{u \in \delta^{-}(v)} \sum_{m=1}^{M_{uv}} x_{uv}^{mk} - \sum_{u \in \delta^{+}(v)} \sum_{m=1}^{M_{vu}} x_{vu}^{mk} = \begin{cases} -d^{k}, & \text{if } v = s^{k}, \\ d^{k}, & \text{if } v = t^{k}, \\ 0, & \text{otherwise} \end{cases} \quad \begin{matrix} \forall v \in V, \\ k = 1 \ldots K \end{matrix} \tag{5.2}$$

$$\sum_{k=1}^{K} x_{uv}^{mk} \leq b_{uv}^{m} y_{uv}^{m} \quad \begin{matrix} \forall uv \in E, \\ m = 1 \ldots M_{uv} \end{matrix} \tag{5.3}$$

$$\sum_{m=1}^{M_{uv}} y_{uv}^{m} \leq 1 \quad \forall uv \in E \tag{5.4}$$

$$x_{uv}^{mk} \in \mathbb{R}^{+}, y_{uv}^{m} \in \{0, 1\} \tag{5.5}$$

In this formulation, the number of continuous and binary variables can be respectively defined by $|E| \cdot M \cdot K$ and $|E| \cdot M$ (assuming that $M_{uv} = M, \forall uv \in E$). The parameters $|E|$ and K are closely related to the size of the network, while the parameter M is defined for the number of modulation schemes available to the microwave radio system (normally a small set). Therefore, for each microwave link, the radio configuration is associated with a discrete space of power-efficient solutions (as illustrated in Figure 5.1).

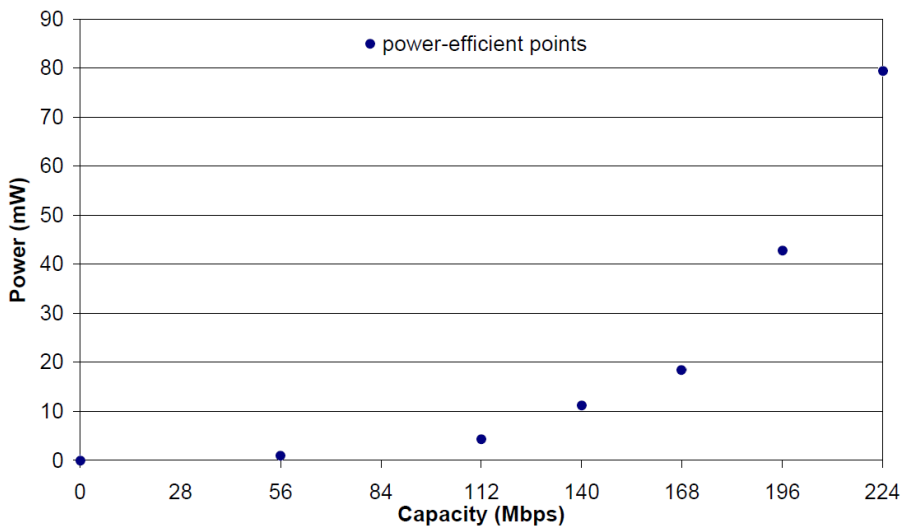

Figure 5.1: Power-efficient configuration points.

As previously discussed, this formulation results in large scale integer linear programs for practical instances, which are very difficult to solve. In order to obtain a lower bound on the total power utilization (and obtain useful information to generate possible network configurations), we can apply a classical linear programming relaxation of this formulation, substituting constraints (5.5) for:

$$x_{uv}^{mk} \in \mathbb{R}^{+}, y_{uv}^{m} \in [0,1] \tag{5.6}$$

In this formulation, we do not consider binary variables anymore, and the number of continuous variables becomes $|E| \cdot M \cdot (K+1)$. For each microwave link, the radio configuration is now defined by a convex linear combination of power-efficient solutions, as illustrated in Figure 5.2. Note that every feasible link configuration for this relaxation – which can or not represent a valid configuration for the exact formulation – is dominated by a configuration obtained from a convex linear combination of two successive (w.r.t the modulation level) power-efficient points. Graphically, for a given charge on the link, the optimal configuration solution lies on the faces of the feasible region in red.

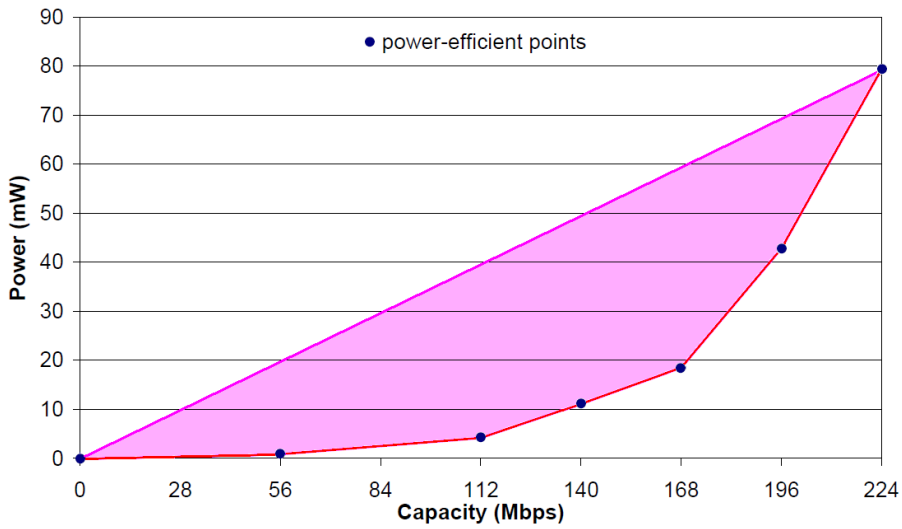

Figure 5.2: Convex linear combination of power-efficient points.

In the sequel, we recall the convexification-based relaxation that makes use of the inherent convex shape of the energy cost functions on the links.

$$\min \sum_{uv \in E} \sum_{m=1}^{M_{uv}} \sum_{k=1}^{K} c_{uv}^{m} x_{uv}^{mk} \tag{5.7}$$

$$s.t. \sum_{u \in \delta^{-}(v)} \sum_{m=1}^{M_{uv}} x_{uv}^{mk} - \sum_{u \in \delta^{+}(v)} \sum_{m=1}^{M_{vu}} x_{vu}^{mk} = \begin{cases} -d^{k}, & \text{if } v = s^{k}, \\ d^{k}, & \text{if } v = t^{k}, \\ 0, & \text{otherwise} \end{cases} \quad \forall v \in V, \; k = 1 \ldots K \tag{5.8}$$

$$\sum_{k=1}^{K} x_{uv}^{mk} \leq b_{uv}^{m} \quad \forall uv \in E, \; m = 1 \ldots M_{uv} \tag{5.9}$$

$$x_{uv}^{mk} \in \mathbb{R}^{+} \tag{5.10}$$

The main advantage of this relaxation consists in reducing the number of variables ($|E| \times M \times K$, instead of $|E| \cdot M \cdot (K+1)$ of the classical linear relaxation) while keeping the problem structure. Note that now every feasible link configuration for this relaxation – which again can or not correspond to a valid configuration for the exact formulation and then a valid radio configuration in practice – can represent an optimal solution, each of them associated with a given level of capacity on the link (as illustrated in Figure 5.3).

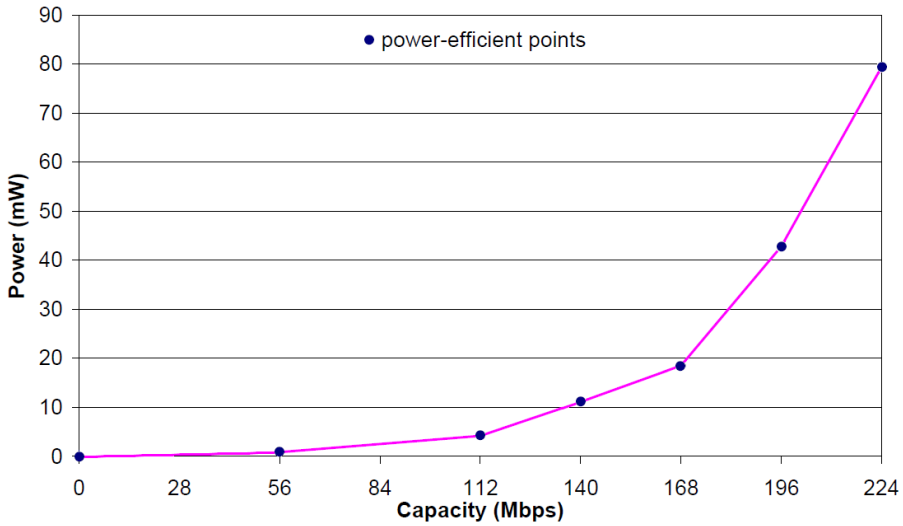

Figure 5.3: Piecewise linear convex combination of power-efficient points.

In order to compare the performance of these relaxations, we carried out computational tests on the standard benchmark grid instances used in the previous chapter. As illustrated in Figure 5.4, the convexification-based relaxation is more time-efficient than the classical linear relaxation.

For the 5×5 grid instances, the execution time of the convexification-based relaxation has never exceeded 1 second, while it has attained 4 seconds for the linear programming relaxation in high-demand scenarios. The 10×10 grid instances are more time-consuming (especially in high-demand scenarios). For these instances, the execution time of the convexification-based relaxation has never exceeded 5 minutes, while it has surpassed 10 minutes for the linear programming relaxation. It is interesting to note that, in low-demand scenarios (when the potential for power mitigation is more important), the convexification-based formulation remained very time-efficient.

5.2 Relaxation improvements

In this section, we propose some refinements to the convexification-based relaxation to reduce the problem size and improve execution performance. In the fol-

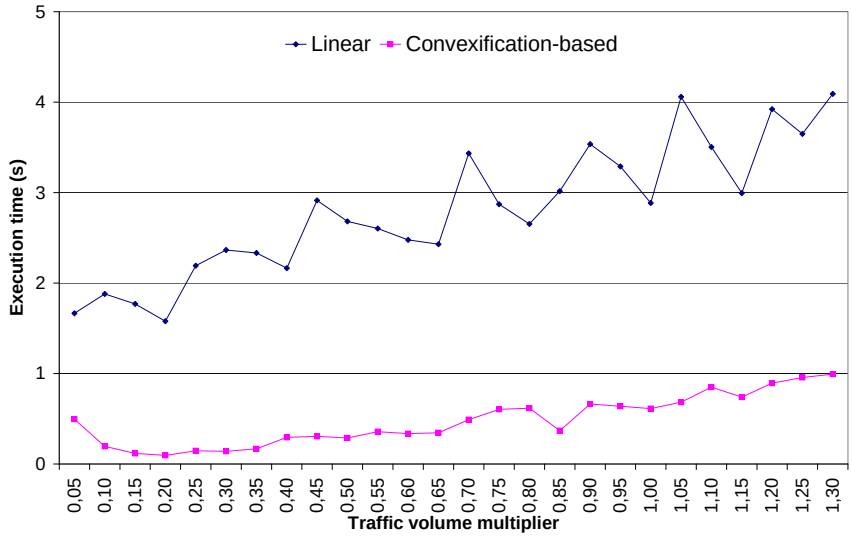

(a) Grid 5×5

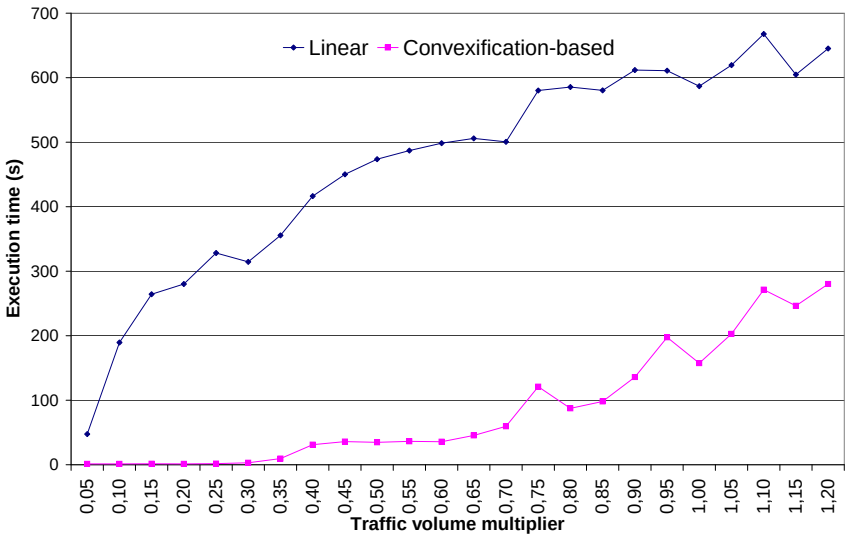

(b) Grid 10×10

Figure 5.4: Execution time for linear and convexification-based relaxations.

lowing, we still use the fact that the marginal energy cost for higher configurations is always increasing, which ensures an utilization of the arcs from the lowest configuration level to the highest one (considering the progressive multi-arc representation of a microwave link). But now x_{uv}^k represents the flow on the arc uv with respect to the traffic requirement k regardless the configuration level. Therefore, to determine the network radio configuration, we need to introduce a new variable z_{uv}^m that represents, for each arc uv, the used capacity with respect to the link configuration m. The optimization problem can be reformulated as follows:

$$\min \sum_{uv \in E} \sum_{m=1}^{M_{uv}} c_{uv}^m z_{uv}^m \tag{5.11}$$

$$s.t. \sum_{u \in \delta^-(v)} x_{uv}^k - \sum_{u \in \delta^+(v)} x_{vu}^k = \begin{cases} -d^k, & \text{if } v = s^k, \\ d^k, & \text{if } v = t^k, \\ 0, & \text{otherwise} \end{cases} \quad \begin{array}{r} \forall v \in V, \\ k = 1...K \end{array} \tag{5.12}$$

$$\sum_{k=1}^{K} x_{uv}^k = \sum_{m=1}^{M_{uv}} z_{uv}^m \qquad \forall uv \in E \tag{5.13}$$

$$z_{uv}^m \leq b_{uv}^m \qquad \begin{array}{r} \forall uv \in E, \\ m = 1 \dots M_{uv} \end{array} \tag{5.14}$$

$$x_{uv}^k \in \mathbb{R}^+, z_{uv}^m \in \mathbb{R}^+ \tag{5.15}$$

The total energy cost is given by a continuous linear function (5.11) of the variables z. The flow conservation constraints (5.12) provide the routes for each demand pair. By (5.13), we say that the level of capacity on each microwave link must be equal to the total flow on it. Finally, by (5.14), we guarantee that, through every link, the flow on each configuration level does not exceed its capacity. The number of continuous variables of this formulation can be defined by $|E| \cdot (K + M)$.

We also applied a widely used approach related to the definition of commodities when they present the same routing cost (equal to zero in our problem). In this case, instead of considering an individual commodity for every demand pair, demands are assumed to be aggregated at their source nodes. This approach significantly reduces the problem size. Figure 5.5 shows a comparison of the execution time for the original convexification-based relaxation (Relaxation 1), the reformulation presented in this section without demand aggregation (Relaxation 2), and the reformulation with demand aggregation (Relaxation 3). The refinements introduced in the original convexification-based formulation produce considerable improvements on the problem solving, particularly in high-demand scenarios where the execution time of the original relaxation tends to increase.

5.3 Lagrangian relaxation

In this section, we present a lagrangian relaxation of the original convexification-based formulation. A straightforward lagrangian relaxation of the minimum cost multicommodity flow problem arises if one relaxes the coupling capacity constraints (5.9) and incorporates them into the objective function [Hol95, BCC10]. The main idea is to decompose the problem into independent subproblems, one for each commodity k, which can be solved efficiently in particular cases [Hol95]. Let us associate nonnegative lagrangian variables λ_{uv}^m with constraints (5.9) and apply lagrangian relaxation. The following lagrangian primal problem $LP(\lambda)$ is obtained:

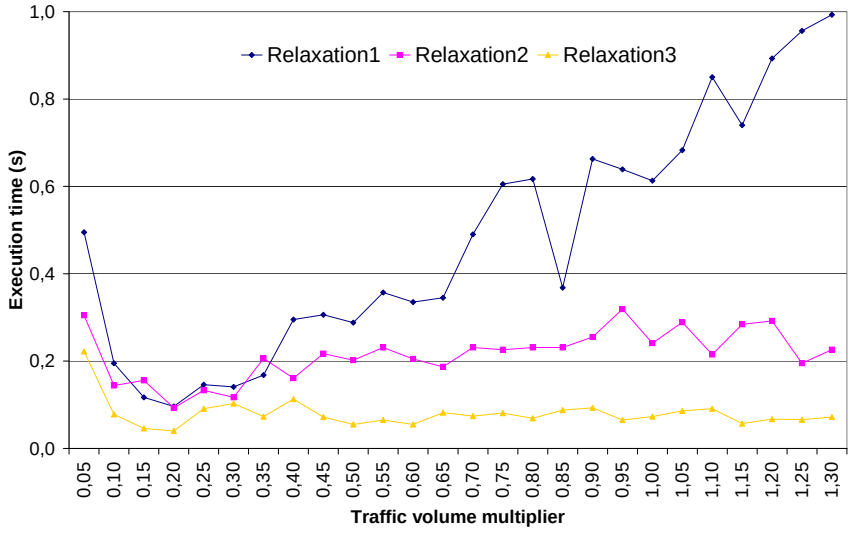

(a) Grid 5×5

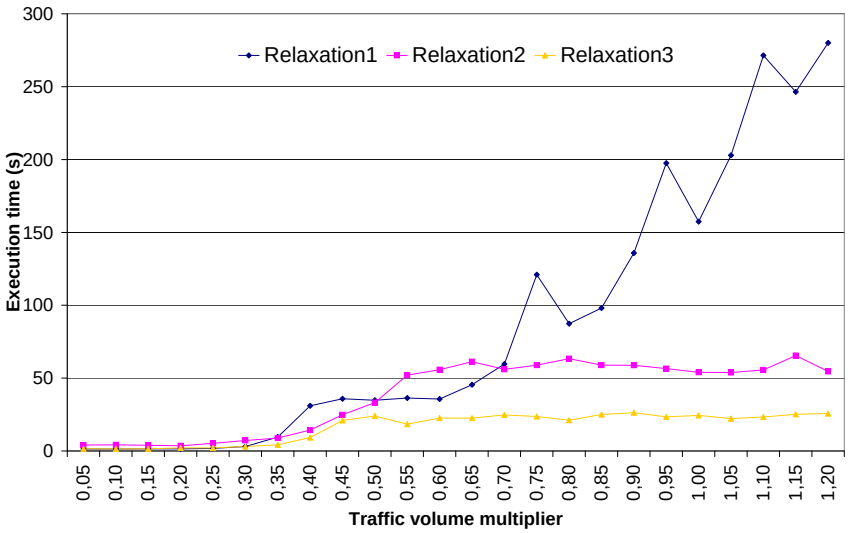

(b) Grid 10×10

Figure 5.5: Execution time for the different relaxations.

$$\min \sum_{uv \in E} \sum_{m=1}^{M_{uv}} \sum_{k=1}^{K} (c_{uv}^m + \lambda_{uv}^m) x_{uv}^{mk} - \sum_{uv \in E} \sum_{m=1}^{M_{uv}} \lambda_{uv}^m b_{uv}^m \tag{5.16}$$

$$s.t. \sum_{u \in \delta^-(v)} \sum_{m=1}^{M_{uv}} x_{uv}^{mk} - \sum_{u \in \delta^+(v)} \sum_{m=1}^{M_{vu}} x_{vu}^{mk} = \begin{cases} -d^k, & \text{if } v = s^k, \\ d^k, & \text{if } v = t^k, \\ 0, & \text{otherwise} \end{cases} \quad \begin{matrix} \forall v \in V, \\ k = 1 \ldots K \end{matrix} \tag{5.17}$$

$$x_{uv}^{mk} \in \mathbb{R}^+ \tag{5.18}$$

Then, the lagrangian dual problem can be written as:

$$D_{LP} = max_{\lambda \geq 0} LP(\lambda) \tag{5.19}$$

The lagrangian dual problem is a nondifferentiable optimization problem that can be approximately solved by any nondifferentiable optimization tool such as subgradient optimization. Subgradient optimization has been used extensively in the literature despite slow convergence and lack of clear stopping criteria [Roc93, Fum01]. In our implementation (see Algorithm 1), we use a subgradient algorithm that starts fixing the value of the lagrangian variables λ and solving for the primal variables x. Then the lagrangian variables are updated based on the violation of the relaxed constraints. The algorithm usually stops when a maximum number of iterations is reached.

Algorithm 1 Subgradient algorithm

```
{Input}
An upper bound LP*
{Initialization}
θ_0 = 2
λ^0 = 0
{Subgradient iterations}
j = 0
while θ_j ≥ 10^(−α) do {stopping criterion}
  γ^j = g(x^j) {gradient of LP(λ^j)}
  t_j = θ_j(LP* − LP(λ^j))/||γ^j||^2 {step size}
  λ^(j+1) = max{0, λ^j + t_j γ^j}
  if ||λ^(j+1) − λ^j|| < ε then
    Stop
  end if
  if no progress in more than β iterations then
    θ_(j+1) = θ_j/2
  else
    θ_(j+1) = θ_j
  end if
  j = j + 1
end while
```

Figure 5.6 shows a comparison of the power utilization bound obtained by the original convexification-based formulation (Relaxation) and the lagrangian relaxation with different parameters and stopping criteria (Lagrangian(α, β)). On the one hand, the lagrangian relaxation with subgradient optimization method clearly converges to the original relaxation solution. On the other hand, we did not obtain time efficiency on the problem solving. As illustrated in Figure 5.7, the original relaxation is solved much faster than the lagrangian relaxation. Actually, different

reasons can explain this behavior. Firstly, we have used the highest network configuration level to obtain the upper bound cost, and a too large value could make the steps too long, and hence slowed down the convergence. Secondly, it is not easy to find the best values for α and β. In general, as these values decrease, the execution time also decreases. However, we have rapidly lost the quality of the relaxation solution for too small values for α and β.

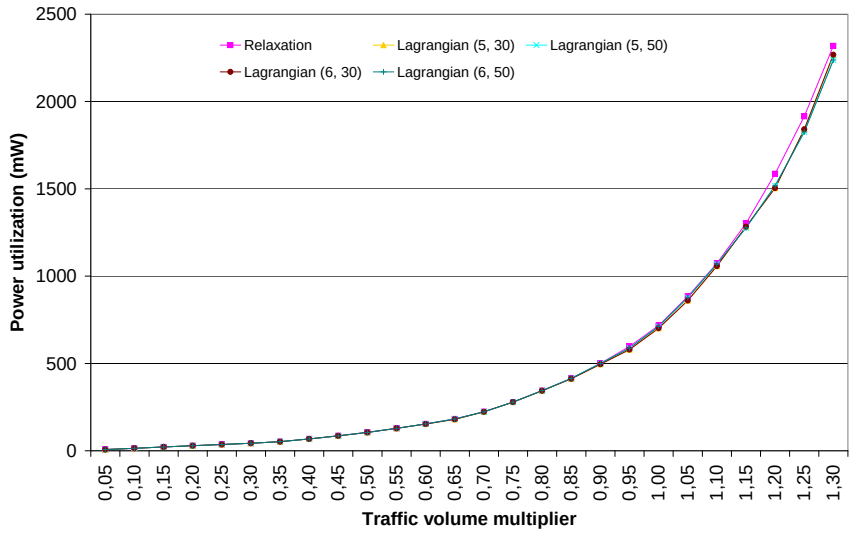

(a) Grid 5×5

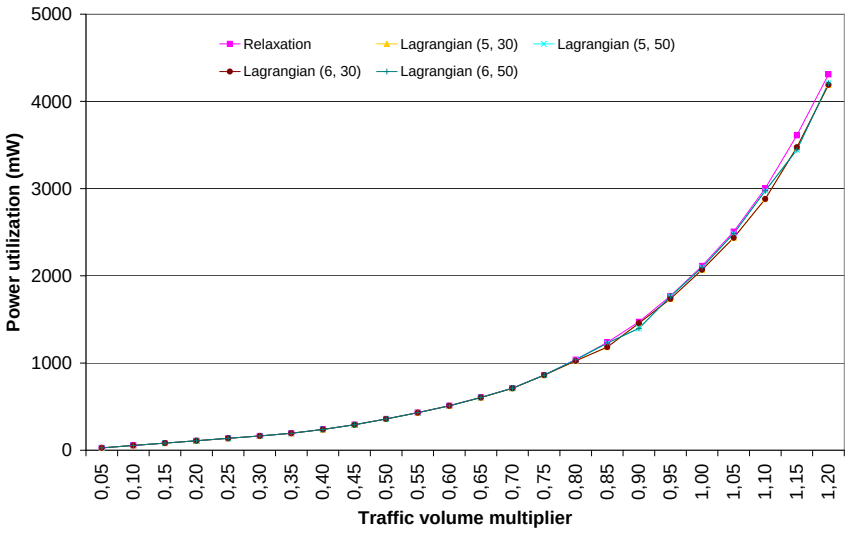

(b) Grid 10×10

Figure 5.6: Convergence of lagrangian relaxations.

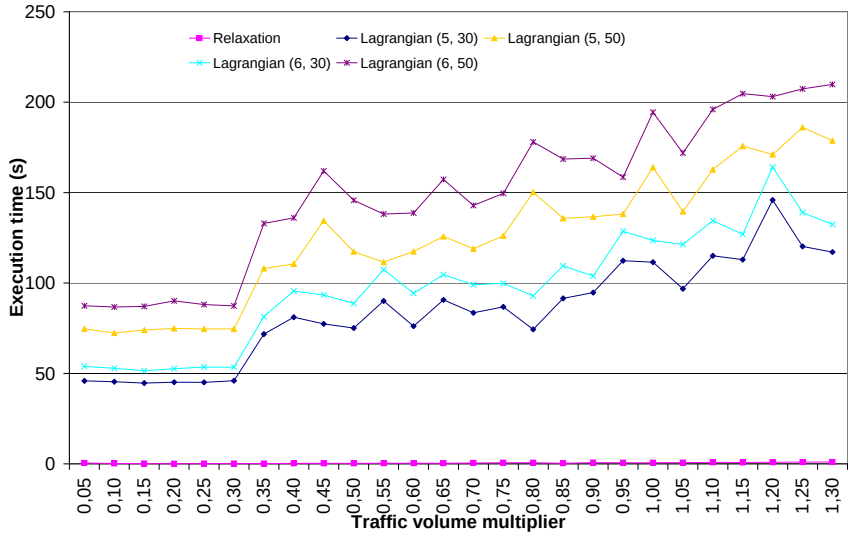

(a) Grid 5×5

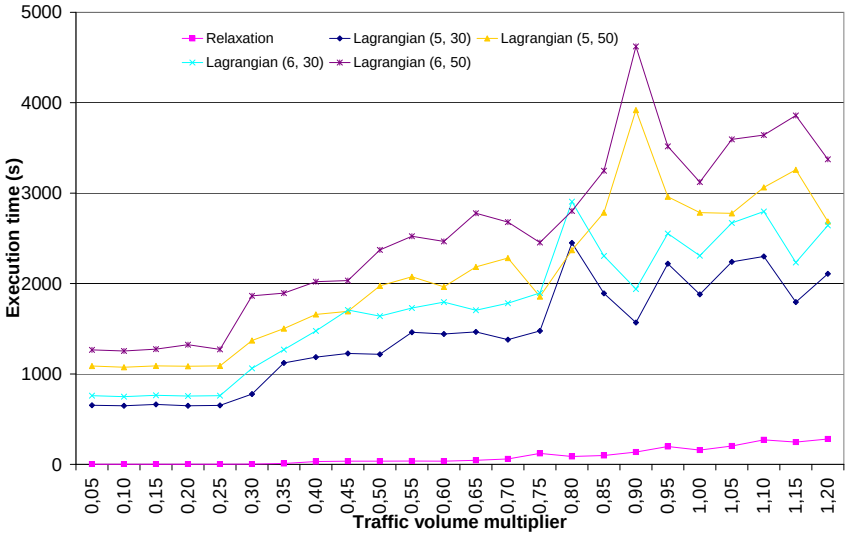

(b) Grid 10×10

Figure 5.7: Execution time for the lagrangian relaxations.

5.4 Benders' decomposition

In this section, we present a Benders' decomposition [Ben62] for the exact formulation with discontinuous step increasing cost functions. Roughly speaking, Benders' decomposition is useful for mixed integer linear programs, when we can distinguish a subset of (integer) variables and decompose the original problem into a master problem involving minimization of the original objective function using only the distinguished variables, and a set of auxiliary problems which iteratively generate inequalities for the master problem.

Note that, in the exact formulation (5.1)– (5.5), the variables x are easily handled as they are continuous in the problem formulation. However, the variables y are constrained to be binary, leading to some difficulty on the problem solving. The basic idea is to partition the original problem into two subproblems (an integer linear program in y and a continuous linear program in x) and use an iterative method to generate only a subset of the constraints for the first subproblem.

Suppose that the vector y is fixed to a given network radio configuration $\overline{y}$. In this case, the objective function reduces to a constant $c\overline{y}$, and we arrive to a simple feasibility program. In other words, the original problem can be rewritten as follows:

$$\min_{y\in\{0,1\}} \left\{ \sum_{uv\in E} \sum_{m=1}^{M_{uv}} c_{uv}^m y_{uv}^m + \min_{x\in\mathbb{R}^+} \{0x : (5.2) - (5.3)\} : (5.4) \right\} \tag{5.20}$$

Let θ_v^k and μ_{uv}^m be the dual variables associated with the constraints (5.2) – (5.3), respectively. Fixing $y = \overline{y}$, the dual of the inner minimization problem (P) is given by the following linear program (D):

$$\max \sum_{v\in V} \sum_{k=1}^{K} f(v,k)\theta_v^k - \sum_{uv\in E} \sum_{m=1}^{M_{uv}} (b_{uv}^m \overline{y}_{uv}^m)\mu_{uv}^m \tag{5.21}$$

$$s.t. \sum_{i\in V} g(uv,i)\theta_i^k - \mu_{uv}^m \leq 0 \qquad \begin{array}{r} \forall uv \in E, \\ m = 1 \ldots M_{uv}, \\ k = 1 \ldots K \end{array} \tag{5.22}$$

$$\theta_i^k \in \mathbb{R}, \mu_{uv}^m \in \mathbb{R}^+ \tag{5.23}$$

where

$$f(v,k) = \begin{cases} -d^k, & \text{if } v = s^k \\ d^k, & \text{if } v = t^k \\ 0, & \text{otherwise} \end{cases}$$

and

$$g(uv,i) = \begin{cases} -1, & \text{if } i = u \\ 1, & \text{if } i = v \\ 0, & \text{otherwise} \end{cases}$$

We have, by strong duality in linear programming, that the primal (P) is feasible if and only if its dual (D) is bounded, since (D) is always feasible. If P_D denotes the feasible domain of (D), it is known that the dual problem (D) is bounded if and only if

$$\sum_{v\in V} \sum_{k=1}^{K} f(v,k)\theta_v^k - \sum_{uv\in E} \sum_{m=1}^{M_{uv}} (b_{uv}^m \overline{y}_{uv}^m)\mu_{uv}^m \leq 0, \quad \forall(\theta,\mu) \in P_D \tag{5.24}$$

We call these the Benders' inequalities (also called a feasibility cut [CCG09]), since they are used as cuts in the Benders' decomposition algorithm. Note that P_D is a full-dimensional polyhedral cone. Any solution in P_D is called a ray.

In the exact formulation (5.1)– (5.5), we can replace (5.2)– (5.3) by the condition (5.24) that states the feasibility of (P). This leads to the pure integer Benders' master problem (M):

$$\min \sum_{uv \in E} \sum_{m=1}^{M_{uv}} c_{uv}^m y_{uv}^m \tag{5.25}$$

$$s.t. \sum_{v \in V} \sum_{k=1}^{K} f(v,k)\theta_v^k - \sum_{uv \in E} \sum_{m=1}^{M_{uv}} (b_{uv}^m y_{uv}^m)\mu_{uv}^m \leq 0, \quad \forall (\theta, \mu) \in P_D \tag{5.26}$$

$$\sum_{m=1}^{M_{uv}} y_{uv}^m \leq 1 \qquad \forall uv \in E \tag{5.27}$$

$$y_{uv}^m \in \{0,1\} \tag{5.28}$$

We can restrict Benders' inequalities to a finite number of such constraints and yet obtain a characterization of the feasibility of (P), since P_D is finitely generated (Theorem 19.1 from [Roc72]). The Benders' decomposition algorithm iteratively generates constraints of (5.26) by obtaining values for the dual variables (θ, μ). For this, we can use an LP solver to solve the multicommodity flow subproblem (P), or its dual (D), at each iteration of the algorithm. The Benders' algorithm first relaxes all feasibility constraints (5.26) in the Benders' master problem. At each iteration, the relaxed master problem provides a lower bound on the optimal solution value of the original problem and a solution y. These variables define a tentative radio configuration for the network, and are used in the dual subproblem.

In case the dual subproblem is unbounded, we can obtain a ray that can be used to generate a violated Benders' inequality. In case the dual subproblem is bounded, the conjunction of the master problem and subproblem solutions is a feasible solution to the original problem (and provides an upper bound). Actually, in this case, this is an optimal solution to the original problem and the extreme point corresponding to the dual optimal solution is obligatory $(\theta, \mu) = (0, 0)$. Therefore, the process iterates until the dual subproblem is bounded, when the values of the lower and upper bounds coincide, and we obtain the optimal network radio configuration.

5.5 Conclusion

In this chapter, we have revisited mathematical formulations for determining feasible radio configurations in microwave backhaul networks. We introduced several refinements to the previous formulations aiming at reducing the execution time of the problem solving. Computational results corroborated the gain in time

efficiency of these improvements. In addition, we implemented a lagrangian relaxation of the convexification-based formulation and presented a Benders' decomposition to the exact formulation based on feasibility constraints generation.

Note that, depending on the scenario of application, the time efficiency plays a key feature of such optimization methods. Today, adaptive modulation and power is now extremely quick, so technically switchovers can be performed even tens of times per second. As a consequence, the heuristic solutions based on the relaxations become more appropriate and could be employed to determine satisfactory power-efficient radio configurations in practice.

CHAPTER 6

Conclusion and perspectives

The increasing demand for bandwidth-intensive services has driven an important development in telecommunications over the last years. With the advances in access technologies, such as WiMAX and LTE, the capacity bottleneck of cellular networks is gradually moving from the radio interface towards the backhaul. Since microwave infrastructure can be deployed rapidly and cost-effectively, it emerges as a key answer to ease backhaul bottlenecks. In fact, business opportunities using microwave is fostering the rise of more capable fixed broadband wireless networks. Nevertheless, backhaul networks available with this technology have received little attention from the scientific community.

In this thesis, we investigated network optimization problems related to the design and configuration of wireless microwave backhaul networks. From a theoretical point of view, the problems studied here are computationally very difficult. And likewise, from a technical point of view, these problems are challenging because of the difficulties inherent to wireless communications, such as the random variations of wireless channels and the dynamic behavior of microwave links. This is the main issue that we addressed in this thesis, nevertheless our contribution is manifold, and it is the result of collaboration with people from different research centers and from the telecommunications industry.

First, we developed a practical activity in close collaboration with the SME 3Roam. The realization of this activity is an optimization tool, *3Link*, for helping engineers on the technical task of conceiving a microwave link. Besides, we studied two interesting applications in wireless microwave backhaul networks. Particularly, we proposed a chance-constrained programming approach to determine the bandwidth assignment for the microwave links of a backhaul network and we introduced heuristic methods combined with linear programming models to generate power-efficient network radio configurations. In parallel, we studied the routing reconfiguration problem that occurs in connection-oriented networks (to be discussed in Appendix A).

However, the field of microwave communications is very large, and many questions that extend across all aspects of this area remain open. For instance, the characterization of wireless channels is a key issue that foments much interest in wireless communications as a whole. Moreover, interfacing the infrastructure of wired networks with the wireless infrastructure with vastly different performance capabilities is still a difficult problem. In addition, the dynamic nature and poor performance of the underlying wireless communication channel require

robust and adaptive network solutions. All these challenges involve interdisciplinary expertise in communications, signal processing, and network design.

In particular, as future research, we are interested in responding some open questions related to the problems discussed in Chapters 3 and 4. For example, with respect to bandwidth assignment for reliable microwave backhaul networks, we consider the random variations into the communications channel, but neglect traffic uncertainty (assuming a static demand matrix). As a natural step, we intend to apply robust optimization approaches to cope with this traffic uncertainty. In addition, we envisage to study other technological solutions used to reduce the vulnerability of wireless networks, such as equipment and frequency diversity. Actually, we think that a global framework which considers the numerous (or at least the main) decisions impacting the design of microwave backhaul networks could be conceived to tackle instances of reasonable size.

With respect to the power-efficient radio configuration problem, many technical questions need to be answered. First, it should be noted that, in reality, adaptive modulation techniques are based on real-time information of the wireless communication channel. Moreover, decisions on the radio configuration are basically taken at the network nodes. Therefore, our approach could be used as a centralized background process (using global information of the network, especially current traffic requirements) to determine the optimal modulation scheme for each microwave link. This network configuration target would be sent to the nodes of the network, while keeping the decisions on the actual radio configuration (based on both information of the communications channel and the configuration target) at the network nodes.

In addition, in collaboration with David Coudert and Issam Tahiri from Mascotte team, we are currently investigating the potential for energy savings in microwave backhaul networks. Since outdoor and indoor units represent the bulk of the energy consumption of microwave radio systems, we aim at saving energy by selectively turning off idle ODU and IDU communication devices in low-demand scenarios. This problem basically relies on a fixed-charge capacitated network design, which is very hard to optimize.

Finally, we have a particular enthusiasm to study alternative models and solution methods to cope better with these challenging optimization problems. The work presented in Chapter 5 is a very first step in this direction. Besides, we intend to carry out theoretical analyses in particular network topologies, such as star, tree, and ring, to obtain optimal solutions and/or bounds to the problems studied here.

APPENDIX A

Tradeoffs in routing reconfiguration problems

We consider a variant of the graph searching games that models the routing reconfiguration problem in WDM networks. In the digraph processing game, a team of agents aims at *processing*, or clearing, the vertices of a digraph D. We are interested in two different measures: 1) the total number of agents used, and 2) the total number of vertices occupied by an agent during the processing of D. These measures respectively correspond to the maximum number of simultaneous connections interrupted and to the total number of interruptions during a routing reconfiguration in a WDM network.

Previous works have studied the problem of independently minimizing each of these parameters. In particular, the corresponding minimization problems are APX-hard, and the first one is known not to be in APX. In this work, we give several complexity results and study tradeoffs between these conflicting objectives. In particular, we show that minimizing one of these parameters while the other is constrained is NP-complete. Then, we prove that there exist some digraphs for which minimizing one of these objectives arbitrarily impairs the quality of the solution for the other one. We show that such bad tradeoffs may happen even for a basic class of digraphs. On the other hand, we exhibit classes of graphs for which good tradeoffs can be achieved. We finally detail the relationship between this game and the routing reconfiguration problem. In particular, we prove that any instance of the processing game, i.e. any digraph, corresponds to an instance of the routing reconfiguration problem.

A.1 Introduction

In this work, we study the *digraph processing* game, analogous to graph searching games [FT08]. This game aims at *processing*, or clearing, the vertices of a contaminated directed graph D. For this, we use a set of agents which are sequentially put and removed from the vertices of D. We are interested in two different measures and their tradeoffs: the minimum number of agents required to *clear* D and the minimum number of vertices that must be *covered* by an agent. The digraph processing game has been introduced in [CPPS05] for its relationship with the routing reconfiguration problem in Wavelength Division Multiplexing (WDM) networks. In this context, the goal is to reroute some connections that are established between pairs of nodes in a communication network, which can lead to interruptions of

service. Each instance of this problem may be represented by a directed graph, called its *dependency digraph*, such that the reconfiguration problem is equivalent to the clearing of the dependency digraph. More precisely, the two measures presented above respectively correspond to the maximum number of simultaneous disruptions, and to the total number of requests disrupted during the rerouting of the connections. The equivalence between these two problems is detailed in Section A.5.

The digraph processing game is defined by the three following operations (or rules), which are very similar to the ones defining the *node search number* [Bre67, DPS02, FT08, KP86, Par78] of a graph, and whose goal is to *process*, or to clear, all the vertices of a digraph D.

R_1 Put an agent at a vertex v of D;

R_2 Remove an agent from a vertex v of D if all its outneighbors are either processed or occupied by an agent, and process v;

R_3 Process an unoccupied vertex v of D if all its outneighbors are either processed or occupied by an agent.

A digraph whose vertices have all been processed is said *processed*. A sequence of such operations resulting in processing all vertices of D is called a *process strategy*. Note that, during a process strategy, an agent that has been removed from a (processed) vertex can be reused. The number of agents used by a strategy on a digraph D is the maximum number of agents present at the same time in D during the process strategy. A vertex is *covered* during a strategy if it is occupied by an agent at some step of the process strategy.

Figure A.1 illustrates two process strategies for a symmetric digraph D of 7 vertices. The strategy depicted in Figure A.1(a) first puts an agent at vertex x_1 (rule R_1), which let y_1 (rule R_3) be processed. A second agent is then put at r (rule R_1) allowing the vertex x_1 to be processed, and the agent on it to be removed (rule R_2). The procedure goes on iteratively, until all the vertices are processed. The depicted strategy uses 2 agents and covers 4 vertices. Another process strategy is depicted in Figure A.1(b) that uses 3 agents and covers 3 vertices. Note that this latter strategy consists in putting agents at the vertices of a feedback vertex set[1] of minimum size.

Clearly, to process a digraph D, it is sufficient to put an agent at every vertex of a feedback vertex set F of D (rule R_1), then the vertices of $V(D) \setminus F$ can be sequentially processed using rule R_3, and finally the vertices of F can be processed and all agents can be removed (rule R_2). In particular, a Directed Acyclic Graph (DAG) can be processed using 0 agent and thus covering no vertices. Indeed, to process a DAG, it is sufficient to process sequentially its vertices starting from the leaves (rule R_3). Note that any process strategy for a digraph D must cover all the vertices

[1] A set F of nodes of D is a feedback vertex set if the removal of all nodes in F makes D acyclic.

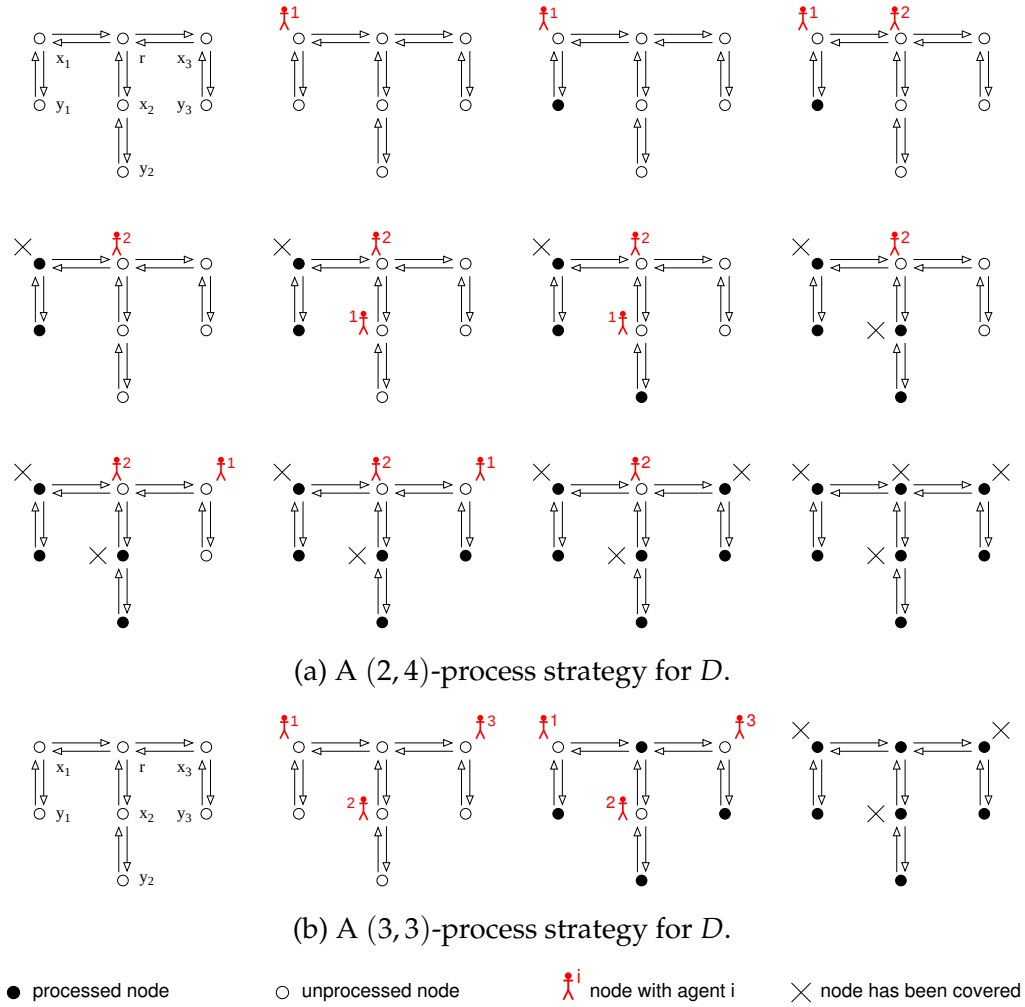

(a) A $(2,4)$-process strategy for D.

(b) A $(3,3)$-process strategy for D.

Figure A.1: Different process strategies for a symmetric digraph D.

of a feedback vertex set of D (not necessarily simultaneously). Obviously, for any process strategy, the number of covered vertices is always at least the number of agents used.

The minimum number of agents required to process a digraph D (without constraint on the number of covered vertices) is called the *process number* [CPPS05, CS07, CHM+09], while the minimum number of covered vertices required to process D (without constraint on the number of agents) equals the size of a *minimum feedback vertex set* of D. In this work, we are interested in trade-offs between the minimum number of agents used by a process strategy and the minimum number of vertices it covers.

A.1.1 Definitions and previous results

Let D be a n-node directed graph. In the following, a (p, q)-*process strategy* for D denotes a process strategy for D using at most p agents and covering at most q vertices. When the number of covered vertices is not constrained, we write (p, ∞)-process strategy. Similarly, when the number of agents is not constrained, we write (∞, q)-process strategy.

Process Number The problem of finding the *process number* of a digraph D, was introduced in [CPPS05] as a metric of the routing reconfiguration problem (see Section A.5). Formally,

Definition 1 *The* process number *of D, denoted by $pn(D)$, is the smallest p such that there exists a (p, ∞)-process strategy for D.*

For instance, the digraph D of Figure A.1 satisfies $pn(D) = 2$. Indeed, Figure A.1(a) describes a process strategy using 2 agents, and it is easy to check that there is no process strategy using at most 1 agent. Digraphs whose process number is equal to 0 or 1 can easily be identified, as they respectively correspond to acyclic digraphs, and to graphs whose strongly connected components have a feedback vertex set of size at most 1 (which can be checked in linear time [CS07]). In [CS07] is also given an polynomial algorithm to recognize digraphs whose process number is equal to 2. However the problem of computing the process number of general digraphs is NP-complete and not in APX (i.e., admitting no polynomial-time approximation algorithm up to a constant factor, unless $P = NP$) [CPPS05]. A distributed polynomial-time algorithm to compute the process number of trees (or forests) with symmetric arcs has been proposed in [CHM08]. Furthermore, a general heuristic to compute the process number of a digraph is described in [CHM+09]. In [Sol09], Solano conjectured that computing the process number of a digraph can be solved, or approximated within a constant factor, in polynomial time if the set of covered vertices is given as part of the input. We disprove this conjecture, showing that computing the process number of a digraph remains not in APX (and so is NP-complete) in this situation (see Theorem 1).

When considering symmetric digraphs, which can be thought of as a directed version of an undirected graph, one notices that the process number is closely related to two other graph invariants, the *node search number* and the *pathwidth*. The node search number of a graph G, denoted by $sn(G)$, is the smallest p such that rules R_1 and R_2 (R_3 is omitted) are sufficient to process G using at most p agents. See [Bre67, DPS02, FT08, KP86, Par78] for more details. The pathwidth of a (undirected) graph G, denoted by $pw(G)$, was introduced by Robertson and Seymour in [RS83]. It has been proved in [EST94] by Ellis *et al.* that the pathwidth and the node search number are equivalent, that is for any graph G, $pw(G) = sn(G) - 1$. The relationship between these parameters and the process number has been described in [CPPS05]: $pw(G) \leq pn(G) \leq pw(G) + 1$ (and so $sn(G) - 1 \leq$

$pn(G) \leq sn(G)$), where $pn(G)$ is the process number of the digraph built from G by replacing each edge by two opposite arcs. Since computing the pathwidth of a graph is NP-complete [MHG+88] and not in APX [DKL87], determining these parameters is as hard.

Minimum Feedback Vertex Set Given a digraph D, the problem of finding a process strategy that minimizes the number of nodes covered by agents is equivalent to the one of computing a *minimum feedback vertex set* (MFVS) of D. Computing such a set is well known to be NP-complete and APX-hard [Kan92]. A 2-approximation algorithm is known in undirected graphs [BBF99] and in symmetric digraph (where a feedback vertex set is a vertex cover of the underlying graph). As far as we know, the best approximation algorithm for computing a MFVS in general n-node digraphs has ratio $\log n \log\log n$ [ENS+95].

We define below the parameter $mfvs(D)$, using the notion of (p,q)-process strategy, corresponding to the size of a MFVS of D.

Definition 2 *Let $mfvs(D)$ denote the smallest q such that there exists a (∞, q)-process strategy for D.*

As an example, the digraph D of Figure A.1 satisfies $mfvs(D) = 3$. Indeed for $i \in \{1,2,3\}$, it is easy to see that either x_i or y_i must be in any feedback vertex set (FVS) of D because of the cycle (x_i, y_i, x_i). Furthermore the removal of x_1, x_2, and x_3 from D is sufficient to break all the cycles. Thus these three nodes form a MFVS of D, and so $mfvs(D) = 3$. The corresponding strategy, covering $mfvs(D) = 3$ nodes by agents, is described in Figure A.1(b).

As mentioned above, $mfvs(D) \geq pn(D)$. Moreover, the gap between these two parameters may be arbitrarily large. For example consider a symmetric path P_n composed of $n \geq 4$ nodes $u_1, u_2, \ldots, u_n$ with symmetric arcs between u_i and u_{i+1} for $i = 1, \ldots, n-1$. We get $mfvs(P_n) = \lfloor \frac{n}{2} \rfloor$ while $pn(P_n) = 2$. Indeed either u_i or u_{i+1} must be in any FVS of P_n, and so we deduce that nodes $u_2, u_4, u_6, \ldots$ form a MFVS of P_n. Furthermore $pn(P_n) \geq 2$ because P_n is strongly connected and $mfvs(P_n) > 1$. We then describe a process strategy for P_n using 2 agents: we put the first agent at u_1 (R_1), we put the second agent at u_2 (R_1), we process u_1 removing the agent from it (R_2), we put this agent at u_3 (R_1), we process u_2 removing the agent from it (R_2), we put an agent at u_4 (R_1), and so on.

Remark that this process strategy for P_n uses the optimal number of agents, $pn(D) = 2$, but all the n nodes are covered by an agent at some step of the process strategy. For this digraph P_n, it is possible to describe a $(pn(D) = 2, mfvs(D) = \lfloor \frac{n}{2} \rfloor)$-process strategy, that is a process strategy for P_n minimizing both the number of agents and the total number of covered nodes. We put the first agent at u_2 (R_1), we process u_1 (R_3), we put the second agent at u_4 (R_1), we process u_3 (R_3), we process u_2 removing the agent from it (R_2), we put this agent at u_6 (R_1), and so on. Unfortunately such good tradeoffs are not always possible (it is the case for the digraph of Figure A.1 as explained later). Actually, we prove in this work that

there exist some digraphs for which minimizing one of these objectives arbitrarily impairs the quality of the solution for the other one. In the following, we define formally the tradeoff metrics we will now study.

Tradeoff Metrics We introduce new tradeoff metrics in order to study the loss one may expect on one parameter when adding a constraint on the other. In particular, what is the minimum number of vertices that must be covered by a process strategy for D using $pn(D)$ agents ? Similarly, what is the minimum number of agents that must be used to process D while covering $mfvs(D)$ vertices ?

Definition 3 *Given an integer $q \geq mfvs(D)$, we denote by $pn_q(D)$ the minimum p such that a (p,q)-process strategy for D exists. We write $pn_{mfvs+r}(D)$ instead of $pn_{mfvs(D)+r}(D)$, $r \geq 0$.*

Definition 4 *Given an integer $p \geq pn(D)$, we denote by $mfvs_p(D)$ the minimum q such that a (p,q)-process strategy for D exists. We write $mfvs_{pn+r}(D)$ instead of $mfvs_{pn(D)+r}(D)$, $r \geq 0$.*

Intuitively $pn_{mfvs}(D)$ is the minimum number of agents required by a process strategy minimizing the number of covered vertices, and $mfvs_{pn}(D)$ is the minimum number of vertices that must be covered by a process strategy using the minimum number of agents. Note that, $pn_{mfvs}(D)$ is upper bounded by the maximum MFVS of the strongly connected components of D. Another straightforward remark is that $mfvs_{mfvs}(D) = mfvs(D)$ for any digraph D.

To illustrate the pertinence of these tradeoff metrics, consider the digraph D of Figure A.1. Recall that $pn(D) = 2$ and $mfvs(D) = 3$. We can easily verify that there does not exist a $(2,3)$-process strategy for D, that is a process strategy minimizing both p and q. On the other hand, we can exhibit a $(2,4)$-process strategy (Figure A.1(a)) and a $(3,3)$-process strategy (Figure A.1(b)) for D. Hence, we have: $pn_{mfvs}(D) = 3$ while $pn(D) = 2$, and $mfvs_{pn}(D) = 4$ while $mfvs(D) = 3$. Intuitively for these two process strategies, we can not decrease the value of one parameter without increasing the other.

We generalize this concept through the notion of *minimal values* of a digraph D. We say that (p,q) is a minimal value of D if $p = pn_q(D)$ and $q = mfvs_p(D)$. Note that $(pn(D), mfvs_{pn}(D))$ and $(pn_{mfvs}(D), mfvs(D))$ are both minimal values by definition (and may be the same). For the digraph of Figure A.1, there are two minimal values: $(2,4)$ and $(3,3)$. Figure A.2 depicts the variations of the minimum number q of vertices covered by a p-strategy for a digraph D ($p \geq pn(D)$), i.e., $mfvs_p(D)$ as a function of p. Clearly, it is a non-increasing function upper bounded by $mfvs_{pn}(D)$ and lower bounded by $mfvs(D)$.

Filled circles of Figure A.2 represent the shape of minimal values of D. Clearly for a given digraph D, the number of minimal values is at most linear in the number of nodes. We now give an example of a family of n-node digraph for which the number of minimal value is $\Omega(\sqrt{n})$. Intuitively, it means that, in those digraphs D,

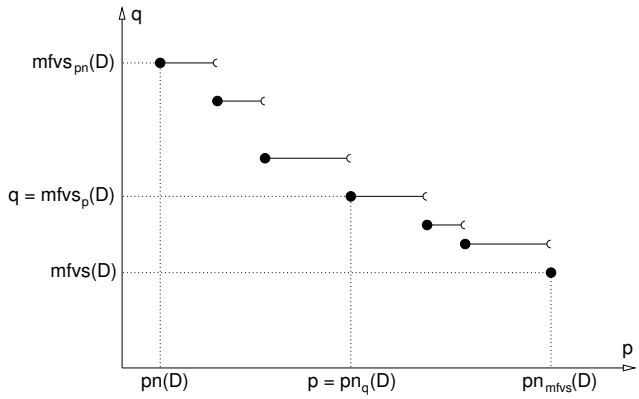

Figure A.2: $mfvs_p(D)$ function of p for a digraph D. Filled circles represent minimal values of D.

starting from the optimal number of agents $pn(D)$, each extra agent added allows to strictly decrease the number of covered vertices, until the optimal, $mfvs(D)$, is reached. Let H_n be the symmetric directed star with $n \geq 3$ branches of length 2 (for instance, H_3 is the digraph of Figure A.1), and let G_k be the graph that consists of the disjoint union of $H_3, \cdots, H_k$, $k \geq 3$. Then, for any $0 \leq i \leq k-2$, $(pn(G_k)+i, mfvs(G_k)+k-2-i) = (2+i, (k(k+1)/2)-5+k-i)$ are minimal values (this can be easily proved using the easy results described in Section A.2.1).

A.1.2 Our results

Our results consist in an analysis of the behaviour of the two given tradeoff measures both in general digraphs and in symmetric digraphs. As mentioned above, in general, no process strategy minimizes both the number of agents and the number of covered vertices (see example in Figure A.1). Hence, we are interested in the loss on one measure when the other is constrained. In particular, we are interested in the ratios $\frac{pn_{mfvs}(D)}{pn(D)}$ and $\frac{mfvs_{pn}(D)}{mfvs(D)}$. This study involves various theorems on the complexity of estimating this loss (Section A.2) and the existence of digraphs for which it can be arbitrarily large (Section A.3). We also study in Section A.4 the case of symmetric digraphs. Finally we describe in Section A.5 the relation between the routing reconfiguration problem and the processing game.

More precisely, we begin by disproving a conjecture from Solano [Sol09] (Theorem 1). Then, we prove that for all $\alpha \in [0,1]$, the problems of determining the parameters $\alpha.pn_{mfvs}(D) + (1-\alpha)pn(D)$ and $\alpha.mfvs_{pn}(D) + (1-\alpha)mfvs(D)$ are NP-complete (Theorem 2). In particular, the problem of determining $pn_{mfvs}(D)$ is not in APX and the problem of determining $mfvs_{pn}(D)$ is APX-hard (Theorem 2). Then, we prove that for any $q \geq 0$ (resp. for any $p \geq 0$), the ratio $\frac{pn_{mfvs+q}(D)}{pn(D)}$ (resp. $\frac{mfvs_{pn+p}(D)}{mfvs(D)}$) is not bounded even in the class of bounded process number digraphs

(Theorem 3 and Theorem 4). However we prove that $\frac{mfvs_{pn}(D)}{mfvs(D)} \leq pn(D)$ for any symmetric digraph D (Lemma 1).

In Section A.5, we detail the relationship between the processing game and the reconfiguration routing problem. In this context, any instance of the routing reconfiguration problem may be represented by a directed graph, called the dependency digraph of this instance, such that the routing reconfiguration problem is equivalent to the processing of this digraph. We prove the reverse, that is, any digraph is the dependency digraph of an instance of the reconfiguration problem (Theorem 5).

A.2 Complexity results

This section is devoted to the study of the complexity of the problems related to the parameters introduced in Section A.1.1. First, we need to define some digraphs.

A.2.1 Definition of some useful digraphs

Let H_n be a symmetric directed star with $n \geq 3$ branches each of which contains two vertices (the root r being at distance 2 from any leaf), with a total of $2n+1$ vertices. H_3 is represented in Figure A.1. It is easy to check that $pn(H_n) = 2$. Indeed 1 agent is obviously not sufficient and there exists a $(2, n+1)$-process strategy for H_n: an agent is put at the central node r, then we successively put an agent at a vertex x adjacent to r, the remaining neighbor of x (different from r) is processed, and we process x itself relieving the agent on it. Then, the same process is applied until all vertices adjacent to r are processed, and finally we process r. Figure A.1(a) represents a $(2,4)$-process strategy for H_3. Moreover, the single MFVS of H_n is the set X of the n vertices adjacent to r. It is easy to check that the single process strategy occupying only the vertices of X consists in putting n agents at all vertices of X. No agent can be removed while all agents have not been put. Thus this strategy is a (n,n)-process strategy, and $pn_{mfvs}(H_n) = n$. See Figure A.1(b) for such a process strategy for H_3. To summarize, the two minimal values of H_n are $(pn(H_n), mfvs_{pn}(H_n)) = (2, n+1)$ and $(pn_{mfvs}(H_n), mfvs(H_n)) = (n,n))$.

Let K_n be a symmetric complete digraph of n nodes. It is easy to check that the unique minimal value of K_n is $(pn(K_n), mfvs(K_n)) = (n-1, n-1)$.

Let $D = (V, A)$ be a symmetric digraph with $V = \{u_1, \ldots, u_n\}$. Let $\hat{D} = (V', A')$ be the symmetric digraph where $V' = V \cup \{v_1, \ldots, v_n\}$, and $\hat{D}$ is obtained from D by adding two symmetric arcs between u_i and v_i for $i = 1, \ldots, n$. It is easy to show that there exists an optimal process strategy for $\hat{D}$ such that the set of occupied vertices is V. Indeed, note that, for all i, at least one of u_i or v_i must be covered by an agent (any FVS of D contains at least one of v_i or u_i). Furthermore if some step of a process strategy for $\hat{D}$ consists in putting an agent at some vertex v_i, then the process strategy can be easily transformed by putting an agent at u_i instead. In particular, $mfvs_{pn}(\hat{D}) = n$.

A.2.2 NP-completeness

Before proving that computing the tradeoff parameters introduced in Section A.1.1 are NP-complete, we disprove a conjecture of Solano about the complexity of computing the process number of a digraph D.

Indeed a possible approach for computing the process number, proposed by Solano in [Sol09], consists of the following two phases: 1) finding the subset of vertices of the digraph at which an agent will be put, and 2) deciding the order in which the agents will be put at these vertices. Solano conjectures that the complexity of the process number problem resides in Phase 1 and that Phase 2 can be solved, or approximated within a constant factor, in polynomial time [Sol09]. We disprove this conjecture :

Theorem 1 *Computing the process number of a digraph is not in APX (and thus NP-complete), even when the subset of vertices of the digraph at which an agent will be put is given.*

Proof. Let D be any symmetric digraph. Let us consider the problem of computing an optimal process strategy for $\hat{D}$ when the set of vertices covered by agents is constrained to be V. By the remark in Section A.2.1, such an optimal strategy always exists. It is easy to check that this problem is equivalent to the one of computing the node search number (and so the pathwidth) of the underlying undirected graph of D which is NP-complete [MHG+88] and not in APX [DKL87]. ■

Theorem 2 *Let $\alpha \in [0,1]$ be fixed. The problem that takes a digraph D as an input and that aims at determining:*

- $\alpha.pn_{mfvs}(D) + (1-\alpha)pn(D)$ *is not in APX,*
- $\alpha.mfvs_{pn}(D) + (1-\alpha)mfvs(D)$ *is APX-hard.*

Proof. The two cases for $\alpha = 0$ clearly holds from the literature.

- We start with $\alpha.pn_{mfvs}(D) + (1-\alpha)pn(D)$.

  Let us first consider the case $\alpha = 1$. That is, let us show that the problem of determining pn_{mfvs} is not in APX. Indeed, let $\mathcal{D}$ be the class of all digraphs $\hat{D}$ obtained from some symmetric digraph D. For any symmetric digraph D, the problem of computing $pw(D)$ (where $pw(D)$ is the pathwidth of the underlying graph of the symmetric digraph of D) is not in APX, and $pn(\hat{D}) = pn_{mfvs}(\hat{D}) = pw(D)+1$ (see Theorem 1). Hence, the problem of determining pn_{mfvs} is not in APX.

  Assume now that $\alpha \in]0,1[$. To prove that determining $\alpha.pn_{mfvs}(D) + (1-\alpha)pn(D)$ is not in APX, let D_1 be the disjoint union of H_n and any n-node digraph D. First, let us note that $pn_{mfvs}(D_1) = pn_{mfvs}(H_n)$ because $pn_{mfvs}(D) \leq n-1$ and $pn_{mfvs}(H_n) = n$. Since $pn(D_1) =$

$\max\{pn(D), pn(H_n)\}$ and $pn(H_n) = 2$, we get that $\alpha.pn_{mfvs}(D_1) + (1-\alpha)pn(D_1) = \alpha.n + (1-\alpha)\max\{pn(D), 2\}$. So, the NP-completeness comes from the NP-completeness of the process number problem.

- We now consider $\alpha.mfvs_{pn}(D) + (1-\alpha)mfvs(D)$.

  When $\alpha = 1$, let us prove that the problem of determining $mfvs_{pn}$ is APX-hard. Let D_2 be the disjoint union of K_n and any n-node digraph D. First let us note that $pn(D_2) = \max\{pn(K_n), pn(D)\}$ because the process number of any digraph is the maximum for the process numbers of its strongly connected components. It is easy to show that $pn(D_2) = pn(K_n) = n-1$ because $pn(D) \leq n-1$. Hence, when D must be processed, $n-1$ agents are available. So, in order to minimize the number of nodes covered by agents, the agents must be placed on a MFVS of D. Thus $mfvs_{pn}(D_2) = n-1+mfvs(D)$, and the result follows because computing $mfvs(D)$ is APX-hard.

  Assume now that $\alpha \in]0,1[$. To prove that determining $\alpha.mfvs_{pn}(D) + (1-\alpha)mfvs(D)$ is APX-hard, let D_3 be the disjoint union of K_n, H_n, and D. Again, $pn(D_3) = \max\{pn(K_n), pn(H_n), pn(D)\}$. It is easy to show that $pn(D_3) = pn(K_n) = n-1$ because $pn(H_n) = 2$ and $pn(D) \leq n-1$. Moreover, any process strategy of D_3 using $n-1$ agents must cover $n-1$ nodes of K_n, $n+1$ nodes of H_n ($mfvs(H_n) = n$ but one extra agent is needed to cover only n nodes), and $mfvs(D)$ nodes of D (because $n-1$ agents are available and $mfvs(D) \leq n-1$). Hence, $mfvs_{pn}(D_3) = (n-1)+(n+1)+mfvs(D)$. Furthermore $mfvs(D_3) = (n-1)+n+mfvs(D)$ because $mfvs(K_n) = n-1$ and $mfvs(H_n) = n$. Thus $\alpha.mfvs_{pn}(D_3) + (1-\alpha)mfvs(D_3) = mfvs(D) + 2n - (1-\alpha)$. The result follows the APX-hardness of the MFVS problem.

■

Corollary 1 *For an input digraph D and two integers $p \geq 0$ and $q \geq 0$, the problems of determining:*

- $\alpha.pn_{mfvs+q}(D) + (1-\alpha)pn(D)$ *are not in APX,*
- $\alpha.mfvs_{pn+p}(D) + (1-\alpha)mfvs(D)$ *are APX-hard.*

A.3 Behaviour of ratios in general digraphs

In this section, we study the behaviours of parameters introduced in Section A.1.1 and their ratios, showing that, in general, good tradeoffs are impossible.

Theorem 3 *For any $C > 0$ and any integer $q \geq 0$, there exists a digraph D such that $\frac{pn_{mfvs+q}(D)}{pn(D)} > C$.*

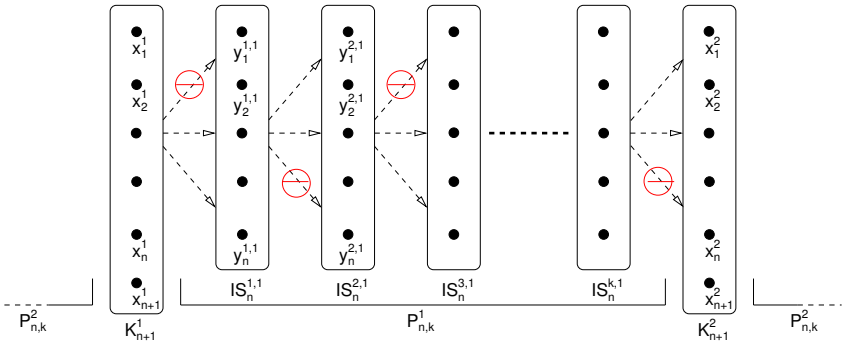

(a) $D_{n,k}$ of Theorem 4 and Corollary 3 (Case k odd). The red symbol $\ominus$ represents the inexistence of arcs between these subgraphs. The arcs from $V(D_{n,k}) \setminus V(K_{n+1}^1)$ to $V(K_{n+1}^1)$ are not represented.

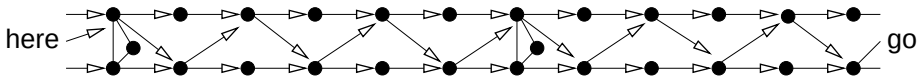

(b) $D_{2,5}$ in Cor. 3 where the arcs from all vertices to one triangle K_3^1 have been omitted.

Figure A.3: Digraph $D_{n,k}$ described in Theorem 4 and Corollary 3.

Proof. Consider the symmetric directed star H_n defined in Section A.2.1. Let now D be the digraph consisting of $q+1$ pairwise disjoint copies of H_n. So D has $q+1$ strongly connected components. We get $mfvs(D) = (q+1)n$. By definition, any $(pn_{mvfs+q}(D), mfvs(D)+q)$-process strategy for D covers at most $q(n+1)+n$ nodes. Therefore, there exists at least one of the $q+1$ strongly connected components for which at most n nodes must be covered. Thus to process this component, n agents are required. Indeed (n,n) is a minimal value of H_n, and by definition we cannot decrease the first value without increasing the second one. Hence, $pn_{mfvs+q}(D) = n$ while $pn(D) = 2$. Taking $n > 2C$, we get $\frac{pn_{mfvs+q}(D)}{pn(D)} > C$. ■

Note that if it is allowed to cover $mfvs(D)+q+1$ nodes during the process strategy (instead of $mfvs(D)+q$), then the number of agents required is $pn(D)$. In other words, for the digraph D described in the proof of Theorem 3, we get $\frac{pn_{mfvs+q+1}(D)}{pn(D)} = 1$ while $\frac{pn_{mfvs+q}(D)}{pn(D)} = \frac{n}{2}$.

Corollary 2 *For any $C > 0$, there exists a digraph D such that $\frac{pn_{mfvs}(D)}{pn(D)} > C$.*

In the sequel, we present similar results for the second ratio.

Theorem 4 *For any $C > 0$ and any integer $p \geq 0$, there exists a digraph D such that $\frac{mfvs_{pn+p}(D)}{mfvs(D)} > C$.*

Proof. Let $n \geq 2$ and let $k \geq 1$ be an odd integer. Let us consider the digraph $D_{n,k}$ built as follows. Let $IS_n^1, \cdots, IS_n^k$ be k independent sets, each IS_n^t ($1 \leq t \leq k$) having n vertices: $y_1^t, y_2^t, \ldots, y_n^t$. Let $P_{n,k}$ be the digraph obtained from the k independent sets IS_n^t ($1 \leq t \leq k$) by adding the arcs from y_i^t to y_j^{t+1}, for $1 \leq j \leq i \leq n$ and $t = 1, 3, \ldots, k-2$, and from y_i^t to y_j^{t+1}, for $1 \leq i \leq j \leq n$ and $t = 2, 4, \ldots, k-1$. Let K_{n+1} be the symmetric clique with $n+1$ nodes: $x_1, x_2, \ldots, x_{n+1}$.

The digraph $D_{n,k}$ is obtained from two copies $P_{n,k}^1, P_{n,k}^2$ of $P_{n,k}$ and two copies K_{n+1}^1, K_{n+1}^2 of K_{n+1}, by adding the following arcs. In what follows, $y_j^{t,a}$ denotes the jth vertex in the tth independent set of $P_{n,k}^a$, where $j \leq n$, $t \in \{1, k\}$, $a \in \{1, 2\}$, and x_j^a denotes the jth vertex of K_n^a, where $j \leq n+1$, $a \in \{1, 2\}$. There are arcs from x_i^a to $y_j^{1,a}$, for $1 \leq i \leq j \leq n$ and $a = 1, 2$, and from $y_i^{k,a}$ to x_j^b, for $1 \leq i \leq j \leq n$, $a = 1, 2$ and $b = 3 - a$. Finally there is an arc from each node of $V(D_{n,k}) \setminus V(K_{n+1}^1)$ to each node of $V(K_{n+1}^1)$. Note that these last arcs are not needed to obtain the results but help make the proof less technical.

Figure A.3(a) shows the general shape of $D_{n,k}$, where the red symbol $\ominus$ represents the inexistence of arcs between these subgraphs. $D_{2,5}$ is depicted in Figure A.3(b). For not overloading the figures, the arcs from $V(D_{n,k}) \setminus V(K_{n+1}^1)$ to $V(K_{n+1}^1)$ are not represented.

Clearly, $mfvs(D_{n,k}) = 2n$, and any MFVS consists of $\{x_1^1, \ldots, x_n^1\}$ plus n vertices of K_{n+1}^2.

First, note that to process one vertex of K_{n+1}^1, there must be a step of any process strategy for $D_{n,k}$ where n agents are simultaneously occupying n nodes of K_{n+1}^1. Hence, $pn(D_{n,k}) \geq n$. Note that, similarly, any process strategy for $D_{n,k}$ must occupy n vertices of K_{n+1}^2. Moreover, because of the arcs from $V(D_{n,k}) \setminus V(K_{n+1}^1)$ to $V(K_{n+1}^1)$, any agent that is placed at some vertex in $V(D_{n,k}) \setminus V(K_{n+1}^1)$ can only be removed when all vertices of K_{n+1}^1 are occupied or processed. Consider any process strategy S for $D_{n,k}$ (in particular, S uses at least n agents) and let s_0 be the first step of S that does not consist in placing an agent at some vertex of K_{n+1}^1. By above remark, after step $s_0 - 1$ of S, n agents are occupying n vertices of $V(K_{n+1}^1)$. Up to reorder the first $s_0 - 1$ steps of S, we obtain a process strategy for $D_{n,k}$ that starts by placing n agents at n vertices of $V(K_{n+1}^1)$, without increasing the number of agents used nor the number of vertices occupied by S. Moreover, if the vertex of $V(K_{n+1}^1)$ that is not occupied is x_i^1 with $i < n+1$, it means that an agent is placed at x_{n+1}^1 during the first n steps of the strategy. Replacing this operation by the placement of an agent at x_i^1 instead of x_{n+1}^1 does not modify the remaining part of the strategy (but the operation "remove the agent from x_{n+1}^1" which is replaced by "remove the agent from x_i^1") since the vertex x_{n+1}^1 can be processed immediately when the n other vertices of K_{n+1}^1 are occupied. Hence, we may assume that S starts by placing agents at $\{x_1^1, \ldots, x_n^1\}$ and then processes x_{n+1}^1.

Second, any process strategy for any graph can easily be modified, without increasing (possibly decreasing) the number of used agents nor the number of occupied vertices, in such a way that the strategy processes all possible vertices

before placing or removing agents. In other words, the rule R_3 can be first applied without increasing the considered parameters. Therefore, any process strategy S for $D_{n,k}$ can be modified , without increasing the number of agents used nor the number of vertices occupied by S, into a strategy that first places n agents at $\{x_1^1, \ldots, x_n^1\}$, then processes x_{n+1}^1 and all vertices of $P_{n,k}^2$, and finally that mimics S. Such a strategy is called a *good* process strategy for $D_{n,k}$.

Third, $pn(D_{n,k}) \leq n+1$ as proved by the following strategy S^*. First, place n agents at $\{x_1^1, \ldots, x_n^1\}$, then process all vertices of $P_{n,k}^2$ and then x_{n+1}^1. In the next sentence, $y_i^{0,1}$ denotes x_i^1 and $y_i^{k+1,1}$ denotes x_i^2, $i \leq n$. Then, for $j = 1 \ldots k+1$, the jth phase of S^* consists of the following: for $i = 1 \ldots n$, place an agent at $y_{n-i+1}^{j,1}$ if j odd (resp., at $y_i^{j,1}$ if j even) and remove the agent at $y_{n-i+1}^{j-1,1}$ (resp., at $y_i^{j-1,1}$ if j even). Finally, process all vertices of K_{n+1}^2.

Let p, $0 \leq p \leq n-2$ (we choose $n \geq p-2$). Let S be a good process strategy for $D_{n,k}$ that uses $n+1+p$ agents (which exists by the previous remarks). We assume that S minimizes the number q of independent sets $IS_n^{t,1}$ of $D_{n,k}$ for which a vertex is occupied during the execution of S. Such an independent set is said *touched*. Note that the transformation that makes a strategy *good* does not increase the number of touched independent sets. Therefore, $2n+q \leq mfvs_{n+1+p}(D_{n,k})$ since any strategy occupies n vertices in each clique plus at least one vertex per touched independent set. In the sequel, we will prove that $q \geq k$, i.e., all independent sets of $P_{n,k}^1$ must be touched, and then, taking $k > 2n(C-1)$, we get that $\frac{mfvs_{pn+p}(D_{n,k})}{mfvs(D_{n,k})} = \frac{mfvs_{pn+p}(D_{n,k})}{2n} \geq \frac{mfvs_{n+1+p}(D_{n,k})}{2n} \geq \frac{2n+k}{2n} > C$.

It remains to prove that S touches all the k independent sets of $P_{n,k}^1$. To do so, we will modify S, possibly increasing the number of occupied vertices but without increasing the number of touched independent sets.

Since S is good, it first places n agents at $\{x_1^1, \ldots, x_n^1\}$, then processes x_{n+1}^1 and all vertices of $P_{n,k}^2$. We set $x_i^1 = y_i^{0,1}$, for all $i \leq n$. Let $S = S^0$. Let $0 \leq j < k$ and let S^j be the strategy that mimics the j first phases of S^* and then performs in the same order those movements of S^0 that concern the unprocessed vertices at this step. We prove by induction on $j < k$ that S^j can be transformed into the good process strategy S^{j+1} for $D_{n,k}$ satisfying the desired properties without increasing the number of touched independent sets. Clearly, S^0 is a good process strategy for $D_{n,k}$ that satisfies these properties.

Assume that, for some $0 \leq j < k-1$, S^j is a good process strategy that satisfies the desired properties. Then, S^j starts by occupying the vertices of $\{x_1^1, \ldots, x_n^1\}$, processes x_{n+1}^1 and the vertices of $P_{n,k}^2$ and then occupies and processes successively all vertices of $IS_n^{r,1}$, $r = 1 \ldots j$ until all vertices of $IS_n^{j,1}$ are occupied. Let s_j be the step of S^j when it occurs. We first prove that S^j touches $IS_n^{j+1,1}$. Indeed, if j is even, there are n vertex-disjoint paths from $y_n^{j+1,1}$ (resp., from $y_1^{j+1,1}$ if j is odd) to $x_1^2, \ldots, x_n^2$. While $y_n^{j+1,1}$ (resp., from $y_1^{j+1,1}$ if j is odd) is not processed, no agent in

$IS_n^{j,1}$ can be removed, and thus only $p+1 \leq n-1$ agents are available. Therefore, the only way to process $y_n^{j+1,1}$ (resp., from $y_1^{j+1,1}$ if j is odd) is to place an agent at it. Hence, there is a step of S^j (hence, of S^0) that consists of placing an agent at $y_n^{j+1,1}$ (resp., $y_1^{j+1,1}$ if j is odd). Hence, S^0 touches $IS_n^{j+1,1}$. To conclude, we modify S^j by adding after step s_j the $j+1^{th}$ phase of S^*. That is, after step j, the strategy successively occupies the vertices of $IS_n^{j+1,1}$ removing the agents at $IS_n^{j,1}$ until all vertices of $IS_n^{j+1,1}$ are occupied and all vertices of $IS_n^{j,1}$ have been processed. Then, the strategy mimics the remaining steps of S^j. The strategy obtained in such a way is clearly S^{j+1} that satisfies all desired properties. In particular, the obtained strategy is a good process strategy for $D_{n,k}$ that touches the same independent sets as S^0. ■

Note that there exists a $(pn(D)+p+1, mfvs(D))$-process strategy for the digraph $D_{n,k}$ described in the proof of Theorem 4 whereas the minimum q such that a $(pn(D)+p, q)$-process strategy for $D_{n,k}$ exists, is arbitrarily large.

Corollary 3 *For any $C > 0$, there exists a digraph D such that $\frac{mfvs_{pn}(D)}{mfvs(D)} > C$.*

We obtain this result by considering the digraph $D_{n,k}$ described in Figure A.3(a), with $n = 2$ and $k \geq 1$ (Figure A.3(b) represents $D_{2,5}$). This digraph is such that $pn(D_{2,k}) = 3$ and $mfvs(D_{2,k}) = 4$ while $\frac{mfvs_{pn}(D_{2,k})}{mfvs(D_{2,k})} = \frac{k+4}{4}$ is unbounded.

Lemma 1 in Section A.4 shows that, in the class of symmetric digraphs with bounded process number, $\frac{mfvs_{pn}(D)}{mfvs(D)}$ is bounded.

A.4 Behaviour of ratios in symmetric digraphs

We address in this section the behaviour of $\frac{mfvs_{pn}(D)}{mfvs(D)}$ for symmetric digraphs D. Note that the behaviours of $\frac{pn_{mfvs+q}(D)}{pn(D)}$ and $\frac{pn_{mfvs}(D)}{pn(D)}$ have already been studied in Section A.3 for symmetric digraphs with bounded process number.

Lemma 1 *For any symmetric digraph D, $\frac{mfvs_{pn}(D)}{mfvs(D)} \leq pn(D)$.*

Proof. Without loss of generality, we prove the lemma for a connected digraph D. Let S be a $(pn(D), mfvs_{pn}(D))$-process strategy for $D = (V, E)$. Let $O \subseteq V$ be the set of vertices occupied by an agent during the execution of S. Let F be a MFVS of D. Let us partition V into $(Y, X, W, Z) = (O \cap F, O \setminus F, F \setminus O, V \setminus (O \cup F))$. Since D is symmetric, $V \setminus F$ is an independent set because it is the complementary of a MFVS. Since the vertices not occupied by S have all their neighbors occupied, $V \setminus O$ is an independent set. Given $V' \subseteq V$, $N(V')$ denotes the set of neighbors of the vertices in V'. The partition is illustrated in Figure A.4.

First, note that $|N(W) \cap X| \leq pn(D)|W|$, because, for any vertex $v \in W$ to be processed, all its neighbors must be occupied by an agent. Thus, the maximum degree of v is $pn(D)$.

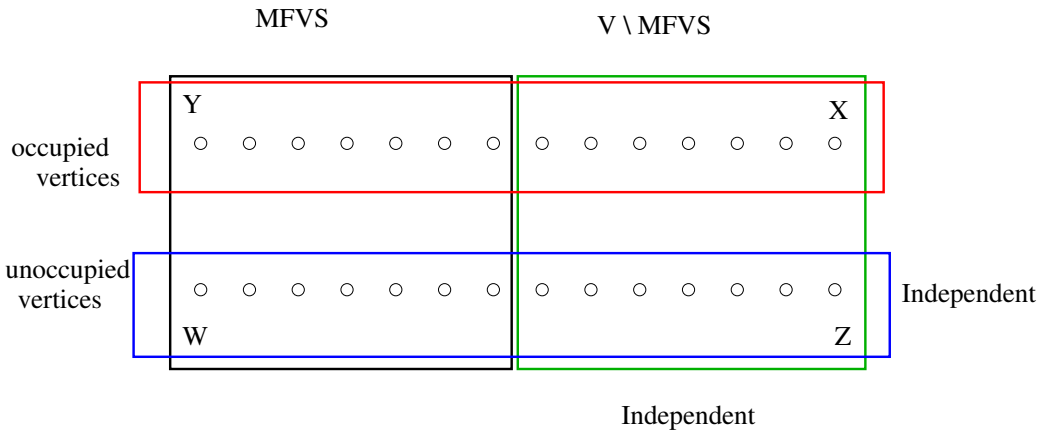

Figure A.4: Proof of Lemma 1

Then, we prove that $|X \setminus N(W)| \leq (pn(D) - 1)|Y|$. Let $R = X \setminus N(W)$. Because $X \cup Z$ is an independent set, for any $v \in R$, $N(v) \subseteq Y$. Let $T = N(R) \subseteq Y$. Note that $N(T) \cap R = R$ because D is connected and symmetric. Let us order the vertices of $T = \{v_1, \cdots, v_t\}$ in the sequence in which they are processed (when the agents are removed) when executing S. For any i, $1 \leq i \leq t$, let $N_i = \bigcup_{j \leq i} N(v_j) \cap R$. We aim at proving that $|N_1| < pn(D)$ and $|N_{i+1} \setminus N_i| < pn(D)$ for any $i < t$. Hence, we obtain $|N_t| = |R| \leq (pn(D) - 1)|T| \leq (pn(D) - 1)|Y|$.

Let us consider the step of S just before an agent is removed from v_1. Let $v \in N_1 \neq \emptyset$. Since the agent will be removed from v_1, either v has already been processed or is occupied by an agent. We prove that there is a vertex in $N(v) \subseteq T$ that has not been occupied yet and thus v must be occupied. Indeed, otherwise, all neighbors of v are occupied (since, at this step, no agents have been removed from the vertices of T) and the strategy can process v without placing any agent on v, contradicting the fact that S occupies the fewest vertices as possible. Therefore, just before an agent is to be removed from v_1, all vertices of N_1 are occupied by an agent. Hence, $|N_1| < pn(D)$.

Now, let $1 < i \leq t$. Let us consider the step of S just before an agent is removed from v_i. Let $v \in N_i \setminus N_{i-1}$ if such a vertex exists. Since the agent will be removed from v_i, either v has already been processed or is occupied by an agent. We prove that there is a vertex in $N(v) \subseteq T \setminus N_{i-1}$ that has not been occupied yet and thus v must be occupied. Indeed, otherwise, all neighbors of v are occupied (since, at this step, no agents have been removed from the vertices of $T \setminus N_{i-1}$) and the strategy can process v without placing any agent on v, contradicting the fact that S occupies the fewest vertices as possible. Therefore, just before an agent to be removed from v_i, all vertices of $N_{i+1} \setminus N_i$ are occupied by an agent. Hence, $|N_{i+1} \setminus N_i| < pn(D)$.

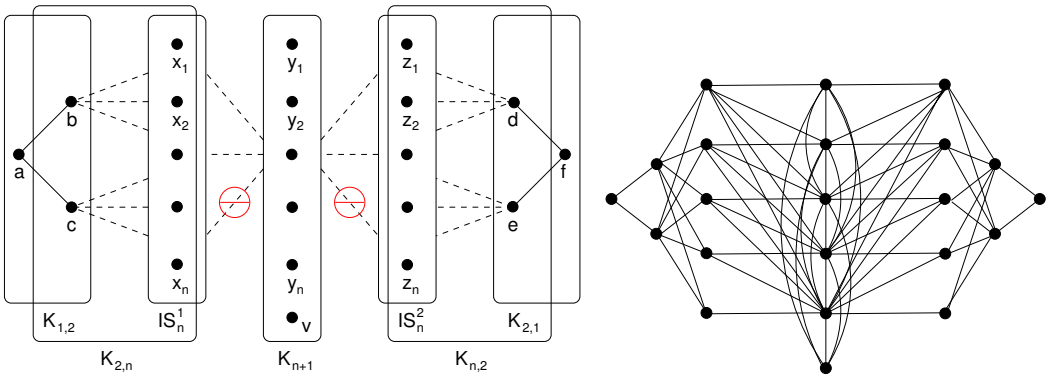

(a) SD_n (b) SD_5

Figure A.5: Symmetric digraph SD_n of Lemma 2 (Figure A.5(a)) and instance of SD_n when $n = 5$ (Figure A.5(b)). The red symbol $\ominus$ represents the absence of arcs.

To conclude: $mfvs_{pn}(D) = |O| = |Y| + |X|$ and $X = |X \setminus N(W)| + |N(W) \cap X|$. Hence, $mfvs_{pn}(D) \leq pn(D)(|Y| + |W|) = pn(D)|F| = pn(D).mfvs(D)$. ■

Lemma 2 *For any given $\varepsilon > 0$, there exists a symmetric digraph D such that $3 - \varepsilon \leq \frac{mfvs_{pn}(D)}{mfvs(D)} < 3$.*

Proof. Let $n \geq 1$. Let us consider the digraph SD_n built as follows. Let IS_n^1 and IS_n^2 be two independent sets of n nodes each: respectively $x_1, \ldots, x_n$ and $z_1, \ldots, z_n$. Let K_{n+1} be a symmetric clique of $n+1$ nodes $y_1, \ldots, y_n, y_{n+1} = v$. The digraph SD_n is built starting from the disjoint union of IS_n^1, IS_n^2, K_{n+1} and 6 isolated vertices $\{a, b, c, d, e, f\}$ by adding the following arcs. There are symmetric arcs between the nodes x_i and y_j and the nodes z_i and y_j, for any $1 \leq i \leq j \leq n$. Furthermore, all symmetric arcs of the complete bipartite graph with partitions $\{b, c\}$ and IS_n^1 are added. Similarly, all symmetric arcs of the complete bipartite graph with partitions $\{d, e\}$ and IS_n^2 are added. Finally, the symmetric arcs $(a, b), (a, c), (d, f), (e, f)$ are added. The general shape of SD_n is depicted in Figure A.5(a). The digraph SD_5 is represented in Figure A.5(b).

Note that the set $F = \{y_1, \ldots, y_n, b, c, d, e\}$ is a feedback vertex set of SD_n, with $|F| = n + 4$. Thus $mfvs(SD_n) \leq n + 4$ (actually, one can easily check that F is a minimum feedback vertex set of SD_n). Clearly, $pn(SD_n) \geq n$. In what follows, we prove that any strategy using $n + 1$ agents needs to cover at least $3n + 2$ vertices, and we present a $(n + 1, 3n + 2)$-process strategy for SD_n. Since $mfvs_{n+1}(D) \leq mfvs_{pn}(D)$ for any digraph D, the result follows.

First, we prove by contradiction that all process strategies for SD_n using $n + 1$ agents must start by processing either the nodes b and c or the nodes d and e, and so by placing the $n + 1$ agents either at vertices a and $x_1, \ldots, x_n$ or at vertices f and $z_1, \ldots, z_n$.

Suppose that the first vertex to be processed is either a or belongs to IS_n^1, and it is processed at step s. Therefore, the vertices b and c must be occupied by agents at this step (such that a can be processed thereafter). Without loss of generality, let us assume that b is processed, say at step s', before c. Since at most $n-1$ agents are available while c and b are occupied, no vertex of the clique K_{n+1} can be processed before step s'. On the other hand, at step s', all vertices of IS_n^1 are processed or occupied by agents such that b can be processed. Let X be the subset of vertices of IS_n^1 that are occupied at step s', and let $Y = V(IS_n^1) \setminus X$. For any $x_i \in Y$, y_i must be occupied at step s' (since x_i is processed and y_i is not). Hence, at step s', at least $2 + |X| + |Y| = n + 2$ agents are occupying some vertices, a contradiction. By symmetry, f and any vertex of IS_n^2 cannot be the first vertex to be processed.

Now suppose that the first vertex to be processed is $y_i \in K_{n+1}$, $i \leq n+1$. Note that all vertices of K_{n+1}, but $y_{n+1} = v$, have at least $n+2$ outneighbors. Therefore, $i = n+1$. When v is processed, the n vertices of $K_{n+1} \setminus \{v\}$ must be occupied, leaving at most one free agent. But now, all vertices of K_{n+1} but v have at least 2 unprocessed outneighbors. Whatever be the placement of the last agent, no other vertex can be processed and no agents can be released. Hence, the strategy fails, a contradiction.

Hence, any process strategy using $n+1$ agents must start by processing b, c, d or e. Without loss of generality, (by symmetry), let us assume that the first vertex to be processed is b. Hence, the strategy must start by placing agents at any vertex in $\{a\} \cup V(IS_n^1)$. At this step, the strategy processes b and c without covering them. Then a can be processed and the agent at it is released. At this step, no other vertex can be processed. Moreover, the only move that can be done is to place the free agent at y_n. Indeed, any other move would let all agents blocked. Then the free agent is placed at node y_n and x_n can be processed and the agent occupying it can be released. Similarly, the strategy sequentially places an agent at y_{n-i}, processes x_{n-i} and removes the corresponding agent, for $1 \leq i \leq n-1$. It is easy to check that any variation of this would make the strategy immediately fail. Once all vertices $y_1, \cdots, y_n$ are occupied, then v can be processed without being covered. Then, the strategy goes on being highly constrained: for $1 \leq i \leq n$, the free agent occupies z_i, allowing to process y_i and to free the agent occupying it. Finally, when all vertices of IS_n^2 are occupied, the free agent must occupy f, and all remaining vertices may be processed. Again, all these moves are forced for, otherwise, the strategy would be blocked.

Such a strategy covers $3n+2$ nodes. Therefore, $mfvs_{pn}(SD_n) \geq mfvs_{n+1}(SD_n) = 3n+2$. Hence, $\frac{mfvs_{pn}(SD_n)}{mfvs(SD_n)} \geq \frac{3n+2}{n+4}$. For $n > \frac{10}{\varepsilon} - 4$, we get $\frac{mfvs_{pn}(SD_n)}{mfvs(SD_n)} \geq 3 - \varepsilon$. Moreover, since SD_n has $3n+7$ vertices, we get $mfvs_{pn}(SD_n) \leq 3n+6$, and so $\frac{mfvs_{pn}(SD_n)}{mfvs(SD_n)} < 3$. ■

Conjecture 1 *For any symmetric digraph D, $\frac{mfvs_{pn}(D)}{mfvs(D)} \leq 3$.*

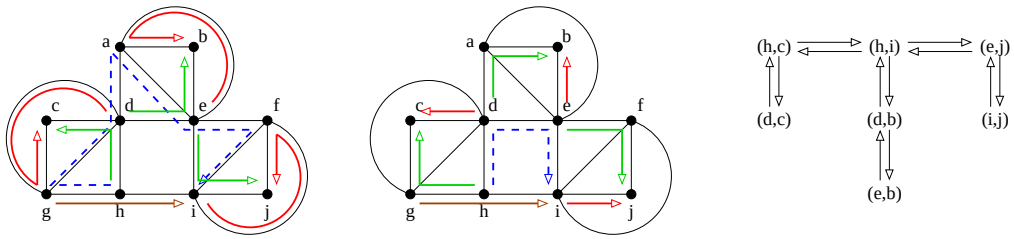

(a) Old set of routes S_1.

(b) New set of routes S_2.

(c) Dependency digraph D from S_1 to S_2.

Figure A.6: Instance of the reconfiguration problem consisting of a network with 10 nodes and symmetric arcs, 8 connections $(h,i),(h,c),(d,c),(d,b),(e,b),(e,j),(i,j),(g,i)$ to be reestablished. Figure A.6(a) depicts the old set of routes S_1, Figure A.6(b) the new set S_2, and Figure A.6(c) the dependency digraph from S_1 to S_2.

A.5 The routing reconfiguration problem

The *routing reconfiguration problem* occurs in connection-oriented networks such as telephone, MPLS, or WDM [CCM+10a, CHM+09, CPPS05, CS07, Sol09, SP09]. In such networks, a connection corresponds to the transmission of a data flow from a source to a destination, and is usually associated with a capacitated path (or a wavelength in WDM optical networks). A *routing* is the set of paths serving the connections. To avoid confusion, we assume here that each arc of the network has capacity one, and that each connection requires one unit of capacity. Consequently, no two paths can share the same arc (valid assumption in WDM networks). When a link of the network needs to be repaired, it might be necessary to change the routing of the connection using it, and incidentally to change the routing of other connections if the network has not enough free resources. Computing a new viable routing is a well known hard problem, but it is not the concern of our work. Indeed, this is not the end of our worries: once a new routing not using the unavailable links is computed, it is not acceptable to stop all the connections going on, and change the routing, as it would result in a bad quality of service for the users (such operation requires minutes in WDM networks). Instead, it is preferred that each connection first establishes the new path on which it transmits data, and then stops the former one. This requires a proper scheduling to avoid conflicts in accessing resources (resources needed for a new path must be freed by other connections first). Furthermore, cyclic dependencies might force to interrupt some connections during that phase. The aim of the routing reconfiguration problem is to optimize tradeoffs between the total number and the concurrent number of connections to interrupt.

As an example, a way to reconfigure the instance depicted in Figure A.6 may be to interrupt connections $(h,c),(d,b),(e,j)$, then set up the new paths of all other

connections, tear down their old routes, and finally, set up the new paths of connections (h, c), (d, b), (e, j). Such a strategy interrupts a total of 3 connections and these ones are interrupted simultaneously. Another strategy may consist of interrupting the connection (h, i), then sequentially: interrupt connection (h, c), reconfigure (d, c) without interruption for it, set up the new route of (h, c), then reconfigure in the same way first (d, b) and (e, b) without interruption for these two requests, and then (e, j) and (i, j). Finally, set up the new route of (h, i). The second strategy implies the interruption of 4 connections, but at most 2 connections are interrupted simultaneously.

Indeed, possible objectives are (1) to minimize the maximum number of concurrent interruptions [CHM+09, CPPS05, Sol09, SP09], and (2) to minimize the total number of disrupted connections [JS03]. Following [CPPS05, JS03], these two problems can be expressed through the theoretical game described in Section A.1.1, on the dependency digraph [JS03]. Given the initial routing and the new one, the dependency digraph contains one node per connection that must be switched. There is an arc from node u to node v if the initial route of connection v uses resources that are needed by the new route of connection u. Figure A.6 shows an instance of the reconfiguration problem and its corresponding dependency digraph. In Figure A.6(c), there is an arc from vertex (d, c) to vertex (h, c), because the new route used by connection (d, c) (Figure A.6(b)) uses resources seized by connection (h, c) in the initial configuration (Figure A.6(a)). Other arcs are built in the same way.

Given the dependency digraph D of an instance of the problem, a (p, q)-process strategy for D corresponds to a valid reconfiguration of the connections where p is the maximum number of concurrent disruptions and q is the total number of interruptions. Indeed the three rules can be viewed in terms of reconfiguration of requests:

R_1 Put an agent at a vertex v of D;
Interrupt the request corresponding to v;

R_2 Remove an agent from a vertex v of D if all its outneighbors are either processed or occupied by an agent, and process v;
Route an interrupted connection when final resources are available;

R_3 Process an unoccupied vertex v of D if all its outneighbors are either processed or occupied by an agent;
Reroute a non-interrupted connection when final resources are available.

The next theorem proves the equivalence between instances of the reconfiguration problem and dependency digraphs.

Theorem 5 *Any digraph D is the dependency digraph of an instance of the routing reconfiguration problem.*

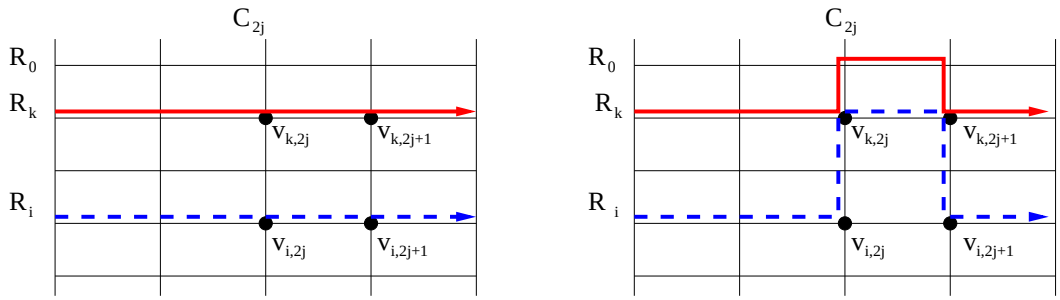

Figure A.7: Scheme of the transformation in the proof of Theorem 5

Proof. Roughly, consider a grid network where each initial lightpath of any connection is some row of the grid. If two connections i and k are linked by an arc (i,k) in the dependency digraph, then we build the new lightpaths of both connections as depicted in Figure A.7 which actually create the desired dependence. Note that the lightpath of connection k is deported on an additional row, i.e., a row corresponding to no connection. For each arc of the dependency digraph, we can use different columns of the grid-network, in such a way that these transformations may be done independently.

More formally, let $D = (V, A)$ be a digraph with $V = \{c_1, \cdots, c_n\}$ and $A = \{a_1, \cdots, a_m\}$. Let us define the network G as a $(n+2) \times (2m)$ grid such that each edge of which has capacity one. Let R_i denotes the ith row of G $(0 \leq i \leq n+1)$ and C_i its ith column $(1 \leq j \leq 2m)$, and let $v_{i,j} \in V(G)$ be the vertex in $R_i \cap C_j$. For any i, $1 \leq i \leq n$, connection i, corresponding to c_i in D, occurs between $v_{i,1} \in V(G)$ the leftmost vertex of R_i and $v_{i,2m} \in V(G)$ the rightmost vertex of R_i, and let the initial lightpath of connection i follows R_i. Now, we present an iterative method to build the new lightpath of each connection. Initially, for any i, $1 \leq i \leq n$, the new lightpath P_i^0 of connection i equals the old lightpath R_i. Now, after the $(j-1)^{th}$ step $(0 < j \leq m)$ of the method, let P_i^{j-1} be the current value of the new lightpath of connection i and assume that in the subgraph of G induced by columns $(C_{2j-1}, \cdots, C_{2m})$, P_i^{j-1} equals R_i. Consider $a_j = (c_i, c_k) \in A$ and let us do the following transformation depicted in Figure A.7. For any $\ell \notin \{i,k\}$, $P_\ell^j = P_\ell^{j-1}$. Now, P_i^j is defined by replacing the edge $(v_{i,2j-1}, v_{i,2j})$ in P_i^{j-1} by the shortest path from $v_{i,2j-1}$ to $v_{k,2j-1}$ (following C_{2j-1}), the edge $(v_{k,2j-1}, v_{k,2j})$, and the shortest path from $v_{k,2j}$ to $v_{i,2j}$ (following C_{2j}). Similarly, P_k^j is defined by replacing the edge $(v_{k,2j-1}, v_{k,2j})$ in P_k^{j-1} by the shortest path from $v_{k,2j-1}$ to $v_{n+1,2j-1}$ if $i < k$ (resp., to $v_{0,2j-1}$ if $i > k$), the edge $(v_{n+1,2j-1}, v_{n+1,2j})$ (resp., $(v_{0,2j-1}, v_{0,2j})$), and the shortest path from $v_{n+1,2j}$ to $v_{k,2j}$ (resp., from $v_{0,2j}$ to $v_{k,2j}$). It is easy to check that the grid G, the sets of initial lightpaths $\{R_1, \cdots, R_n\}$ and final lightpaths $\{P_1^m, \cdots, P_n^m\}$ admit D as dependency digraph. ■

Note that a digraph may be the dependency digraph of various instances of the reconfiguration problem. Since any digraph may be the dependency digraph of a realistic instance of the reconfiguration problem, Theorem 5 shows the relevance of studying these problems through dependency digraph notion.

A feasible reconfiguration may be defined by a (p, q)-process strategy for the corresponding dependency digraph. Problem (1) is equivalent to minimize p (Section A.1.1) and Problem (2) is similar to the one of minimizing q (Section A.1.1). Consider the dependency digraph D of Figure A.6. From Section A.1.1, we can not minimize both p and q, that is the number of simultaneous disrupted requests and the total number of interrupted connections. Indeed there does not exist a $(2, 3)$-process strategy while $(2, 4)$ and $(3, 3)$ exist (Figure A.1(a) and Figure A.1(b)).

It is now easy to make the relation between tradeoff metrics introduced in Section A.1.1 and tradeoffs for the routing reconfiguration problem. For example, pn_{mfvs} introduced in Definition 3 represents the minimum number of requests that have to be simultaneously interrupted during the reconfiguration when the total number of interrupted connections is minimum. Also Section A.2 shows that the problems of computing these new tradeoffs parameters for the routing reconfiguration problem are NP-complete and not in APX. Finally Section A.3 proves that the loss one can expect on one parameter when minimizing the other may be arbitrarily large.

A.6 Conclusion

In this work, we address the routing reconfiguration problem through a game played on digraphs. We introduce the notion of (p, q)-process strategy and some tradeoff metrics in order to minimize one metric under the constraint that the other is fixed. We proved that the problems of computing these parameters are APX-hard and some are not in APX. We also proved that there exist digraphs for which minimizing one parameter may increase the other arbitrarily. For further research, we plan to continue our study for symmetric digraphs in order to (dis)prove Conjecture 1. Moreover, it would be interesting to design exact algorithms and heuristics to compute (p, q)-process strategies.

Bibliography

[AHK+07] K. Aardal, S. V. Hoesel, A. M. C. A. Koster, C. Mannino, and A. Sassano. Models and solution techniques for frequency assignment problems. *Annals of Operations Research*, 153(1):79–129, 2007. 3

[And03] H. Anderson. *Fixed broadband wireless system design*. John Wiley & Sons, 2003. 9, 12, 14, 15, 16, 19, 20, 21, 22

[ARC07] Décret n2007-1532. `http://www.arcep.fr/fileadmin/reprise/textes/decrets/d2007-1532.pdf`, 2007. 13

[ASR09] D. Dentcheva A. Shapiro and A. Ruszczynski. *Lectures on Stochastic Programming: Modeling and Theory*. SIAM, 2009. 32

[AT02] L. T. H. An and P. D. Tao. D.C. programming approach for multicommodity network optimization problems with step increasing cost functions. *Journal of Global Optimization*, 22(1):205–232, 2002. 51

[Bar72] W. T. Barnett. Multipath propagation at 4, 6 and 11 GHz. *Bell System Technical Journal*, 51(2):311–361, 1972. 19, 20

[BBF99] V. Bafna, P. Berman, and T. Fujito. A 2-approximation algorithm for the undirected feedback vertex set problem. *SIAM J. Discrete Math*, 12:289Ð297, 1999. 85

[BCC10] T. Bektaş, M. Chouman, and T. G. Crainic. Lagrangean-based decomposition algorithms for multicommodity network design problems with penalized constraints. *Networks*, 55(3):171–180, 2010. 65, 70

[BCGT98] D. Bienstock, S. Chopra, O. Günlük, and C. Y. Tsai. Minimum cost capacity installation for multicommodity network flows. *Mathematical Programming*, 81(2):177–199, 1998. 37

[Ben62] J. F. Benders. Partitioning procedures for solving mixed variable programming problems. *Numerische Mathematik*, 4:238–252, 1962. 74

[Ber98] D. Bertsekas. *Network optimization: continuous and discrete models*. Athena Scientific, 1998. 4

[BG96] D. Bienstock and O. Günlük. Capacitated network design – polyhedral structure and computation. *INFORMS Journal on Computing*, 8(3):243–259, 1996. 37

[Boc09] E. Boch. High-capacity Ethernet backhaul radio systems for advanced mobile data networks. *IEEE Microwave Magazine*, 10(5):108–114, 2009. 1, 2, 11

[BR03] C. Blum and A. Roli. Metaheuristics in combinatorial optimization: overview and conceptual comparison. *ACM Computing Surveys*, 3(35):268–308, 2003. 54

[Bre67] R. L. Breisch. An intuitive approach to speleotopology. *Southwestern Cavers*, VI(5):72–78, 1967. 82, 84

[CCG09] A. M. Costa, J.-F. Cordeau, and B. Gendron. Benders, metric and cutset inequalities for multicommodity capacitated network design. *Computational Optimization and Applications*, 42(3):371–392, 2009. 37, 65, 76

[CCKN] G. Claßen, D. Coudert, A. M. C. A. Koster, and N. Nepomuceno. Bandwidth allocation for reliable fixed broadband wireless networks. (Submitted). 5

[CCM+10a] N. Cohen, D. Coudert, D. Mazauric, N. Nepomuceno, and N. Nisse. Tradeoffs in process strategy games with application in the WDM reconfiguration problem. In *5th International Conference on Fun with Algorithms (FUN'10)*, volume 6099 of *Lecture Notes in Computer Science*, pages 121–132. Springer, 2010. 6, 98

[CCM+10b] N. Cohen, D. Coudert, D. Mazauric, N. Nepomuceno, and N. Nisse. Tradeoffs in routing reconfiguration problems. In *12èmes Rencontres Francophones sur les Aspects Algorithmiques des Télécommunications (AlgoTel'10)*, 2010. 6

[CGB09] S. Chia, M. Gasparroni, and P. Brick. The next challenge for cellular networks: backhaul. *IEEE Microwave Magazine*, 10(5):54–66, 2009. 2

[CHM08] D. Coudert, F. Huc, and D. Mazauric. A distributed algorithm for computing and updating the process number of a forest. In G. Taubenfeld, editor, *22nd International Symposium on Distributed Computing (DISC)*, volume 5218 of *Lecture Notes in Computer Science*, pages 500–501, Arcachon, France, September 2008. Springer. brief announcement. 84

[CHM+09] D. Coudert, F. Huc, D. Mazauric, N. Nisse, and J-S. Sereni. Routing reconfiguration/process number: Coping with two classes of services. In *13th Conf. on Optical Network Design and Modeling (ONDM)*, 2009. 83, 84, 98, 99

[CMN09] L. Chiaraviglio, M. Mellia, and F. Neri. Reducing power consumption in backbone networks. In *IEEE International Conference on Communications (ICC'09)*, pages 1–6, 2009. 62

[CNR09a] D. Coudert, N. Nepomuceno, and H. Rivano. Joint optimization of routing and radio configuration in fixed wireless networks. In *11ème*

Rencontres Francophones sur les Aspects Algorithmiques des Télécommunications (AlgoTel'09), 2009. 5

[CNR09b] D. Coudert, N. Nepomuceno, and H. Rivano. Minimizing energy consumption by power-efficient radio configuration in fixed broadband wireless networks. In *1st IEEE WoWMoM Workshop on Hot Topics in Mesh Networking (HotMESH'09)*. IEEE, 2009. 5

[CNR10] D. Coudert, N. Nepomuceno, and H. Rivano. Power-efficient radio configuration in fixed broadband wireless networks. *Computer Communications, Special Section on Hot Topics in Mesh Networking*, 33(8):898–906, 2010. 5

[COS10] Introduction to chance-constrained programming. `http://stoprog.org/index.html?SPIntro/intro2ccp.html`, 2010. 32

[CPL10] IBM ILOG CPLEX website. `http://www.ilog.com/products/cplex`, 2010. 40, 57

[CPPS05] D. Coudert, S. Perennes, Q.-C. Pham, and J.-S. Sereni. Rerouting requests in WDM networks. In *7ème Rencontres Francophones sur les Aspects Algorithmiques des Télécommunications (AlgoTel'05)*, pages 17–20, mai 2005. 81, 83, 84, 98, 99

[Cra80] R. K. Crane. Prediction of attenuation by rain. *IEEE Transactions on Communications*, 28(9):1717–1732, 1980. 19, 20

[Cra96] R. K. Crane. *Electromagnetic wave propagation through rain*. John Wiley & Sons, 1996. 19, 20

[CS07] D. Coudert and J-S. Sereni. Characterization of graphs and digraphs with small process number. Research Report 6285, INRIA, September 2007. 83, 84, 98

[Dar07] B. Darties. *Problèmes algorithmiques et de complexité das les réseaux sans fil*. PhD thesis, Université Montpellier II, 2007. 3, 27

[DKL87] N. Deo, S. Krishnamoorthy, and M. A. Langston. Exact and approximate solutions for the gate matrix layout problem. *IEEE Tr. on Comp.-Aided Design*, 6:79–84, 1987. 85, 89

[DPS02] J. Díaz, J. Petit, and M. Serna. A survey on graph layout problems. *ACM Comp. Surveys*, 34(3):313–356, 2002. 82, 84

[DXC+08] L. Dai, Y. Xue, B. Chang, Y. Cao, and Y. Cui. Optimal routing for wireless mesh networks with dynamic traffic demand. *Mobile Networks and Applications*, 13(2):97–116, 2008. 47

[ENS+95] G. Even, J. Naor, B. Schieber, , and M. Sudan. Approximating minimum feedback sets and multi-cuts in directed graphs. In *Proc. 4th Int. Conf. on Integer Prog. and Combinatorial Optimization*, volume LNCS 920, 1995. 85

[EST94] J.A. Ellis, I.H. Sudborough, and J.S. Turner. The vertex separation and search number of a graph. *Information and Computation*, 113(1):50–79, 1994. 84

[FCC10] The FCC website. `http://www.fcc.gov`, 2010. 12

[FKNP07] M. Flammini, R. Klasing, A. Navarra, and S. Pérennes. Improved approximation results for the minimum energy broadcasting problem. *Algorithmica*, 49(4):318–336, 2007. 48

[FT08] F. Fomin and D. Thilikos. An annotated bibliography on guaranteed graph searching. *Theo. Comp. Sci.*, 399(3):236–245, 2008. 81, 82, 84

[Fum01] F. Fumero. A modified subgradient algorithm for lagrangean relaxation. *Computers and Opererations Research*, 28(1):33–52, 2001. 72

[GC97] A. Goldsmith and S.-G. Chua. Variable-rate variable-power MQAM for fading channels. *IEEE Transactions on Communications*, 45(10):1218–1230, 1997. 30

[GC98] A. Goldsmith and S.-G. Chua. Adaptive coded modulation for fading channels. *IEEE Transactions on Communications*, 46(5):595–602, 1998. 30

[GK03] F. W. Glover and G. A. Kochenberger. *Handbook of Metaheuristics*. Kluwer Academic Publishers, 2003. 54

[GKM99] V. Gabrel, A. Knippel, and M. Minoux. Exact solution of multicommodity network optimization problems with general step cost functions. *Operations Research Letters*, 25(1):15–23, 1999. 4

[GM97] V. Gabrel and M. Minoux. LP relaxations better than convexification for multicommodity network optimization problems with step increasing cost functions. *Acta Mathematica Vietnamica*, 22(1):123–145, 1997. 4, 51

[Gol05] A. Goldsmith. *Wireless Communications*. Cambridge University, 2005. 9

[GPR08] C. Gomes, S. Pérennes, and H. Rivano. Bottleneck analysis for routing and call scheduling in multi-hop wireless networks. In *4th IEEE Workshop on Broadband Wireless Access (BWA'08)*, pages 1–6, 2008. 48

[GS03] M. Gupta and S. Singh. Greening of the internet. In *ACM Conference on Applications, Technologies, Architectures, and Protocols for Computer Communications (SIGCOMM'03)*, pages 19–26, 2003. 11

[HART10] S. Hurley, S. Allen, D. Ryan, and R. Taplin. Modelling and planning fixed wireless networks. *Wireless Networks*, 16(3):577–592, 2010. 27

[Hol95] K. Holmberg. Lagrangian heuristics for linear cost multicommodity network flow problems. Technical Report OPT-WP-1995-01, LiTH-MAT, 1995. 65, 70

[HTRS10] N. Himayat, S. Talwar, A. Rao, and R. Soni. Interference management for 4G cellular standards WIMAX/LTE UPDATE. *IEEE Communications Magazine*, 48(8):86–92, 2010. 3

[ICT10] The ICT regulation toolkit website. `http://icttoolkit.infodev.org`, 2010. 12, 13

[IOR+10] F. Idzikowski, S. Orlowski, C. Raack, H. Woesner, and A. Wolisz. Saving energy in IP-over-WDM networks by switching off line cards in low-demand scenarios. In *14th Conference on Optical Networks Design and Modeling (ONDM'10)*, pages 1–6, 2010. 62

[ITU10] The ITU website. `http://www.itu.int`, 2010. 11

[JS03] N. Jose and A.K. Somani. Connection rerouting/network reconfiguration. In *4th International Workshop on Design of Reliable Communication Networks (DRCN)*, pages 23–30. IEEE, October 2003. 99

[Kan92] V. Kann. *On the Approximability of NP-complete Optimization Problems*. PhD thesis, Department of Numerical Analysis and Computing Science, Royal Institute of Technology, Stockholm., 1992. see also: http://www.csc.kth.se/ viggo/wwwcompendium/node19.html. 85

[Ken78] J. Kennington. A survey of linear cost multicommodity network flows. *Operations Research*, 26(2):209–236, 1978. 4, 29, 47

[KGV83] S. Kirkpatrick, C. D. Gelatt, and M. P. Vecchi. Optimization by simulated annealing. *Science*, 220(4598):671–680, 1983. 55, 56

[Klo10] O. Klopfenstein. Solving chance-constrained combinatorial problems to optimality. *Computational Optimization and Applications*, 45(3):607–638, 2010. 29, 34

[KP86] M. Kirousis and C.H. Papadimitriou. Searching and pebbling. *Theoretical Comp. Sc.*, 47(2):205–218, 1986. 82, 84

[LAN10] J. Luedtke, S. Ahmed, and G. L. Nemhauser. An integer programming approach for linear programs with probabilistic constraints. *Mathematical Programming*, 122(2):247–272, 2010. 29

[Leh10] H. Lehpamer. *Microwave transmission networks: planning, design, and deployment*. McGraw-Hill, 2010. 9, 11, 13, 14, 15, 16, 22, 48

[Lit09] S. Little. Is microwave backhaul up to the 4G task? *IEEE Microwave Magazine*, 10(5):67–74, 2009. 1, 3

[LY04] T. Larsson and D. Yuan. An augmented lagrangian algorithm for large scale multicommodity routing. *Computational Optimization and Applications*, 27(2):187–215, 2004. 39, 57, 65

[Man09] T. Manning. *Microwave radio transmission design guide*. Artech House, 2009. 9, 10, 14, 22, 48

[MHG+88] N. Megiddo, S. L. Hakimi, M. R. Garey, D. S. Johnson, and C. H. Papadimitriou. The complexity of searching a graph. *J. Assoc. Comput. Mach.*, 35(1):18–44, 1988. 85, 89

[Min06] M. Minoux. Multicommodity network flow models and algorithms in telecommunications. In P. Pardalos and M. Resende, editors, *Handbook of Optimization in Telecommunications*, pages 163–184. 2006. 4, 29, 47

[MMV93] T. L. Magnanti, P. Mirchandani, and R. Vachani. The convex hull of two core capacitated network design problems. *Mathematical Programming*, 60(2):233–250, 1993. 37

[MMV95] T. L. Magnanti, P. Mirchandani, and R. Vachani. Modelling and solving the two-facility capacitated network loading problem. *Operations Research*, 43(1):142–157, 1995. 37

[MPR08] C. Molle, F. Peix, and H. Rivano. An optimization framework for the joint routing and scheduling in wireless mesh networks. In *19th IEEE International Symposium on Personal, Indoor and Mobile Radio Communications (PIMRC'08)*, pages 1–5, 2008. 48

[OPTW10] S. Orlowski, M. Pióro, A. Tomaszewski, and R. Wessäly. SNDlib 1.0 – Survivable Network Design Library. *Networks*, 55(3):276–286, 2010. 45

[ORV10] A. Ouni, H. Rivano, and F. Valois. Capacity of wireless mesh networks: determining elements and insensible properties. In *IEEE Wireless Communications and Networking Conference Workshops (WCNCW'10)*, pages 1–6, 2010. 48

[Par78] T. D. Parsons. Pursuit-evasion in a graph. In *Theory and applications of graphs*, volume 642 of *Lecture Notes in Mathematics*, pages 426–441. Springer, Berlin, 1978. 82, 84

[PM04] M. Pióro and D. Medhi. *Routing, flow, and capacity design in communication and computer networks*. Morgan Kaufmann, 2004. 4

[PR05] J. Puchinger and G. R. Raidl. Combining metaheuristics and exact algorithms in combinatorial optimization: a survey and classification. In J. Mira and J. R. Álvarez, editors, *1st International Work-Conference on the Interplay Between Natural and Artificial Computation (IWINAC'05)*, pages 41–53, 2005. 54

[Pré95] A. Prékopa. *Stochastic Programming*. Kluwer, 1995. 32

[Put00] S. Puthenpura. Interesting optimization problems in the planning of microwave transmission networks. In *25th Annual IEEE Conference on Local Computer Networks (LCN'00)*, pages 384–391, 2000. 2

[Rai06] G. R. Raidl. A unified view on hybrid metaheuristics. In F. Almeida, M. J. B. Aguilera, C. Blum, J. M. Moreno-Vega, M. P. Pérez, A. Roli, and M. Sampels, editors, *3rd International Workshop on Hybrid Metaheuristics (HM'06)*, pages 1–12, 2006. 54

[Rap02] T. Rappaport. *Wireless communications: principles and practice*. Prentice Hall, 2002. 9, 13, 15

[RKOW10] C. Raack, A. M. C. A. Koster, S. Orlowski, and R. Wessäly. On cut-based inequalities for capacitated network design polyhedra. *Networks*, 2010. 37, 38

[Roc72] R. T. Rockafellar. *Convex Analysis*. Princeton, 1972. 76

[Roc93] R. T. Rockafellar. Lagrange multipliers and optimality. *SIAM Review*, 35(2):183–238, 1993. 72

[RS83] N. Robertson and P. D. Seymour. Graph minors. I. Excluding a forest. *J. Comb. Th. Ser. B*, 35(1):39–61, 1983. 84

[San09] J. M. Sandri. Microwave backhaul as a business: taking the next step. *IEEE Microwave Magazine*, 10(5):34–46, 2009. 3, 11

[Sha48] C. Shannon. A mathematical theory of communication. *Bell System Technical Journal*, 27:379–423, 1948. 14

[Sol09] F. Solano. Analyzing two different objectives of the WDM network reconfiguration problem. In *IEEE Global Communications Conference (Globecom)*, 2009. 84, 87, 89, 98, 99

[SP00] V. Sridhar and J. S. Park. Benders-and-cut algorithm for fixed-charge capacitated network design problem. *European Journal of Operational Research*, 125(3):622–632, 2000. 65

[SP09] F. Solano and M. Pióro. A mixed-integer programing formulation for the lightpath reconfiguration problem. In *VIII Workshop on G/MPLS Networks (WGN8)*, 2009. 98, 99

[SRSW05] D. Simplot-Ryl, I. Stojmenovic, and J. Wu. Energy efficient backbone construction, broadcasting, and area coverage in sensor networks. In I. Stojmenovic, editor, *Handbook of Sensor Networks*, pages 343–380. 2005. 48

[TLM84] R. T. Wong T. L. Magnanti. Network design and transportation planning: models and algorithms. *Transportation Science*, 18(1):1–55, 1984. 4

[Vig75] A. Vigants. Space-diversity engineering. *Bell System Technical Journal*, 54(1):103–142, 1975. 19, 20

[Wol98] L. A. Wolsey. *Integer Programming*. John Wiley & Sons, 1998. 37

[ZP00] J. Zyren and A. Petrick. Tutorial on basic link budget analysis. Technical Report AN-9804.1, Intersil, 2000. 14

[ZWZL05] J. Zhang, H. Wu, Q. Zhang, and B. Li. Joint routing and scheduling in multi-radio multi-channel multi-hop wireless networks. In *2nd IEEE International Conference on Broadband Networks (BROADNETS'05*, pages 678–687, 2005. 48